TUTKIMUSRAPORTTI
REPORT OF INVESTIGATION 90

Risto Puranen

Susceptibilities, iron and magnetite content of Precambrian rocks in Finland

GEOLOGIAN TUTKIMUSKESKUS
GEOLOGICAL SURVEY OF FINLAND

Espoo 1989

GEOLOGIAN TUTKIMUSKESKUS
Tutkimusraportti 90

GEOLOGICAL SURVEY OF FINLAND
Report of Investigation 90

Risto Puranen

SUSCEPTIBILITIES, IRON AND MAGNETITE CONTENT OF PRECAMBRIAN ROCKS IN FINLAND

Espoo 1989

Puranen, Risto, 1989. Susceptibilities, iron and magnetite content of Precambrian rocks in Finland. *Geological Survey of Finland, Report of Investigation 90.* 45 pages, 25 figures, 7 tables and 3 appendices.

A summary is presented of magnetic susceptibilities measured during the last two decades from about 40 000 rock samples provided by geologists. These samples collected for bedrock mapping are representative of the Precambrian rocks in Finland both areally and lithologically. The susceptibility data were originally measured for magnetic interpretations but the data also have petrologic applications. Application methods have been developed by comparisons of susceptibility data with density, remanent magnetization, chemistry and mineralogy of the most common rock types.

Frequency distributions of susceptibilities are composed of dia-, para- and ferrimagnetic components, which can often be identified. The components are most clearly distinguished in susceptibility-density diagrams, which also reflect variations in the iron content of mafic minerals. The paramagnetic component dominates the susceptibility distributions in most areas and rock types. With the aid of para- and ferrimagnetic susceptibility of rocks their iron and magnetite content can be estimated. Average formulae are presented for such estimation based on abundant experimental data. Relations between remanence and susceptibility (Q-ratios) are studied to determine the total magnetization of rocks for magnetic interpretations. The Q-ratios are also used to characterize grain sizes and types of ferrimagnetic minerals.

The methods and relations presented are applied for comparison of geologic provinces in Finland. Mica schists and especially granites are more uniformly magnetized in northern Finland (Lapland) than in central and southern Finland, which is consistent with regional aeromagnetic data. In Lapland more than 70 % of granite samples are ferrimagnetic as compared to about 20 % in other areas, although the total iron content of granites is at lowest in Lapland. This difference in magnetite distribution can be inherited from source material, which may have been more homogeneously oxidized in Lapland. The Wiborg rapakivi granites of southern Finland contain exceptionally iron-rich mafic silicates, which have partly been decomposed into small amounts of fine-grained iron oxides.

Key words: magnetic susceptibility, iron, magnetite, rocks, density, remanent magnetization, chemical composition, mineral composition, oxidation, Precambrian, Finland

Risto Puranen
Geological Survey of Finland
SF-02150 Espoo
Finland

ISBN 951-690-352-5
ISSN 0781-4240

CONTENTS

INTRODUCTION

The physical properties of Precambrian rocks in Finland have been studied in the laboratories of Geological Survey (GSF) since the early 1960's. At first, only the densities and magnetic susceptibilities of rocks were measured. The intensity of remanent magnetization was added to the measuring program in 1975, after the construction of a suitable meter for hand specimens. At about the same time a more sensitive meter was built for studies of anisotropic and paramagnetic susceptibilities. In 1983 the development of new remanence and resistivity meters was completed, and the measuring apparatus was installed under computer control. Measurement data have accumulated during the last 20 years so that the petrophysical register in 1985 contained the density and susceptibility of more than 40 000 bedrock samples and the remanence of about 20 000 samples. Originally the petrophysical measurements were intended to assist the quantitative interpretation of geophysical maps, and although they are still made for this purpose, the abundant data can also be applied to petrologic investigations.

The petrophysical data have already been summarized with respect to densities (Puranen et al., 1978), and the present report will mostly concentrate on the magnetic susceptibilities of rocks. A statistical summary is presented for the effective susceptibilities of common rock types for the purpose of magnetic interpretations, but the petrologic application of susceptibility measurements will be the main subject of this report. Petrologic interpretations are facilitated by comparisons of the susceptibility data with rock density, remanent magnetization, chemistry and mineralogy. The comparisons are made for ten example rock types, which are representative of the Finnish bedrock and divide the sample material into more homogeneous strata. Para- and ferrimagnetic parts of susceptibility distributions are distinguished, and their mean relations to iron and magnetite contents of rocks are quantified. The abundant data is summarized into various diagrams based on averages so that the effects of local geologic variation are smoothed out. The mean results for the whole of Finland provide a frame of reference, within which geologic provinces and smaller units are compared. The geologic recycling of iron and magnetite is also discussed in the light of the results and on the basis of the excellent review articles by McIntyre (1980) and Grant (1985).

PREVIOUS STUDIES

The relations of rock magnetic properties to magnetic minerals and bedrock geology on one hand and to magnetic maps on the other hand have been actively studied since the 1950's (Mooney & Bleifuss, 1953; Balsley & Buddington, 1958; Pecherskiy, 1965; Puranen et al., 1968; Henkel, 1976; Krutikhovskaya et al., 1979; Clark, 1983). Summaries of magnetic properties and densities of rocks have also been published from many areas for geophysical interpretations (Dudarev, 1964; Fox & Opdyke, 1973; Cornwell, 1975; Jäger & Kopf, 1975; Gupta & Burke, 1977; Mutton & Shaw, 1979; Subrahmanyam & Verma, 1981; Yudin & Katseblin, 1981; Imaoka & Nakashima, 1983). During this time the significance of petrophysical data for the geologic interpretation of geophysical maps has often been emphasized (Lauterbach, 1959; Puranen et al., 1968; Emerson, 1979; Paterson & Reeves, 1985), but in spite of these recommendations, there are relatively few published examples of interpretations based on the synthesis of geophysical, petrophysical and geologic data.

Petrophysical data have also been applied directly to the petrographic classification of rocks and in the qualitative description of rock alteration processes (Kopf, 1976). Density-susceptibility diagrams were used by Henkel (1976) to characterize the magmatic differentiation and serpentinization of rocks. In the serpentinization process the susceptibility of rock (magnetite content) increases, whereas in other hydrothermal alteration processes the susceptibility usually decreases. In fractured zones of bedrock, magnetite can be oxidized into hematite or hydrated to Fe-hydroxide, which decreases the susceptibility of rocks (Henkel & Guzmán, 1977; Criss & Champion, 1984). These alteration products in fracture zones indicate low temperatures, high oxygen fugacities and the presence of water. The regional progression of such alteration processes has been estimated with the aid of susceptibility measurements (Lapointe et al., 1986).

During regional metamorphism rock magnetization commonly increases (Lidiak, 1974; Mutton & Shaw, 1979) so that rocks formed at granulite facies conditions are often most strongly magnetic (Krutikhovskaya et al., 1979). In some contact aureoles around granite intrusions a strongly magnetic zone is observed (Mutton & Shaw, 1979; Speer, 1981). In such zones the conditions of contact metamorphism have thus been favourable for magnetite formation. On the other hand, the progressive deformation of tholeiitic dykes seems to destroy magnetite, decreasing the susceptibility as dolerites are first transformed into metadolerites and finally into amphibolites (Hageskov, 1984). In the early stages of granitization, magnetization of rocks can be slightly increased, while in the final stages it clearly decreases (Krutikhovskaya et al., 1979). In recent studies of granitoids, susceptibility measurements have often been applied, as the proposed relations between magnetic properties and mineralizations of granitoids (Pecherskiy, 1965; Ishihara, 1977) have been tested in practice.

Pecherskiy (1965) reported that the intensity of magnetization in granitoids depends on their level of emplacement. The most magnetic granitoid intrusions were emplaced into a fractured environment at a depth of about 1 km. The magnetization seemed to decrease toward greater depths, and the most weakly magnetic intrusions had been emplaced near the earth's surface. The magnetite content of granitoids was sufficient to explain their magnetization, which was almost independent of the total iron content and petrography of the rocks. Tin deposits were mainly associated with nonmagnetic granitoids and gold deposits with magnetic intrusions. Ishihara (1977) suggested that the granitic rocks could be divided into the magnetite series and ilmenite series granitoids. The magnetite series rocks contain by definition at least 0.1 % of primary magnetite, whereas the ilmenite series granitoids are practically devoid of magnetite. It is thus easy to identify the rocks of these series with the aid of susceptibility measurements.

On the basis of mineral assemblages and ferric/ferrous-ratios of rocks Ishihara (1977) concluded that the magnetite series granitoids were formed in more oxidizing conditions than the ilmenite series rocks. The magnetite series granitoids were possibly generated at great depths (lower crust or upper mantle), where they could avoid the reducing effect of crustal carbon. The oxidation of granitoid magmas could have taken place by dissociation of water and the preferential escape of hydrogen. The ilmenite series granitoids have presumably originated at shallower levels, where the presence of carbonaceous material has prevented their oxidation. Sulfide deposits are mainly found in conjunction with the magnetite series granitoids, whereas tin deposits are associated with the ilmenite series rocks (Ishihara, 1981). The susceptibility measurements can thus be used to estimate the petrogenesis and ore potential of granitic rocks.

In most common rock types, magnetite is the dominant ferrimagnetic (oxide) mineral, and when present it determines both the susceptibility of rocks and the character of magnetic anomalies (McIntyre, 1980). The most important iron sulfide magnetically is ferrimagnetic pyrrhotite, which causes many of the magnetic anomalies associated with black schists and iron-rich sulfide deposits. Compared with magnetite however, pyrrhotite is rather rare, forming under special conditions in geologic units which are of restricted extent in Finland and evidently on a global basis as well (Grant, 1985). Pyrrhotite is petrophysically characterized by high values of Q-ratio and strongly anisotropic susceptibilities (Nagata, 1961). In this work pyrrhotite is only considered in passing with respect to its possible presence in the samples. The physical properties of pyrrhotite-bearing rocks in Finland have been thoroughly reported earlier in connection with a survey of black schists (Kukkonen et al., 1985).

Previous investigations have described qualitatively how the petrophysical character of rocks is changed by geologic processes. The descriptions are based on the relation of density to major mineral composition and particularly on the dependence between ferrimagnetic susceptibilities and the magnetite content of rocks. Less use has been made of the relation between paramagnetic susceptibility and the iron content of rocks, which can also be observed in the susceptibility distributions of geologic units (Chernyuk, 1971; Dortman, 1976; Puranen, 1976). The petrophysical description of geologic processes has mostly remained at a semiquantitative level. More advanced descriptions can be expected only after the development of a systematic methodology, which relates the physical properties of rocks more accurately to their mineralogy and chemistry. Such relations can be determined by the statistical analysis of extensive data, which will be attempted in the present paper.

SAMPLE MATERIAL

This study is based on sample material, which has mostly been collected by geologists during regional mapping of the Finnish bedrock. The distribution of sampling points is shown in Fig. 1. The samples are arbitrarily shaped hand specimens that have been obtained from the outcrops by hammer. The average sample has a weight of 500 g and a volume of 200 cm^3. Most of the samples represent the predominant rock types. The rock types have usually been named after visual inspection of the samples in the field. The samples represent only the exposed bedrock, which comprises less than 3 % of the total area of Finland (Okko, 1964). The sample material is thus to some extent biased, as the samples mainly characterize the most resistant part of bedrock. Additional bias can be caused by the uneven areal distribution of the sampled outcrops within geologic provinces. The results of regional sampling are the main subject of this report, but more local examples from outcrops and drilling-cores are also presented.

Glacial erosion has substantially removed the regolith cover, particularly in southern Finland. Therefore, most of the samples represent fresh rocks, which has also been visually verified. Due to generally weaker glacial erosion and postglacial action of frost, weathered rocks and the preglacial regolith are more common in northern Finland. The effects of weathering are demonstrated by susceptibility and density measurements of core-samples drilled from the Nattanen granite in Sodankylä, Lapland (see Fig. 2). The susceptibilities show more variation and lower values in the topmost 50 meters of the drilling-core compared with the deeper sections. Similarly, in the topmost part of the core the density values are lower than in the deeper parts. These systematic differences are due to local weathering of the surficial bedrock, which is also recorded visually as a change in the colour of granite. Microscopic observations revealed that magnetite was locally martitized to hematite, which often decreases the susceptibility values as reported by Henkel & Guzmán (1977).

The regional sample material is represented with the aid of ten example rock types, which were selected for the purpose of demonstrating susceptibility variations in the bedrock of Finland. These rock types (and numbers of samples) are granite (4244), granodiorite (3030), quartz diorite (1133), diorite (596), gabbro (1288), quartzite (2745), quartz-feldspar schist/gneiss (758), mica schist/gneiss (5553), amphibolite (1951) and (meta)diabase (2151). The lithologies thus represent magmatic, sedimentogenous and metamorphic origin and the compositions vary from acid to basic. Reasonable amounts of chemical and

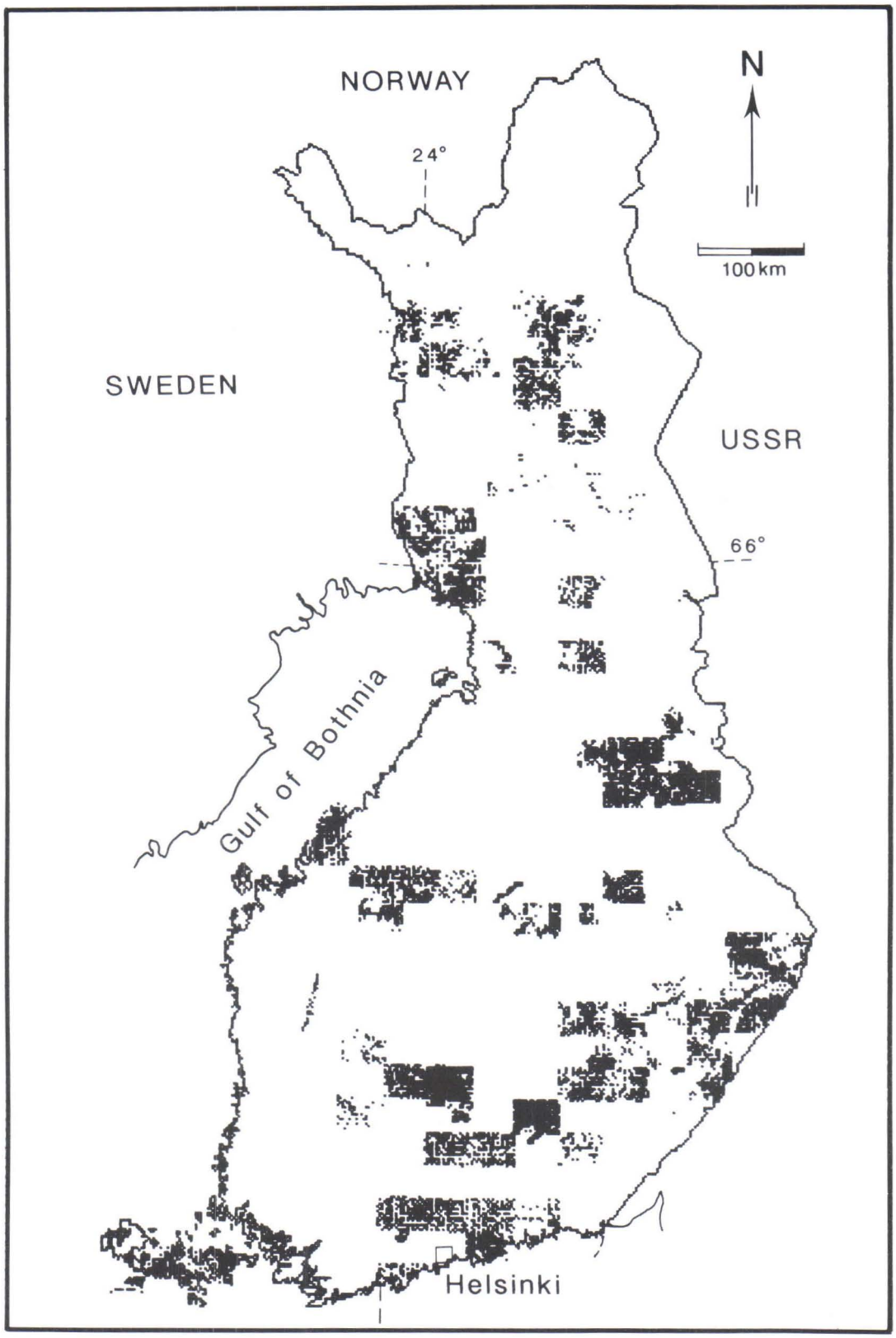

Fig. 1. Areal distribution of petrophysical sample material in Finland (41 696 samples).

mineralogic data are available from Finland for these rock types, which also areally comprise the bulk of Finnish bedrock (cf. Simonen, 1980). The areal coverage is further improved by inclusion of the rapakivi varieties of southern Finland and the greenstones of northern Finland, which are treated in this report, too.

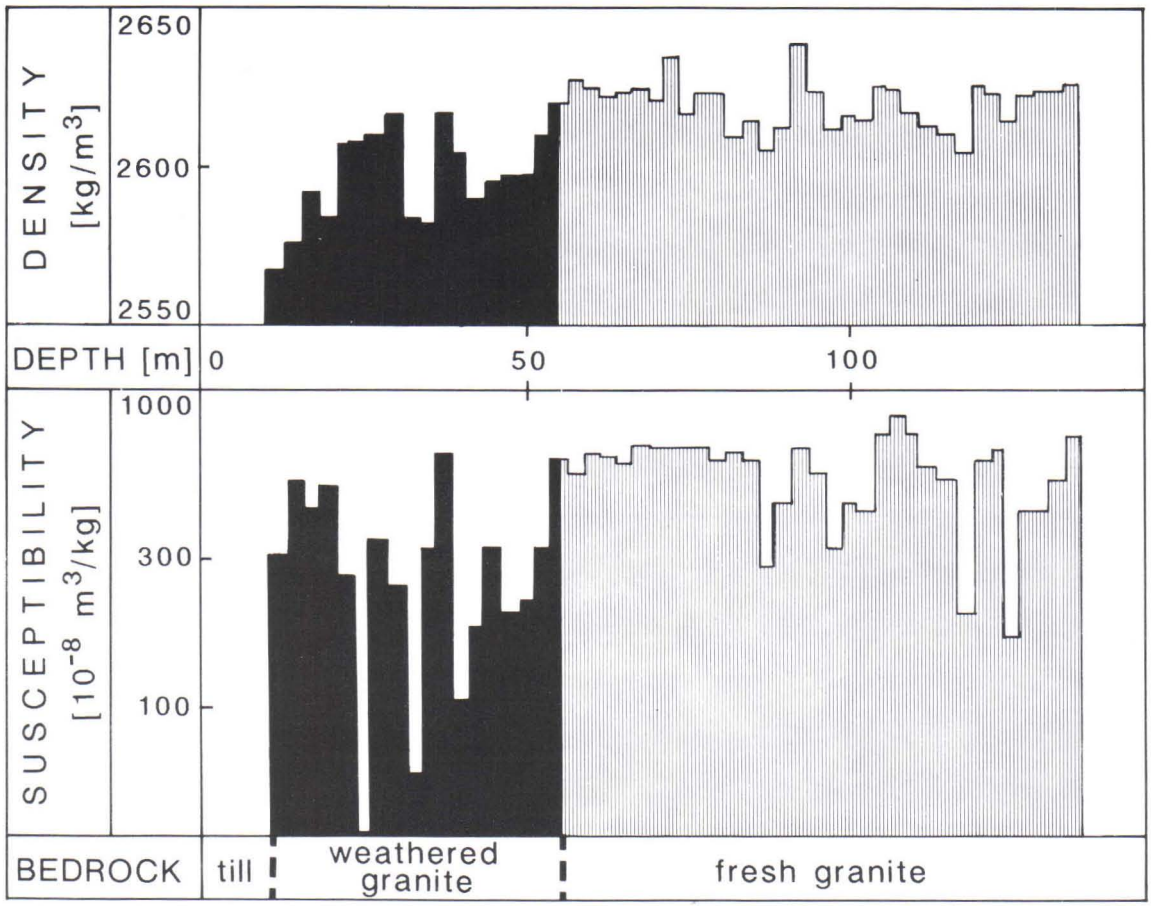

Fig. 2. Effect of weathering on susceptibility and density profiles measured from drill-core samples of Nattanen granite from northern Finland (cf. Fig. 11).

With the aid of example lithologies the sample material is divided into more homogeneous strata, which reduces the petrophysical variation and simplifies the petrologic interpretation of results. The interpretations naturally also require information on the chemical and mineralogic composition of the example rock types. Chemical data were collected from published reports (Lokka, 1934; Lokka, 1950) and from the open data register, which contains the results of classical silicate analyses made at GSF during the years 1957—1981. The samples chemically analysed provide a reasonable areal coverage of Finland. Mineralogic data for the example lithologies were obtained from the modal analyses that have been published by GSF in the explanations to the geologic maps of Finland. These references have been listed in Appendix A, which also describes the areal distribution of mineralogic data according to map sheets. The combined treatment of various data was made with a microcomputer after creation of data bases, which contain the results of about 600 chemical and 900 modal analyses of the example rock types.

MEASURING APPARATUS

All results of measurements are expressed in SI-units in this report. It is practical to express susceptibilities with respect to mass units when studying their relationship to the chemical composition (weight %) of rocks. The mass susceptibility is often also referred to as specific susceptibility. The unit of mass susceptibility is m^3/kg or the inverse unit of density, because the volume susceptibility is a dimensionless quantity in the SI-system.

Correspondingly, the unit Am^2/kg is obtained for the specific intensity of remanent magnetization, which will be abbreviated here to mass remanence. In geophysical interpretations it is more practical to use volume susceptibilities, because geological bodies are generally described by volumes in the interpretation formulae. The statistics of effective and bulk susceptibilities, which will be presented for interpretation purposes (see Table 5), are expressed with respect to volume units.

Almost all of the susceptibility data treated in this work have been measured with two instruments that have both analysed about 20 000 samples. During the years 1965—1975 a commercial meter (Magnetic Susceptibility Bridge Model MS-2, manufacturer: Geophysical Specialties Co., USA) was used. The operation principles of this instrument (AC-bridge) are described in detail by Mooney (1952). For the measurement of hand specimens an outer coil (diameter = 100 mm, height = 73 mm) was constructed at GSF for the AC-bridge. The commercial instrument was replaced in 1975 by a more sensitive susceptibility bridge K-3A, which was designed and built at GSF (Puranen & Puranen, 1977). The meter K-3A can be used for the determination of anisotropic susceptibility as well, because the measuring field in this low-field AC-bridge is homogeneous. Susceptibilities have also been measured directly on some outcrops with a portable meter constructed at GSF. This meter is in principle a resonance bridge (Westerlund, 1973), and its sensing element is a thin surface coil with a diameter of about 230 mm.

In the case of weakly magnetic samples (susceptibility below $50 \cdot 10^{-8}$ m^3/kg), the standard errors of repeated measurements are about 10^{-8} and 10^{-9} m^3/kg for the susceptibility meters MS-2 and K-3A, respectively. When more strongly magnetic samples are measured, the relative standard errors are correspondingly 5 % and 2 %. The relative errors are largely due to the varying position of arbitrarily shaped hand specimens and their ferrimagnetic inclusions within the measuring coils. The effect of shape demagnetization in the most strongly magnetic samples is also corrected for. The correction is calculated using the demagnetization coefficients of rotational ellipsoids, which are fitted to the samples by length and volume. The precision of the portable susceptibility meter is about $5 \cdot 10^{-8}$ m^3/kg. According to measurements of standard materials (paramagnetic salts), the absolute measuring error with the susceptibility bridge K-3A is lower than 2 %. The susceptibility meters MS-2 and K-3A give average results that are consistent within ± 5 %.

The susceptibility data will be related to the chemical and mineralogic composition, magnetite content, density and remanent magnetization of rocks. The estimates of chemical composition are based on classical silicate analyses, which also provide a value for the ferric/ferrous ratio or the oxidation ratio of iron. The estimates of mineralogic composition are based on the results of modal analyses determined by counting at least 1 000 points per sample. The magnetite content in some samples was measured with a saturation magnetization analyser (Satmagan apparatus, manufacturer: Outokumpu Oy, Finland). The manufacturer states that the amount of magnetic material with constant saturation magnetization can be measured to an accuracy of 0.1 weight %. The Satmagan apparatus has been described in detail by Laurila (1964).

Rock densities have been determined by weighing the samples in air and water. The weighing accuracy is 0.1 g and the standard error of repeated density determinations is less than 2 kg/m^3. The determinations are made on dry samples, which causes underestimation of densities due to porosity. The porosity of crystalline rocks is, however, low and usually varies in the range 0—3 % (Wenk & Wenk, 1969). Hence, for crystalline rocks the systematic density error caused by porosity is generally lower than 1 % (Henkel, 1976).

The intensity of remanent magnetization has been measured with two instruments (R1 and R2) both assembled at GSF. In these instruments the measuring space is shielded with two Mu-metal cylinders (diameter about 20 cm, length 80 cm). The magnetic field strength in the shielded space is less than 50 nT. The control electronics and sensor unit (two fluxgate elements) of the first meter R1 were constructed at GSF (Puranen, 1978). In the later model R2 (Puranen & Sulkanen, 1985) a commercial fluxgate magnetometer (DM-2220, manufacturer: Schonstedt Instrument Co., USA) is used as the sensor. The remanence error is less than 10 %, when the meter R1 is used for measurement of average samples (weight 500 g) whose intensity of remanence exceeds the threshold value $40 \cdot 10^{-6}$ Am^2/kg. The corresponding threshold is $20 \cdot 10^{-6}$ Am^2/kg for the meter R2. The remanence results of this report are based on approximately 15 000 measurements with the meter R1 and 5 000 determinations with the meter R2. Since 1983 the susceptibility, density and remanence measurements have been carried out in a computer-controlled laboratory described by Puranen and Sulkanen (1985).

SUSCEPTIBILITY DISTRIBUTIONS

The forms of susceptibility distributions have been studied in connection with early paleomagnetic work (Irving et al., 1966; Tarling, 1966), magnetic interpretations (Puranen et al., 1968; Henkel, 1976) and geologic applications (Dudarev, 1964; Chernyuk, 1971; Magnusson, 1983). The frequency distributions of susceptibilities are asymmetric and positively skewed when viewed on arithmetic susceptibility scales. On logarithmic scales the distributions are more symmetric, which means that they resemble more closely lognormal than normal distributions (Irving et al., 1966; Tarling, 1966; Puranen et al., 1968). The susceptibility distributions are often bimodal (Dudarev, 1964; Puranen et al., 1968) and in the case of basic rock types even multimodal (Henkel, 1976). The bimodal distributions of intrusive rocks show a susceptibility peak at low values, caused by paramagnetism of mafic minerals, and a mode at higher susceptibilities due to the presence of ferrimagnetic minerals (Chernyuk, 1971). This interpretation is in harmony with the results obtained from the igneous rocks of Finland (Puranen, 1976).

The susceptibility of rocks can be determined as the weighted sum of mineral susceptibilities with the mineral fractions as weights. The most common felsic minerals are quartz and feldspars, which are diamagnetic. Their susceptibility values are negative with the orders of magnitude 10^{-8} m³/kg (Schön, 1983). The most important mafic minerals — micas, amphiboles and pyroxenes — are paramagnetic and have susceptibilities varying in the range $(10—50) \cdot 10^{-8}$ m³/kg depending on iron content (Vernon, 1961). The most magnetic as well as the most common ferrimagnetic mineral is (titano)magnetite with typical susceptibilities of about $100\,000 \cdot 10^{-8}$ m³/kg. The (approximate) susceptibilities of other ferrimagnetic minerals, such as hematite ($100 \cdot 10^{-8}$ m³/kg) and pyrrhotite ($10\,000 \cdot 10^{-8}$ m³/kg), are clearly lower (Schön, 1983). Negative susceptibilities are thus expected for a rock that contains more than 95 % diamagnetic minerals and no ferrimagnetic minerals. Low positive susceptibilities (below $50 \cdot 10^{-8}$ m³/kg) should characterize a rock that contains more than 5 % paramagnetic minerals without magnetite. In rocks containing more than 0.1 % magnetite, the susceptibility value should be higher than $100 \cdot 10^{-8}$ m³/kg, the value being proportional to the amount of magnetite.

Frequency distributions of susceptibilities in Finnish rocks will next be considered with the aid of data contained in the petrophysical register of GSF. The susceptibility distribution of all samples in the register (irrespective of rock type) is shown using an arithmetic susceptibility scale in Fig. 3A and with a logarithmic scale in Fig. 3B. The arithmetic diagram is asymmetric and positively skewed consistently with the results published earlier. The distribution diagram is more symmetric when the data is presented on logarithmic scale. The logarithmic diagram is composed of two parts. A dominant maximum is located at low susceptibility values around $(10—15) \cdot 10^{-8}$ m³/kg, and a weaker but broader frequency plateau extends towards higher susceptibilities. The dominant maximum can be explained either by paramagnetic mafic minerals or by small amounts of ferrimagnetic magnetite. The broad susceptibility plateau at higher values is caused by samples with widely varying magnetite contents. The effect of other ferrimagnetic minerals like hematite and pyrrho-

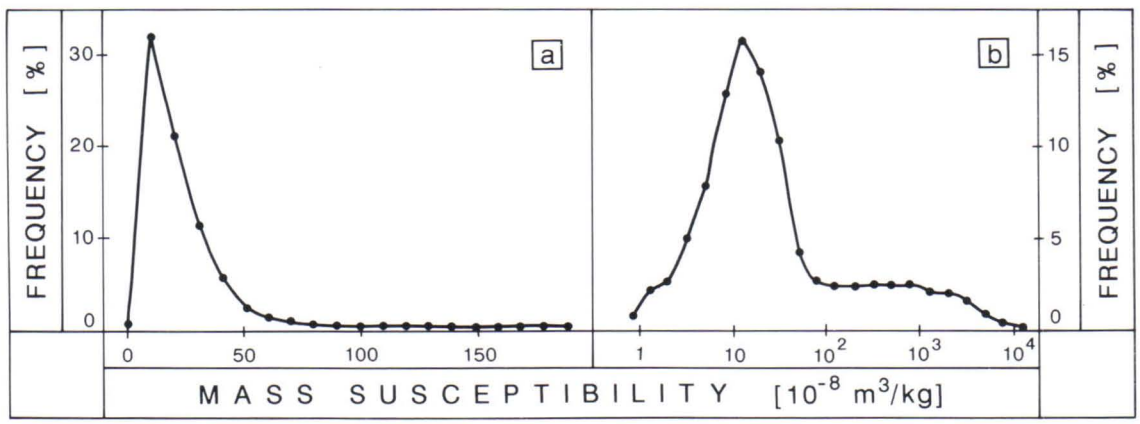

Fig. 3. Frequency distributions of susceptibilities presented on A) arithmetic and B) logarithmic susceptibility scales. Both distributions are based on 41 696 samples from the petrophysical register, and are truncated at left and right margins.

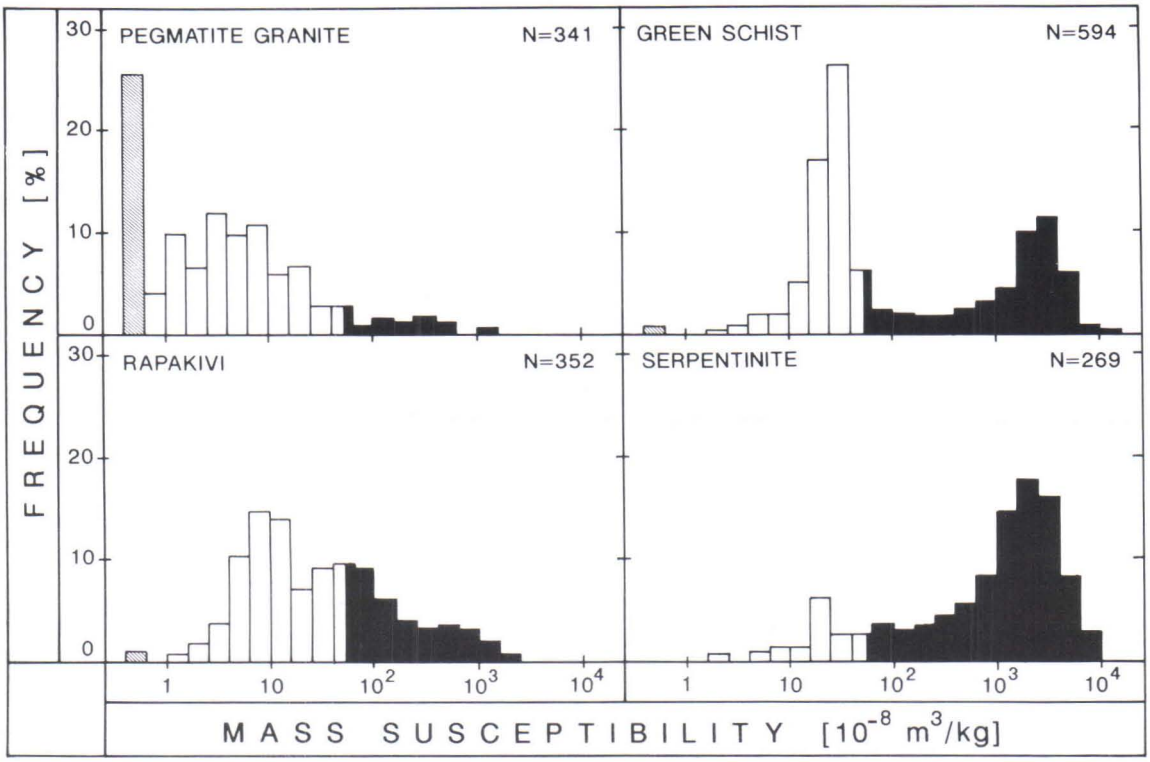

Fig. 4. Frequency histograms of susceptibility for magnetically different rock types divided into dia- (grey), para- (white) and ferrimagnetic (black) parts. Susceptibility value 0 separates dia- and paramagnetic parts, and value $50 \cdot 10^{-8}$ m³/kg distinguishes para- and ferrimagnetic parts. Left- and rightmost classes of histograms are open, and N = number of samples.

tite should be negligible in the example rocks of this work, because these minerals are magnetically weak and rare in the most common rock types (Grant, 1985).

The logarithmic susceptibility scale is applied in Figures 4—6 because it is more practical than the arithmetic scale for the presentation of broad distributions. The rock types of Fig. 4 have been chosen so that proportions of dia-, para- and ferrimagnetic mineral components vary from one histogram to the next. Negative and zero susceptibilities indicate the dominance of diamagnetic minerals, and higher positive values imply the presence of ferrimagnetic minerals. The susceptibility peak in the intermediate range $(0—50) \cdot 10^{-8}$ m³/kg may be caused by either paramagnetic or ferrimagnetic minerals, but the peak is tentatively described as the paramagnetic maximum. The susceptibility histogram for pegmatite granites (Fig. 4) shows a clear diamagnetic peak, a dominant paramagnetic maximum and a weak ferrimagnetic tail. The paramagnetic samples still predominate in the histogram of Lapland greenstones, but the ferrimagnetic samples with magnetite also produce a strong maximum. The ferrimagnetic maximum becomes dominant in the serpentinite histogram, while the proportion of paramagnetic samples is very low. The histogram for rapakivi varieties contains both paramagnetic and ferrimagnetic maxima, which are both fairly strong and so close to each other that their discrimination is difficult.

The susceptibility histograms of all example rock types (Figures 5 and 6) show a major paramagnetic maximum, and a minor ferrimagnetic tail located at higher susceptibility values. The density distributions, which characterize the chemical composition of rocks (Henkel, 1976) and the amount of mafic minerals (Puranen et al., 1978), are shown alongside the susceptibilities. The change toward more basic composition of rocks is reflected in the density histograms as a movement of frequency maxima toward higher densities. A corresponding displacement is also observed in the susceptibility histograms, whose paramagnetic maximum is shifted toward higher values in the basic rocks. The total shift of the paramagnetic maximum is about $20 \cdot 10^{-8}$ m³/kg and the density growth is approximately 300 kg/m³. In principle, the susceptibility shift could be caused by a small increase (about 0.02 wt %) in the magnetite content. Such a small addition of magnetite cannot however, explain the observed density growth from 2 600 to 2 900 kg/m³.

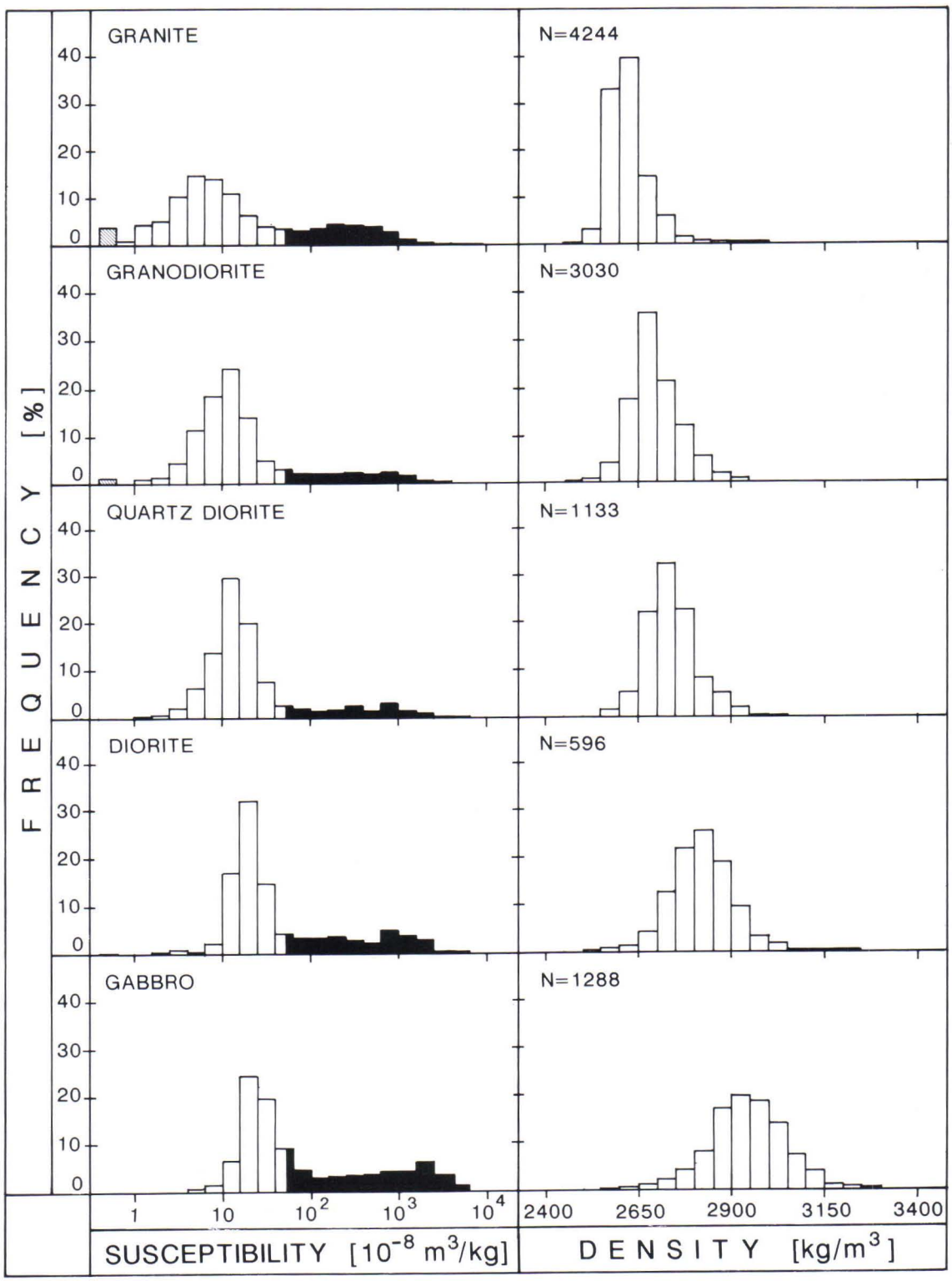

Fig. 5. Frequency distributions of susceptibility and density for igneous rock types. Additional explanations as in Fig. 4.

The density increase clearly indicates a corresponding increase in the amount of mafic minerals, which also means that the iron content of the rocks increases. The values of paramagnetic susceptibility are proportional to the amount of iron and, as will be shown later, the variation in iron content of the example rocks is large enough to cause the observed susceptibility shift. For now we merely conclude that the concomitant increase in densities and susceptibilities can be explained by the increasing amount of paramagnetic mafic minerals. In addition, the susceptibility histograms of sedimentogenous and meta-

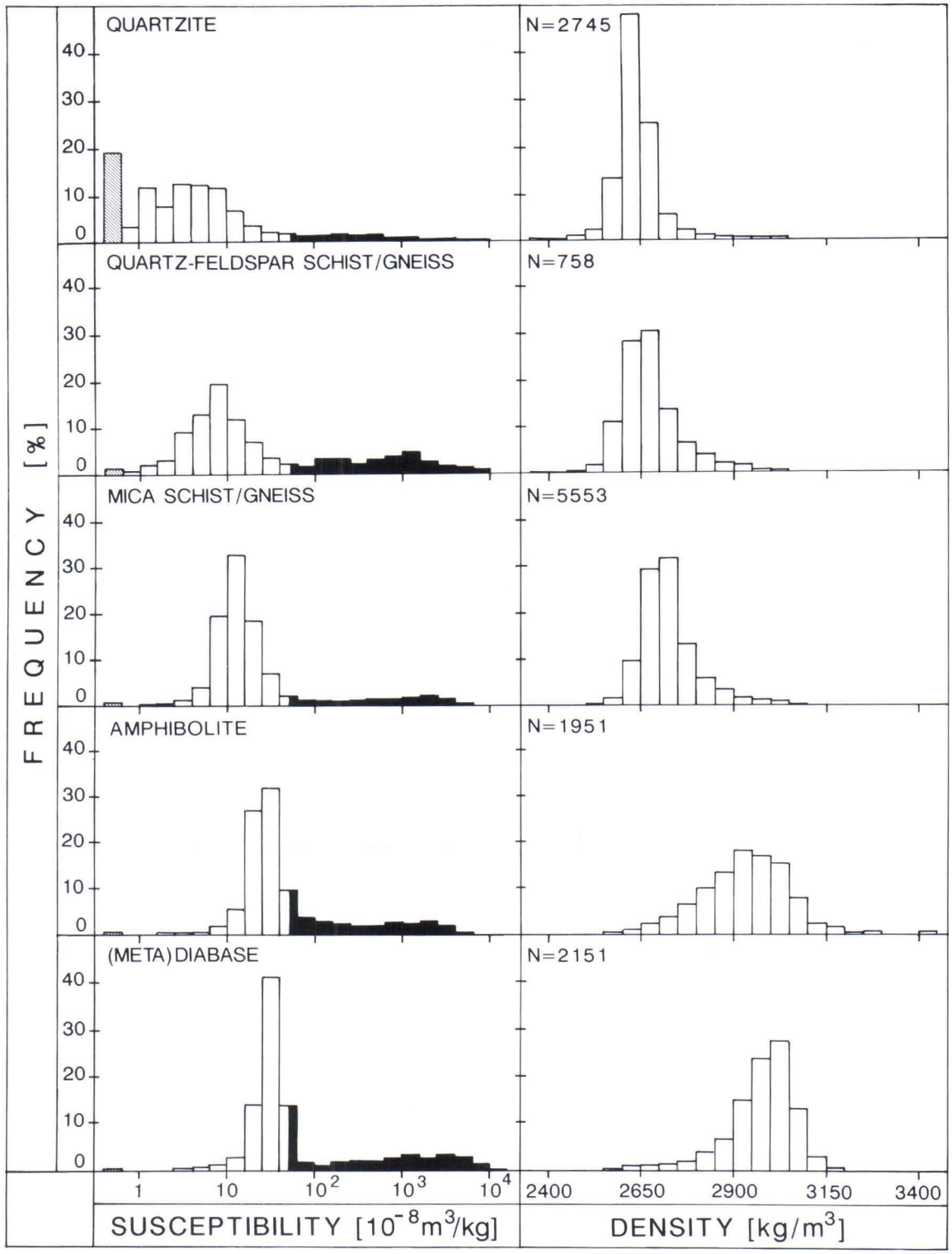

Fig. 6. Frequency distributions of susceptibility and density for sedimentogenous and metamorphic rock types. Additional explanations as in Fig. 4.

morphic rocks (Fig. 6) show a diamagnetic peak in the case of quartzites. In all example rock types the group of paramagnetic samples is largest, the ferrimagnetic group comes next and the diamagnetic samples remain a minority. The proportions of these groups can be seen more precisely in the cumulative histograms of Fig. 7. The proportion of ferrimagnetic samples is at a minimum in the quartzites (about 10 %) and maximum in the gabbros (over 40 %). Diamagnetic samples constitute almost 20 % of the quartzites, whereas other example rock types are practically devoid of purely diamagnetic samples.

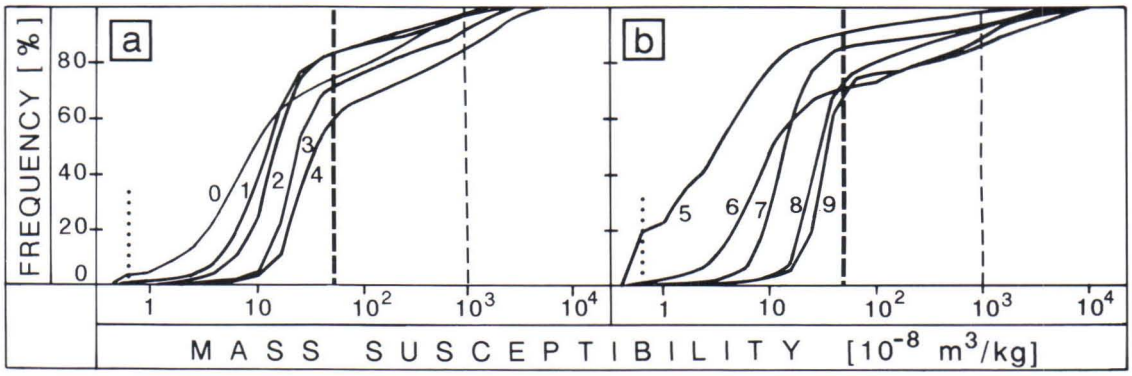

Fig. 7. Cumulative frequency distributions of susceptibility for A) igneous and B) other example rocks. Rock type codes are 0 = granite, 1 = granodiorite, 2 = quartz diorite, 3 = diorite, 4 = gabbro, 5 = quartzite, 6 = quartz-feldspar schist/gneiss, 7 = mica schist/gneiss, 8 = amphibolite, 9 = (meta)diabase. Numbers of samples as in Figures 5—6. Dotted lines separate dia- from paramagnetic data, and thick dashed lines para- from ferrimagnetic data (cf. Fig.4). Thin dashed lines mark magnetite content of about 1.5 wt % (cf. Fig. 11).

Let us finally examine at what areal scale the different kinds of susceptibilities can be identified. Strong susceptibility variations have been reported even at single outcrops within short distances of some meters (Mooney & Bleifuss, 1953; Magnusson, 1983). The susceptibility variations on granitoid and mica shist outcrops in the Hyvinkää-Riihimäki area are demonstrated by the histograms in Figures 8 and 9. The volume susceptibilities measured directly on the outcrops have been transformed into mass susceptibilities using average densities, which were determined for each outcrop with the aid of 10 samples. The length of all outcrops studied was less than 100 meters and the distance between outcrops was typically a few kilometers. The susceptibility histograms of most outcrops show only one frequency maximum, located at either low or high susceptibilities. When the histograms of individual outcrops are combined into a common histogram for the whole area, the resulting distribution is bimodal for both the granitoids and the mica schists. In this case the bimodality is mainly caused by the variation between the outcrops over a distance of some kilometers.

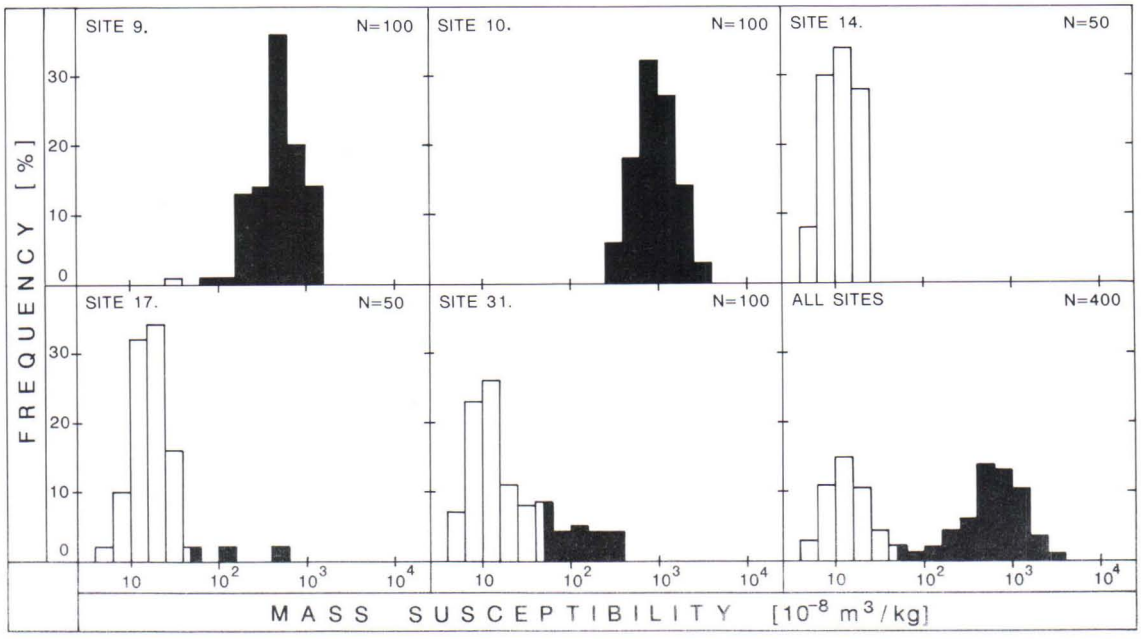

Fig. 8. Typical susceptibility distributions from granitoid outcrops in the Hyvinkää area. Additional explanations as in Fig. 4.

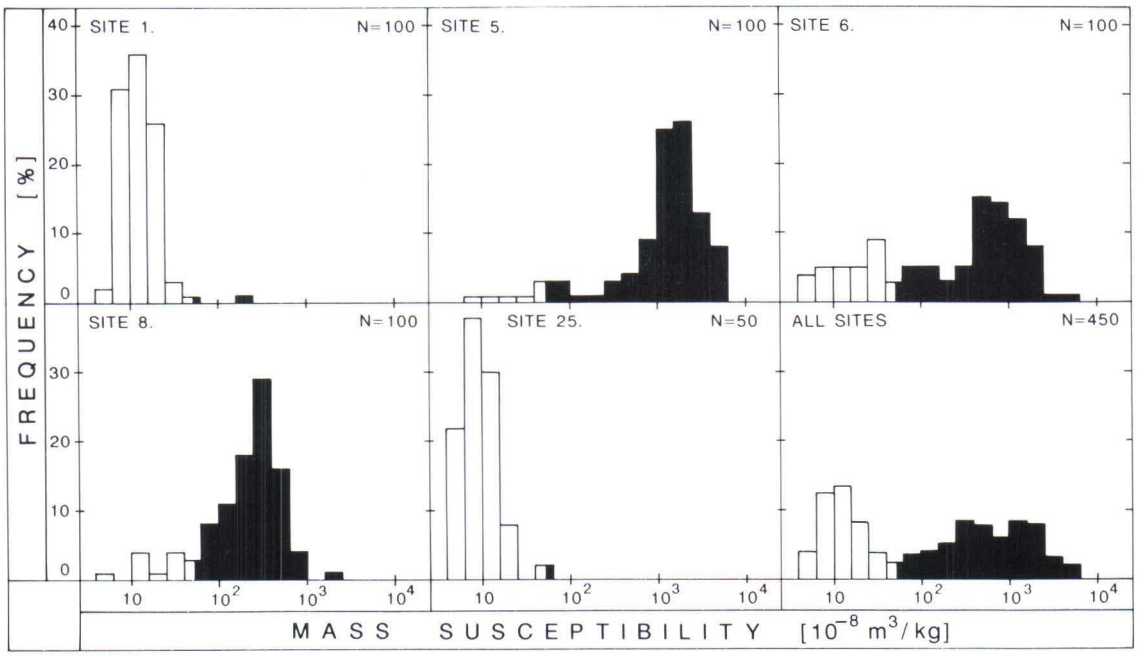

Fig. 9. Typical susceptibility distributions from mica schist outcrops in the Hyvinkää area. Additional explanations as in Fig. 4.

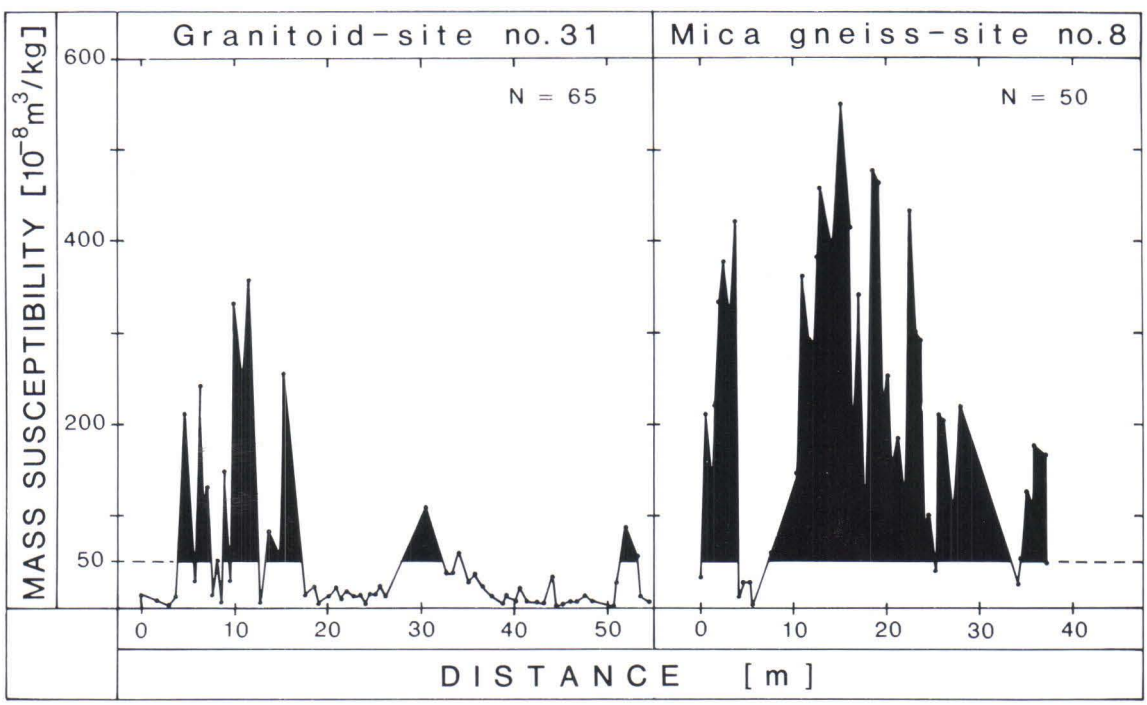

Fig. 10. Susceptibility profiles for two example outcrops from the Hyvinkää area. Ferrimagnetic parts are black and N = number of measurements.

The susceptibility profiles from two example outcrops (Fig. 10) show great variations even between adjacent points of the profiles separated by only a few meters. Variation mainly takes place within ferrimagnetic values on the mica gneiss outcrop, reflecting changes in the magnetite content. At the granitoid site, susceptibilities vary back and forth between paramagnetic and ferrimagnetic values. This means that conditions have changed between adjacent points from favourable to unfavourable for magnetite formation (or preservation). Because changes in pressure and temperature are expected to be gradual and con-

tinuous, they cannot account for these abrupt jumps in conditions. Suitable PT-conditions are naturally required as a prerequisite for magnetite formation, but the decisive differences between adjacent sample points probably reside in rock composition and oxygen fugacity, which are interrelated and can vary strongly even within short distances.

FERRIMAGNETIC SUSCEPTIBILITIES

The most common application of susceptibility measurements is in the estimation of magnetite content. This is understandable since ferrimagnetic magnetite is an ore mineral and also the most wide spread iron oxide in bedrock. The relationship between susceptibility and magnetite content had already been investigated both theoretically and experimentally in the 1940's (Puzicha, 1942; Werner, 1945). Subsequently, the relation has been determined for several rock types (Mooney & Bleifuss, 1953; Balsley & Buddington, 1958; Puranen et al., 1968; Pesonen & Stigzelius, 1972). This relationship, which has usually been expressed in volume units, has proven to be approximately linear for low concentrations of magnetite. Volume susceptibilities have varied in the range $(3\ 200—3\ 800) \cdot 10^{-5}$ SI-units for rocks containing 1 volume % of magnetite. By using the known density of magnetite (5 200 kg/m^3), the relation can be transformed into the following average dependence

$$W_m = 1.5 \cdot 10^{-3} \cdot X \qquad (1)$$

between magnetite content W_m (weight %) and mass susceptibility X (10^{-8} m^3/kg).

The susceptibility-magnetite relation has also been studied from till samples of northern Finland (Puranen, 1977; Pulkkinen et al., 1980). Tills are representative of the underlying bedrock, from which they have been crushed by glaciers. In the studies of tills the magnetite content was determined with a saturation magnetization analyser (Laurila, 1964), which requires powdered samples. The till samples could thus be measured directly as such without grinding contamination. High correlation coefficients characterized the susceptibility-magnetite relations, which were tightly linear. Depending on the till fraction and investigation area, the relations could be described with regression lines, whose slope coefficients varied in the range $(1.3—1.7) \cdot 10^{-3}$, in good accordance with formula (1). The coefficients tended to increase slightly as the grain size of till decreased, which might be due to the lower susceptibility of fine grained magnetite (Pulkkinen et al., 1980). Susceptibility distributions further indicated (Puranen, 1977) that the most common grain size range of magnetite in till was 0.06—0.2 mm, consistently with the microscopically estimated average grain size of magnetite in igneous rocks (Feniak, 1944).

The magnetic investigations of tills in Lapland have since been extended to several other parts of Finland (Fig. 11A), utilizing samples of both till and powdered rock in the grain size range 0.06—0.6 mm. These more recent studies also produce linear susceptibility-magnetite relations as demonstrated by examples from the Hyvinkää gabbro (Fig. 11B) and Poksaselkä tills (Fig. 11C). The summary of new results (Table 1) gives the value $1.48 \cdot 10^{-3}$ for the average slope coefficient of regression lines, which is in good agreement with both earlier results and with formula (1). The regression coefficients show some variation according to (areal) composition and grain size of magnetite, but the average relation (1) should be accurate enough for most practical comparisons of magnetite content. On the basis of formula (1), rock samples contain about 1.5 wt % of magnetite if their mass susceptibility is $1\ 000 \cdot 10^{-8}$ m^3/kg. This susceptibility limit is exceeded by less than 10 % of example rock types (see Fig. 7). Therefore, most ferrimagnetic samples contain magnetite less than 1.5 wt %, and about 60—80 % of all samples are so weakly magnetic that they can be regarded as diamagnetic or paramagnetic.

The extrinsic mass suceptibility of coarse (diameter about 0.1 mm) grains of pure magnetite is $0.53 \cdot 10^{-3}$ m^3/kg, according to theoretic considerations by Stacey & Banerjee (1974) and experimental work by Parry (1965). If low concentrations of such magnetite are dispersed in a non-magnetic matrix, the theoretic relation $W_m = 1.88 \cdot 10^{-3} \cdot X$ is obtained between magnetite content W_m (wt %) and mass susceptibility X (10^{-8} m^3/kg) of the mixture. The theoretic coefficient $1.88 \cdot 10^{-3}$ is higher than the experimental estimates presented above, which could be due to impurities of magnetite as proposed by Pulkkinen

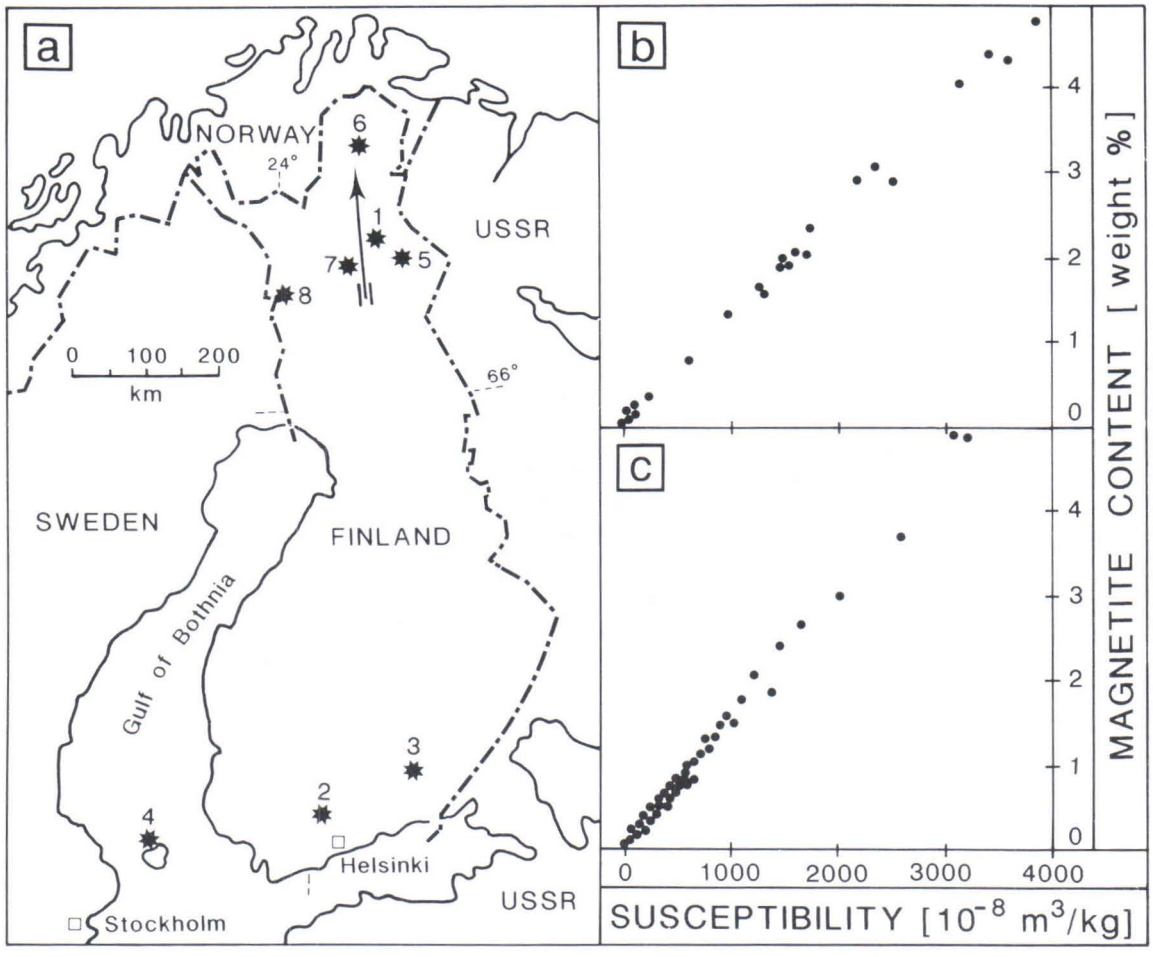

Fig. 11. Dependence between mass susceptibility and magnetite content. A) Location of investigation areas and example results from B) Hyvinkää gabbro powder and C) Poksaselkä glacial till (cf. Table 1). Localities are 1 = Nattanen, 2 = Hyvinkää, 3 = Lovaskoski, 4 = Geta, 5 = Lokka, 6 = Kaamanen, 7 = Poksaselkä and 8 = Rautuvaara.

Table 1. Relations between mass susceptibility X (10^{-8} m^3/kg) and magnetite content W_m (weight %) in samples of glacial till and rock powder from eight investigation areas (see Fig. 11). Relations are described with correlation coefficients R and regression lines $W_m = A + B \cdot X$ fitted to N observations.

STUDY AREA	SAMPLE MATERIAL	GRAIN SIZE (mm)	REGRESSION PARAMETERS			
			$A \cdot 10^3$	$B \cdot 10^3$	R	N
Nattanen	Granite powder	0.06—0.60	20.5	1.44	0.990	19
Hyvinkää	Gabbro powder	0.06—0.60	68.0	1.25	0.998	26
Lovaskoski	Diabase powder	0.07—0.25	291	1.39	0.987	33
Geta	Rapakivi powder	0.06—0.60	5.0	1.36	0.997	14
Lokka	Till fraction	0.06—0.25	24.8	1.60	0.960	38
Kaamanen	Till fraction	0.06—0.25	33.7	1.52	0.950	107
Poksaselkä	Till fraction	0.06—0.25	42.1	1.49	0.997	96
Rautuvaara	Till fraction	0.06—0.20	6.6	1.75	0.999	40

et al. (1980). If this interpretation is correct, then magnetite grains seem to contain more impurities in the bedrock of southern Finland than in Lapland. This conclusion is based on the fact that regression coefficients (Table 1) are systematically somewhat lower for the powdered rock samples of southern Finland $(1.25—1.44) \cdot 10^{-3}$ than for the till samples of Lapland $(1.49—1.75) \cdot 10^{-3}$. Alternatively, the difference could be due to artificial grinding of rock samples or to areal variations in the grain size spectrum of magnetite.

PARAMAGNETIC SUSCEPTIBILITIES

The paramagnetic susceptibilities of mafic silicates (biotite, amphibole, pyroxene, olivine) were actively studied during the 1950's (Nagata et al., 1957; Akimoto et al., 1958; Chevallier & Mathieu, 1958; Chevallier & Martin, 1959; Syono, 1960). Studies were summarized by Vernon (1961), who also presented new data on biotites and amphiboles. According to these works the paramagnetic susceptibility obeys Curie's law and is dependent on the abundance of paramagnetic ions (Fe^{2+}, Fe^{3+}, Mn^{2+}) in the mafic minerals. In most rock types the main paramagnetic ion is Fe^{2+}. For substances that obey the Curie's law, the specific susceptibility X can be calculated by the relation

$$X = u_o u_B^2 n p^2/(3kT) \quad (2)$$

where u_o = permeability of vacuum, u_B = Bohr magneton, n = number of atoms per unit mass, p = effective Bohr magneton number, k = Boltzmann's constant and T = absolute temperature.

The effective Bohr magneton number has been experimentally determined, yielding the result $p^2 = 28.7$ for the ion Fe^{2+}, and $p^2 = 34.0$ for ions Fe^{3+} and Mn^{2+} (Bleaney & Bleaney, 1976). After insertion of the room temperature (T = 298 K) and the constant values into formula (2), the mass susceptibility X_i (10^{-8} m^3/kg) can be expressed with the aid of the abundances of paramagnetic ions W_i (wt %) by the following numerical relations

$$X_{Fe2} = 2.71 \cdot W_{Fe2} \quad (3)$$

$$X_{Fe3} = 3.21 \cdot W_{Fe3} \quad (4)$$

$$X_{Mn2} = 3.26 \cdot W_{Mn2} \quad (5)$$

The mass susceptibility of mafic silicates is then obtained as the sum $X_{Fe2} + X_{Fe3} + X_{Mn2}$. In order to calculate the susceptibilities of mafic minerals, data would be needed on their chemical composition. Because such data are only scarce in Finland, the paramagnetic susceptibilities of rocks will not be calculated from their mineralogic composition but according to their total iron content.

The abundances of paramagnetic ions in the example rock types are statistically summarized in Table 2, based on silicate analyses of rocks. The chemical data were also used to calculate a theoretic value of paramagnetic susceptibility for each sample with the aid of formulae (3)—(5). The calculated susceptibilities may be somewhat overestimated, because they are based on the iron content of both silicates and oxides. However, for most of the example rock types, magnetite (iron oxides) is present in less than 30 % of the samples and abundantly present (over 1.5 wt %) in less than 10 % of sample material (see Fig. 7). Therefore, iron oxides should cause only small errors in the calculated values of paramagnetic susceptibilities, and the possible errors should be observed by comparisons of theoretic with measured susceptibilities.

Table 2. Averages M and standard deviations S for abundances of paramagnetic ions (wt %) in example rock types, and mean values of oxidation ratio $Ox = W_{Fe3}/(W_{Fe2} + W_{Fe3})$ and coefficient $C = 1/(2.71 + Ox/2)$ for formula (6). Rock type codes as in Fig. 7 and N = number of samples.

ROCK TYPE	Mn^{2+} (%)		Fe^{2+} (%)		Fe^{3+} (%)		Fe(%) sum	Ox (—)	C (—)	N (—)
	M	S	M	S	M	S				
0	0.03	0.04	1.29	0.96	0.68	0.68	1.97	0.35	0.347	120
1	0.06	0.03	2.50	1.23	0.81	0.61	3.31	0.24	0.353	48
2	0.05	0.05	3.60	1.38	0.83	0.53	4.43	0.19	0.356	34
3	0.10	0.08	4.99	1.19	1.19	0.65	6.18	0.19	0.356	33
4	0.10	0.08	6.02	2.05	1.27	0.83	7.29	0.17	0.358	74
5	0.02	0.04	0.75	1.45	0.86	1.42	1.61	0.53	0.336	31
6	0.04	0.04	2.35	1.51	0.58	0.43	2.93	0.20	0.356	26
7	0.05	0.03	4.05	1.80	1.37	1.53	5.42	0.25	0.353	54
8	0.11	0.07	6.31	2.23	1.52	1.25	7.83	0.19	0.356	57
9	0.14	0.13	7.44	3.07	2.30	1.54	9.74	0.24	0.353	94
M	0.07		3.93		1.14		5.07	0.26	0.352	

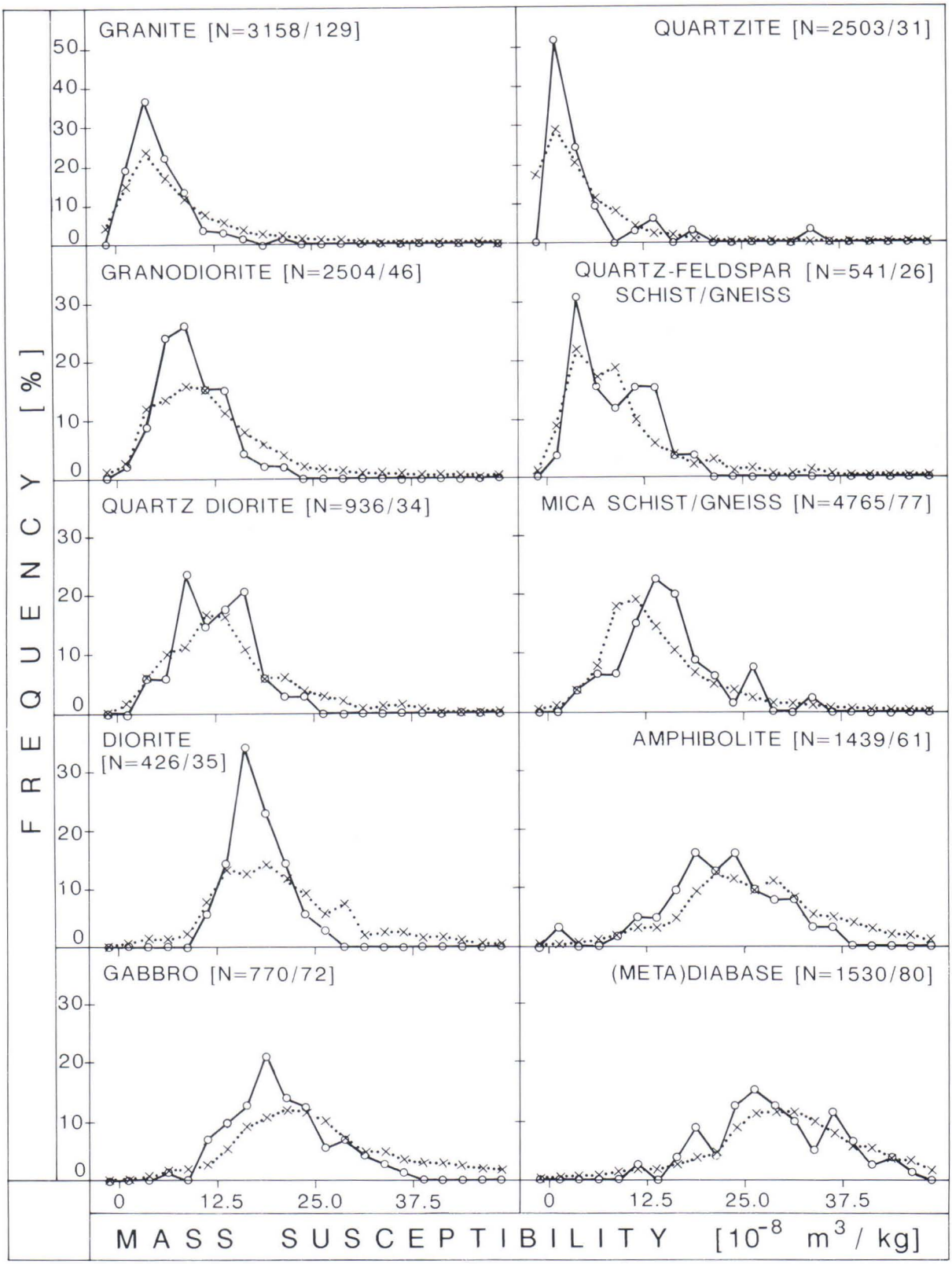

Fig. 12. Frequency diagrams of paramagnetic susceptibilities based on measurements of example rocks (crosses) and calculated from chemical analyses (circles). Leftmost class is open and arithmetic susceptibility scale is truncated at $50 \cdot 10^{-8}$ m³/kg corresponding to about 18 wt % of iron. N = number of susceptibility measurements/chemical analyses.

The frequency diagrams for calculated and measured values of paramagnetic susceptibilities are compared in Fig. 12. The measured curves show smoother variations than the theoretic diagrams, which is probably due to the fact that the measured curves are based on much larger data. The theoretic peaks are sharper than the measured modes particu-

larly in the case of igneous rocks. This possibly reflects the precision of rock classification, which is better in the theoretic case because of the known chemistry. The modes of measured and theoretic diagrams are located rather close to each other for all rock types, although perfect congruence is not to be expected, the diagrams being based on different samples from somewhat different locations. On the whole however, the measured and theoretic susceptibility curves of Fig. 12 show quite good agreement.

The preceding data indicate that for weakly magnetic rocks, susceptibilities (below $50 \cdot 10^{-8}$ m³/kg) are dominantly due to paramagnetism of mafic silicates, and this interpretation will be later confirmed by density and remanence data. Therefore, the paramagnetic susceptibilities of rocks can be used to estimate the iron contents by relations (3)—(5). Because the abundance of the ion Mn^{2+} is below 0.15 wt % in all example rock types (see Table 2), formula (5) can be ignored without significant loss of accuracy. The relations (3) and (4) can be combined into a new formula (6), where the total abundance of iron is $W_{Fe} = W_{Fe2} + W_{Fe3}$ and the oxidation ratio of iron is $Ox = W_{Fe3}/W_{Fe}$. The iron content W_{Fe} (wt %) is obtained from the paramagnetic susceptibility X (10^{-8} m³/kg) by the relation

$$W_{Fe} = C \cdot X \text{ , where } C = 1/(2.71 + Ox/2) \tag{6}$$

The minimum value of the oxidation ratio $Ox = 0$ (no Fe^{3+}-ions) gives the maximum value for the coefficient $C = 0.369$, which leads to overestimation of the iron content W_{Fe}. The maximum value $Ox = 1$ gives a minimum value $C = 0.312$, which leads to underestimation of W_{Fe}. The best estimates of iron content W_{Fe} are obtained by formula (6) by applying the C-values of Table 2, which have been calculated from the average oxidation ratio of each rock type. Inserting the overall means of C- and Ox-values (Table 2) into formula (6), leads to the average formula

$$W_{Fe} = 0.35 \cdot X \tag{7}$$

which is sufficiently accurate for the estimation of iron contents in many situations.

Before the relations (6) or (7) can be applied to the determination of iron contents, representative estimates are needed for the paramagnetic susceptibilities of rock units. According to Fig. 12 the frequency distributions of paramagnetic susceptibilities are rather symmetric even on arithmetic susceptibility scales. The paramagnetic susceptibilities can thus be described reasonably well with ordinary arithmetic means of observations, after the ferrimagnetic observations have first been eliminated by truncation of the distribution. In some cases it is difficult to select the correct truncation point between the para- and ferrimagnetic parts of susceptibility distributions (cf. Fig. 4). In such cases it is better to characterize the paramagnetic susceptibilities with the aid of mode Mo, which can be determined from the formula

$$Mo = L_1 + L \cdot E_1/(E_1 + E_2) \tag{8}$$

where L = size of modal class interval, L_1 = lower class boundary of modal class, E_1 = excess of modal frequency over frequency of next lower class, and E_2 = excess of modal frequency over frequency of next higher class. The modes are not affected by truncation and they are less affected by ferrimagnetic impurities than the averages of truncated distributions.

Formula (7) can be used, for instance, to determine the average iron content of Finnish bedrock, which has been estimated as 3.3 wt % by Sederholm (1925). The average iron content of the whole lithosphere has been calculated by Beus (1976), who presented the estimate 3.4 wt % for sedimentary rocks, 5.6 wt % for volcanic rocks, 2.9 wt % for magmatic rocks and 4.5 wt % for metamorphic rocks. The paramagnetic mode in the combined susceptibility distribution of all Finnish rocks (Fig. 3) is $11.5 \cdot 10^{-8}$ m³/kg. Insertion of this value into relation (7) gives the estimate 4.0 wt % for the average iron content of rocks in Finland. The average is somewhat higher than the earlier result quoted above, but in good accordance with the iron averages presented for the whole lithosphere. The distribution of Fig. 3 was prepared from all samples of the petrophysical register without areal weighting of data, which leads to overrepresentation of basic rock types (Puranen et al., 1978). This kind of bias could partially explain the difference between the two estimates for average iron content in Finnish rocks.

SUSCEPTIBILITY AND DENSITY

Henkel (1976) showed that the combined use of susceptibilities and densities can increase the geologic resolution of petrophysical measurements. Susceptibility distributions characterize the iron and magnetite contents of rocks, which can be related through density values to mineralogic and chemical compositions (Henkel, 1976) and to the abundance of mafic minerals (Puranen et al., 1978). The serpentinization process and magmatic differentiation of igneous rocks were demonstrated by Henkel (1976) with the aid of density-susceptibility distributions whose major trends were manually outlined from unsmoothed data. In the case of scattered data however, this practice can lead to rather broad outlines, which may obscure some of the systematic features.

In the following considerations, susceptibility is regarded as the basic quantity that is compared with density, intensity of remanence and Q-ratio. For this reason susceptibilities are presented on the horizontal axis and the other quantities on the vertical axis, contrasting with the convention adopted by Henkel (1976). The susceptibility-density graphs will for convenience be referred to as XD-diagrams. The smoothing effects on XD-diagrams are demonstrated with the aid of quartz diorite data (cf. Fig. 5), representing intermediate rocks. The data are first arranged into a sequence of rising susceptibilities, then divided into successive groups of equal size, and finally characterized by group means of densities and susceptibilities. The effect of smoothing is intensified by increasing the size of groups from 1 sample (no smoothing) to 30 samples.

Fig. 13 demonstrates how the plot of scattered points is transformed gradually into a compact XD-graph as the intensity of smoothing increases. The left half of the graph rises linearly and the right half forms a concave curve. The linear relation between the low susceptibilities and densities of quartz diorites is due to the simultaneously increasing abundance of iron and mafic minerals. The linear part of the XD-diagram covers the density range 2 650—2 800 kg/m^3. The corresponding susceptibility range is about $(3—30) \cdot 10^{-8}$ m^3/kg, which could be caused by a magnetite content of 0.005—0.05 wt % according to formula (1) or an iron content of 1—10 %, based on formula (7). This range of magnetite content is too low to explain the density rise of quartz diorites. The rise could however, be caused by an increasing amount of mafic minerals, which could also easily

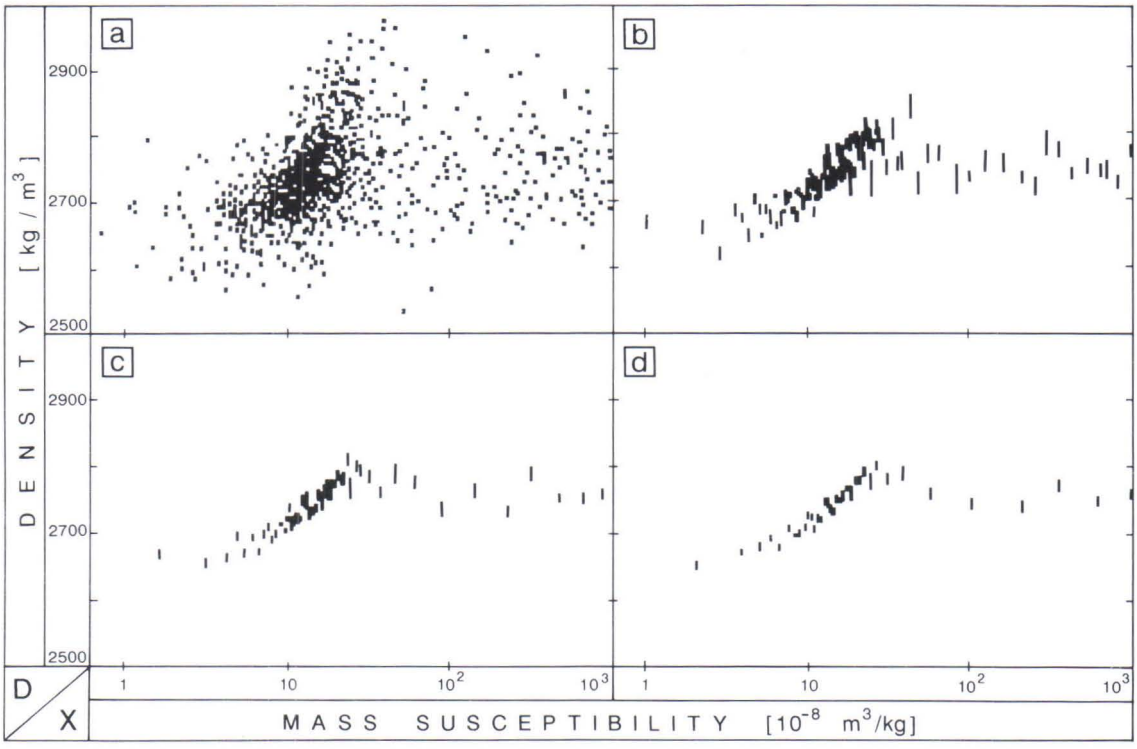

Fig. 13. Susceptibility-density diagrams for quartz diorites shown A) without smoothing (1133 samples), B) using group means of 10 samples, C) 20 samples and D) 30 samples. Vertical bars describe standard errors of densities, and horizontal distances between adjacent points constrain susceptibility errors. Additional explanations in text.

accomodate the proposed iron contents. The discontinuity between the linear and concave parts of the XD-graph reflects the shift from paramagnetic to ferrimagnetic susceptibilities.

The main features of the quartz diorite XD-graph are repeated in the diagrams for other example rock types (Fig. 14). The number of points and the degree of smoothing in the

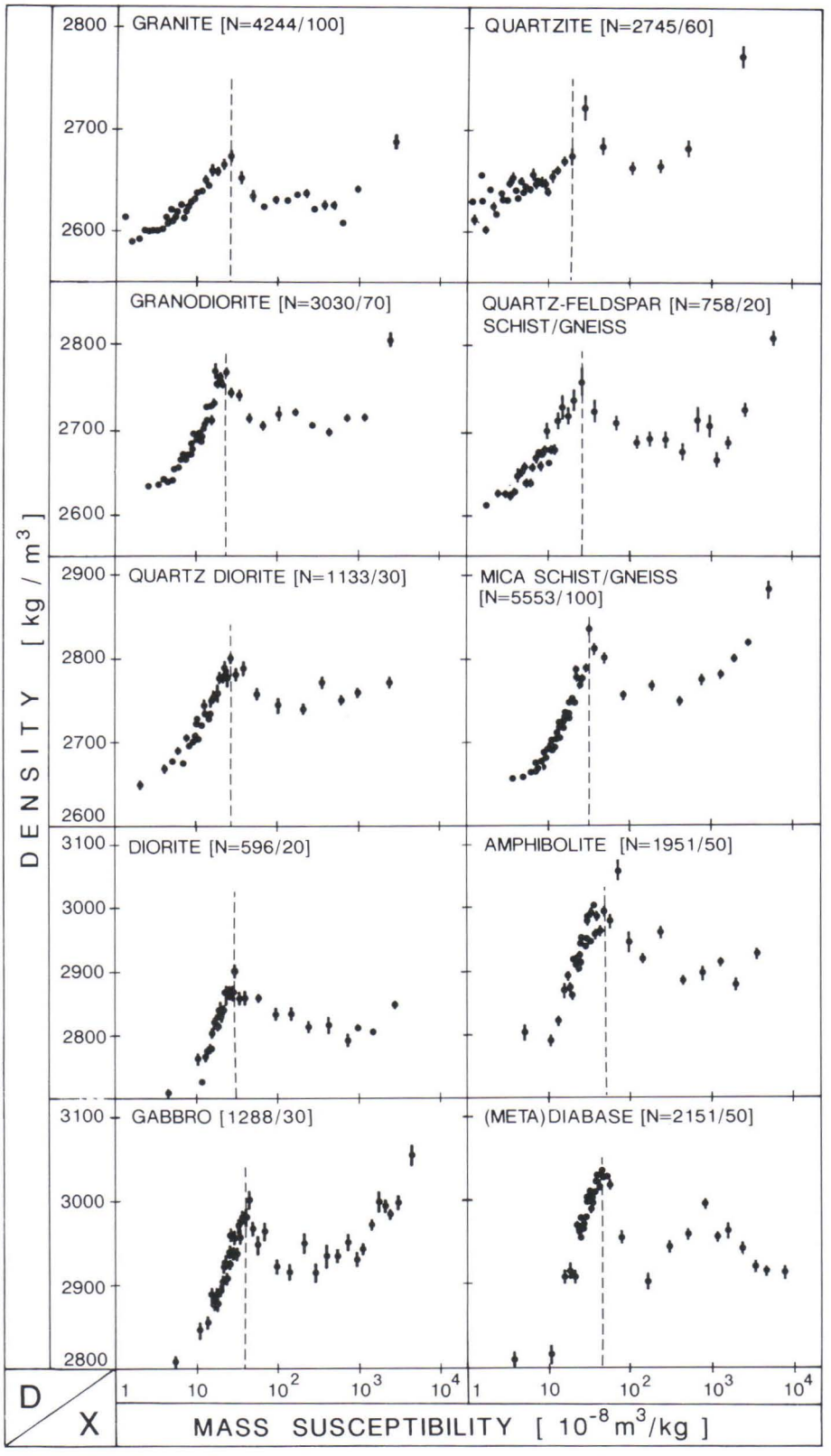

Fig. 14. Susceptibility-density diagrams for example rock types. Vertical bars describe standard errors of densities and dashed lines divide data into para- and ferrimagnetic parts. N = number of samples/size of smoothing group.

diagrams have been experimentally chosen to make the XD-graphs reasonably compact. About 30—50 points proved to be sufficient for outlining the paths, which means that the size of smoothing groups varies in the range 20—100 depending on rock type. The paramagnetic (linear) and ferrimagnetic (curved) parts of XD-diagrams are separated by limiting susceptibilities X_b (see Table 3) that are indicated by dashed lines. The linear parts are called XD-lines and the concave parts XD-curves. In most diagrams a few points near the left margin are slightly displaced from the paramagnetic XD-line. This displacement of the most weakly magnetic samples is probably due to diamagnetism of felsic minerals.

Table 3. Sample numbers N, averages M, standard deviations S and limiting susceptibilities X_b (10^{-8} m^3/kg) of para- and ferrimagnetic parts of susceptibility data for example rock types. Magnetite content W_m (wt %) and iron content W_{Fe} (wt %) are estimated by relations (1) and (7). Fraction of ferrimagnetic samples is $F = N_f/(N_f + N_p)$ and rock type codes as in Fig. 7.

ROCK TYPE CODE	SUSCEPTIBILITIES							ABUNDANCES		
	Paramagnetic			Limit X_b	Ferrimagnetic			F (—)	W_m (%)	W_{Fe} (%)
	M	S	N_p		M	S	N_f			
0	7.6	6.2	2988	29	383	731	1247	0.29	0.6	2.7
1	10.6	5.5	2301	25	366	521	728	0.24	0.5	3.7
2	13.0	6.0	866	28	478	753	267	0.24	0.7	4.6
3	18.5	6.2	380	32	603	830	216	0.36	0.9	6.5
4	24.1	8.9	749	46	1085	1207	539	0.42	1.6	8.4
5	4.2	4.4	2326	22	469	1037	347	0.13	0.7	1.5
6	8.6	5.9	517	30	1118	1602	239	0.31	1.7	3.0
7	13.5	6.4	4598	34	1074	1408	954	0.17	1.6	4.7
8	26.1	9.5	1449	52	867	1146	502	0.26	1.3	9.1
9	28.6	9.0	1453	45	1645	2261	697	0.32	2.5	10.0
M	15.5			34	809			0.27	1.2	5.4

The limiting susceptibility values X_b have been used to divide the sample material of each example rock type into paramagnetic and ferrimagnetic parts. The (relative) sizes of these parts and their susceptibility statistics are presented in Table 3. The mean susceptibilities have been further used to estimate the average abundances of magnetite (W_m) and iron (W_{Fe}) in example rocks by relations (1) and (7). These petrophysical estimates are somewhat higher than the results of chemical analyses (cf. Table 2). The largest differences between the estimates (about 1 %) are observed in amphibolites, gabbros and granites, which represent the most basic and acid types of the example rocks. For the intermediate rock types the discrepancy is less than 0.5 %.

The small differences between chemical and petrophysical estimates can result from a real variation in the iron contents of the two sets of samples. On the other hand, the differences could also be due to the sharp division of susceptibility distributions into two parts. The samples in the paramagnetic part may contain minute amounts of magnetite, which would raise the susceptibilities and lead to somewhat overestimated abundances of paramagnetic iron. The truncated distributions of para- and ferrimagnetic susceptibilities can also lead to underestimation of the standard deviations of these distributions. However, according to the comparisons above, the possible bias in petrophysical averages is fairly small and will not be significant in most applications.

The ferrimagnetic XD-curves as a whole are mostly located in the high density field for each rock type (see Fig. 14). High densities reflect high iron content, which thus seems to favour magnetite formation. Both ends of the XD-curves are characterized by rising densities. The density rise is caused by high magnetite contents at the right end of the curve, whereas the rise near the left end at low susceptibilities is not due to magnetite but rather to the abundance of iron. The iron content of rocks (W_{Fe}) can also be estimated from their densities (D) using the proper relations. Such relations are presented in Table 4 together with density statistics for the example rock types. The relations were determined by fitting regression lines to (D, W_{Fe})-data, which were obtained by relation (7) from the data points of XD-lines.

Table 4. Averages M and standard deviations S of densities D (kg/m³) in example rock types based on N samples. Relations between densities and iron content W_{Fe} (weight %) are determined from paramagnetic XD-lines of Fig. 14 after replacement of X-values with W_{Fe}-values from formula (7). Relations are described with regression lines $W_{Fe} = A + B \cdot D$ and correlation coefficients R. Rock type codes as in Fig. 7.

ROCK TYPE	Density statistics			Regression parameters		
	M	S	N	A	B	R
0	2625	66	4244	−237	0.091	0.95
1	2698	76	3030	−122	0.047	0.98
2	2737	72	1133	−144	0.054	0.96
3	2820	85	596	−121	0.045	0.98
4	2935	107	1288	−184	0.066	0.96
5	2644	75	2745	−221	0.084	0.75
6	2677	85	758	−133	0.051	0.95
7	2726	87	5553	−146	0.056	0.98
8	2930	129	1951	−144	0.052	0.90
9	2970	102	2151	−148	0.053	0.94

The linear dependence between density and iron content is characterized by high values for regression coefficients (see Table 4). Because of the varying composition of the example rocks, the regression lines show significant differences. The slope of regression lines is at a maximum for the acid quartzites and granites. This means that the mafic minerals of acid rocks are the most iron-rich, which is consistent with petrologic observations. This result can also be deduced from the simplified XD-diagrams of example rock types (Fig. 15), which were drawn and smoothed by hand from the data of Fig. 14. When any fixed value of paramagnetic susceptibility (iron content) is considered in the diagrams, the cor-

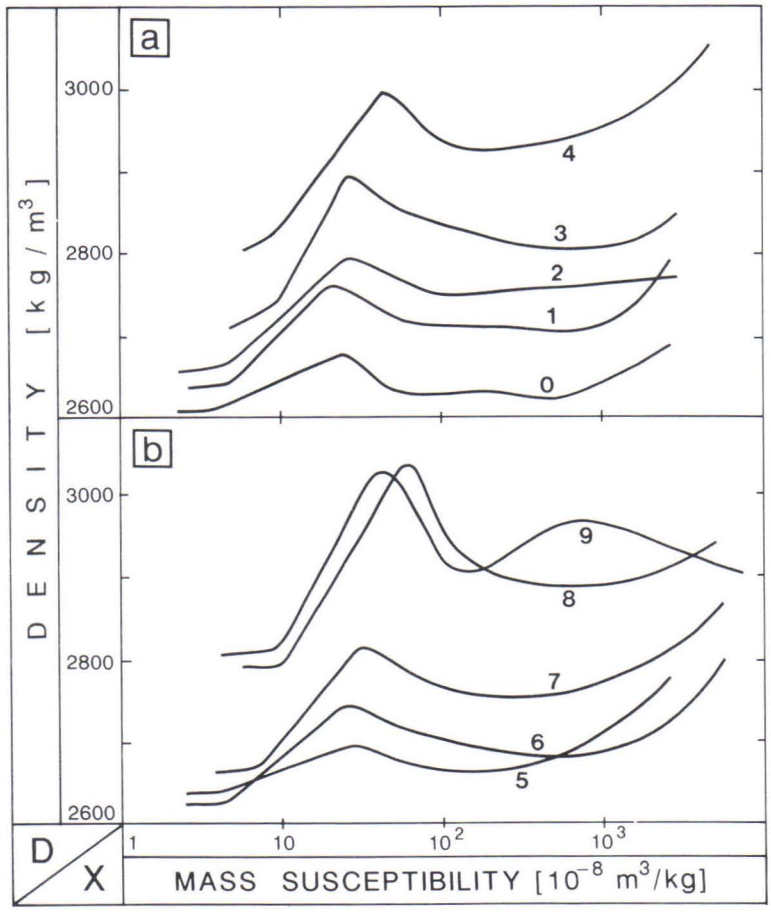

Fig. 15. Simplified susceptibility-density curves for A) igneous and B) other example rock types. Rock type codes as in Fig. 7.

responding density is lower in the light granites than in the heavy gabbros. In granites iron is thus concentrated into a smaller amount of mafic minerals, which makes them accordingly more iron-rich.

The XD-diagrams of Fig. 15 characterize the average behaviour of example rock types for the whole of Finland. The diagrams will be later applied as petrophysical standard curves in areal comparisons. Each diagram starts with a small flex at the left, which is caused by the diamagnetic samples. The slope of paramagnetic XD-lines increases from the felsic rocks toward the mafic rocks (from bottom to top), which results from changes in the main mineral components of the rocks. Areal differences can also be observed in the length, location and slope of XD-lines and in the form of XD-curves within each rock type. Such differences can be used to estimate variations in rock composition, providing that suitable model curves are prepared. Preparation of model curves must be based on sample material, which is analysed petrophysically and chemically as well as mineralogically. Because such material is not available at present, preliminary model considerations are made by combining different data sets through lithologic names.

SUSCEPTIBILITY AND REMANENCE

The dependence between remanent magnetization J_r and susceptibility of rocks can be described with the aid of Königsberger's ratio $Q = J_r/J_i$, where the induced magnetization J_i is determined as the product of susceptibility and magnetic field strength H. The values of the Q-ratio are naturally independent on whether magnetizations are expressed with respect to mass or volume units. On the one hand the Q-ratios reflect magnetic mineralogy (grain type, size), and on the other they describe the significance of remanence in the formation of magnetic anomalies. Coarse (multi-domain) grains of magnetite are characterized by low Q-ratio values (Stacey & Banerjee, 1974; Criss & Champion, 1984), whereas the Q-ratios of fine-grained (single-domain) magnetite are typically greater than 0.5 (Stacey, 1967; Magnusson, 1983). Very high Q-ratios (above 10) are often connected with hematite and pyrrhotite (Nagata, 1961). The values of the Q-ratio characterize the relative magnitudes of magnetization components but not their absolute strengths, which ultimately determine the intensity of magnetic anomalies. Therefore, in magnetic interpretations the effective susceptibility of rocks is often a more useful parameter than the Q-ratio.

In the calculation of effective susceptibilities the remanent and induced magnetizations are assumed to be parallel, which means that the total magnetization J_t is obtained directly as the sum $J_t = J_r + J_i$. This assumption can be regarded as effectively valid at least in Scandinavia, where the directions of natural remanence are often scattered, but on average still parallel with the Earth's magnetic field (Cornwell, 1975; Enmark & Nisca, 1983). Remanences are somewhat overestimated when determined as averages of intensities, because scattering of directions tends to reduce the effect of remanence. This bias should be corrected when directional data are available, but otherwise a reasonable estimate can be obtained for the effective susceptibility from the formula $K_{eff} = J_t/H = (Q + 1) \cdot J_i/H = (Q + 1) \cdot k$, where k is the volume susceptibility. In geophysical interpretations the volume susceptibilities and remanences are mostly applied, because geologic bodies are usually outlined by volumes. The magnetic properties expressed in volume units have been summarized in Table 5 for the example rock types and some other rocks of interest.

The effective susceptibilities indicate that basic (meta)diabases, amphibolites and gabbros are the most magnetic example rocks, whereas acid granites and quartzites are most weakly magnetic. The susceptibilities of felsic quartz-feldspar schists are also notably high. The effect of remanent magnetization is lower in the igneous rocks than in other rock types, but in all example rocks the remanence forms a significant part of the total magnetization ($Q > 0.5$). The most magnetic rocks of Table 5 are serpentinites, tuffites and ultrabasic rocks. Amongst granitoids rapakivi varieties are the most magnetic and the least magnetic are pegmatitic granites. The highest Q-ratio values are observed in black schists, skarns and tuffites. In tuffites the high Q-ratios and susceptibilities are probably due to fine-grained magnetite, which can form during rapid crystallization. The high Q-ratios of skarns and black schists may be caused by pyrrhotite or hematite, because the susceptibilities of these rocks are low. The physical properties of black schists and other graphite bearing rocks in Finland have been reported earlier in the course of a special project (Kukkonen et al., 1985).

Table 5. Averages M and standard deviations S of volume susceptibilities k and remanences J_r of main Precambrian rock types. Estimates based on these averages are presented for Königsberger's ratio $Q = J_r/k/H$ and effective susceptibilities $K_{eff} = (1 + Q) \cdot k$. Magnetic field is H = 41 A/m and N = number of samples.

ROCK TYPES	k (10^{-5} SI)		N	J_r (10^{-2} A/m)		Q	K_{eff}
	M	S		M	S		
Granite	427	1362	1833	12	110	0.69	722
Granodiorite	322	981	1337	16	139	1.21	712
Quartz diorite	466	1619	305	14	33	0.73	806
Diorite	635	1852	239	19	62	0.73	1099
Gabbro	1113	2698	630	59	202	1.29	2549
Quartzite	148	1344	975	17	119	2.80	562
Quartz-feldspar schist/gn.	1129	3352	512	43	309	0.93	2179
Mica schist/gneiss	314	1469	2726	28	201	2.18	999
Amphibolite	530	1966	651	85	480	3.91	2602
(Meta)diabase	2853	6394	714	133	1352	1.14	6105
Porphyrites	647	1832	155	17	42	0.64	1061
Volcanites	804	2435	257	154	855	4.67	4559
Tuffites	1295	5362	156	593	3670	11.17	15760
Black schist	306	824	139	417	1733	33.25	10480
Conglomerate	1969	4332	92	34	67	0.42	2796
Greywacke	229	1513	182	20	92	2.13	717
Pegmatite granite	21	116	91	4	3	4.65	119
Microcline granite	136	596	236	9	50	1.61	355
Aplite granite	234	745	136	6	18	0.63	381
Rapakivi granites	647	1074	104	24	44	0.91	1236
Porphyritic granite	782	1204	298	13	51	0.41	1103
Porphyritic granodiorite	140	690	644	7	36	1.22	311
Ultrabasic rocks	2413	4366	99	363	874	3.67	11269
Serpentine rocks	6175	5710	94	1042	2242	4.12	31616
Greenstone	1606	3643	177	125	693	1.90	4657
Amphibole gneiss	1186	3294	257	70	444	1.44	2894
Skarns	302	994	143	184	616	14.87	4793
Veined gneiss	118	677	269	8	30	1.65	313
Granite gneiss	327	974	945	12	135	0.90	621
Biotite-plagioclase gneiss	682	3650	113	21	111	0.75	1194

Abundant data are still to be interpreted from the aeromagnetic maps of Finland, which presently cover the whole country. The most reliable interpretations are obtained, if petrophysical data are available for the investigation area in question, but for preliminary interpretation the national averages of Table 5 can also be useful. The susceptibility and remanence averages as such are characteristic of rock types, but only the differences in effective susceptibilities between neighbouring rock units can cause magnetic anomalies. A susceptibility difference of at least $40 \cdot 10^{-5}$ (SI) is needed (in Finland) between an anomalous zone and its surroundings, before the maximum anomaly above the center of the zone exceeds 10 nT, according to the approximate model presented by Parasnis (1973) for extremely deep and long vertical zones. This small difference, which could characterize mafic and felsic zones of paramagnetic rocks, is easily lost amongst the noise of aeromagnetic measurements. Correspondingly, a zone anomaly of 1000 nT is caused by a susceptibility difference of $4\,000 \cdot 10^{-5}$ (SI). Such differences are not to be expected in more than 10 % of the example rocks, as can be deduced from Fig. 7 after the transformation of susceptibility units.

The magnetic properties of rocks can vary strongly within short distances of some meters, but these local variations cannot be observed on aeromagnetic maps due to insufficient resolution. From these maps only mean estimates can be obtained for the magnetic properties of rocks even with the most sophisticated interpretation techniques. These estimates reflect average mixtures of para- and ferrimagnetic minerals that may be rare in real samples of bedrock. Therefore, when petrophysical measurements are used to identify the source rocks of magnetic anomalies, the identification must be based on averages of large sample materials. The importance of remanence for magnetic interpretations must also be stressed, because the mean Q-ratio of the example rocks is about 1.6, and over half of the total magnetization is thus due to remanence. Following this short digression into magnetic interpretations, the petrophysical considerations will be resumed by comparison of mass susceptibilities and remanences (Fig. 16).

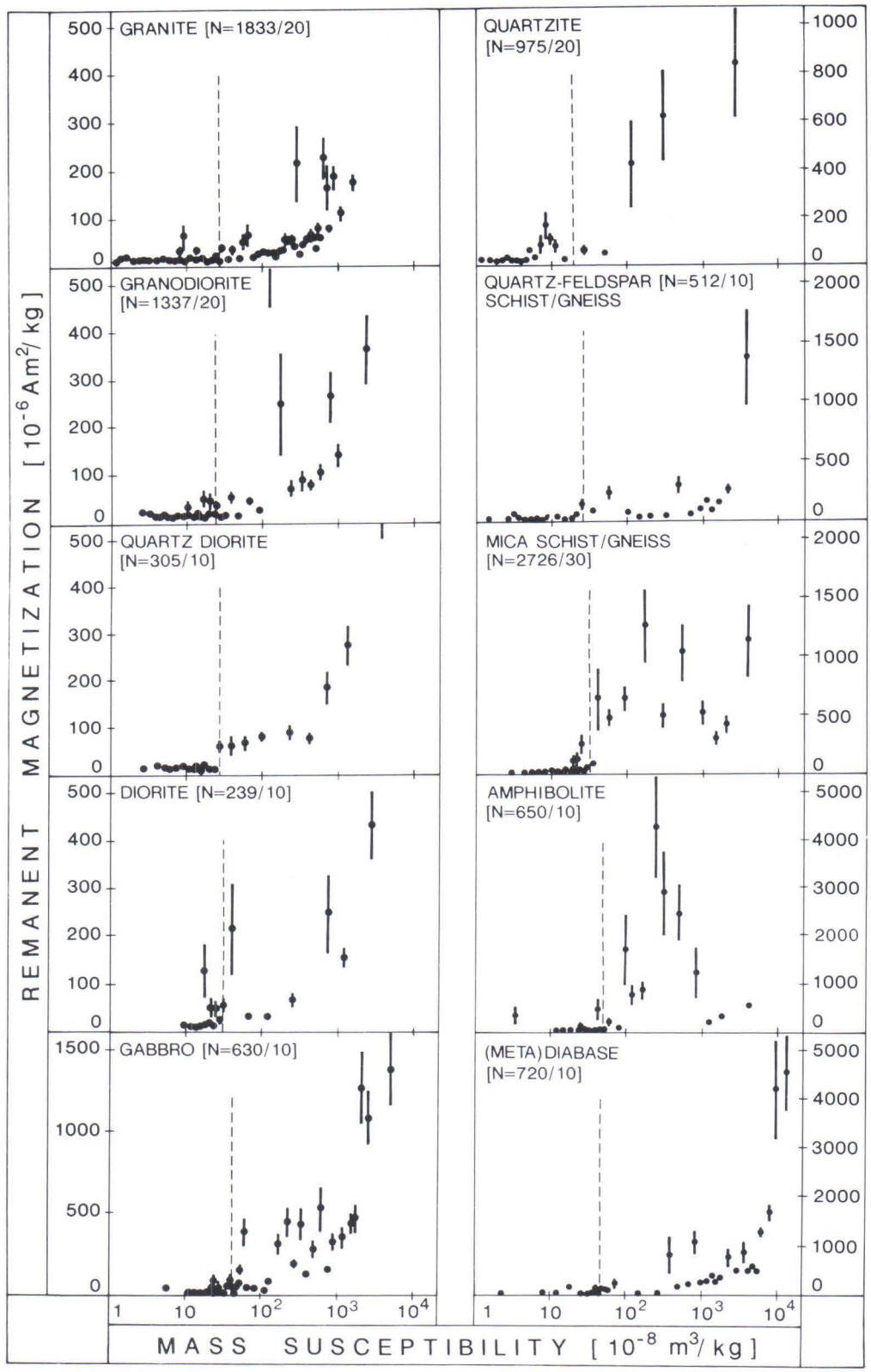

Fig. 16. Dependence between mass susceptibility and mass remanence of example rock types. Vertical bars describe standard errors of remanences and dashed lines divide data into para- and ferrimagnetic parts. N = number of samples/size of smoothing group.

The data of Fig. 16 have been smoothed and are presented in a similar form to the data of XD-diagrams. The standard errors of remanences are large in strongly magnetic samples. Despite this scatter, the average remanences clearly increase together with susceptibilities, and the remanence is thus roughly proportional to the abundance of magnetite. The samples characterized by paramagnetic susceptibilities have mostly such weak rem-

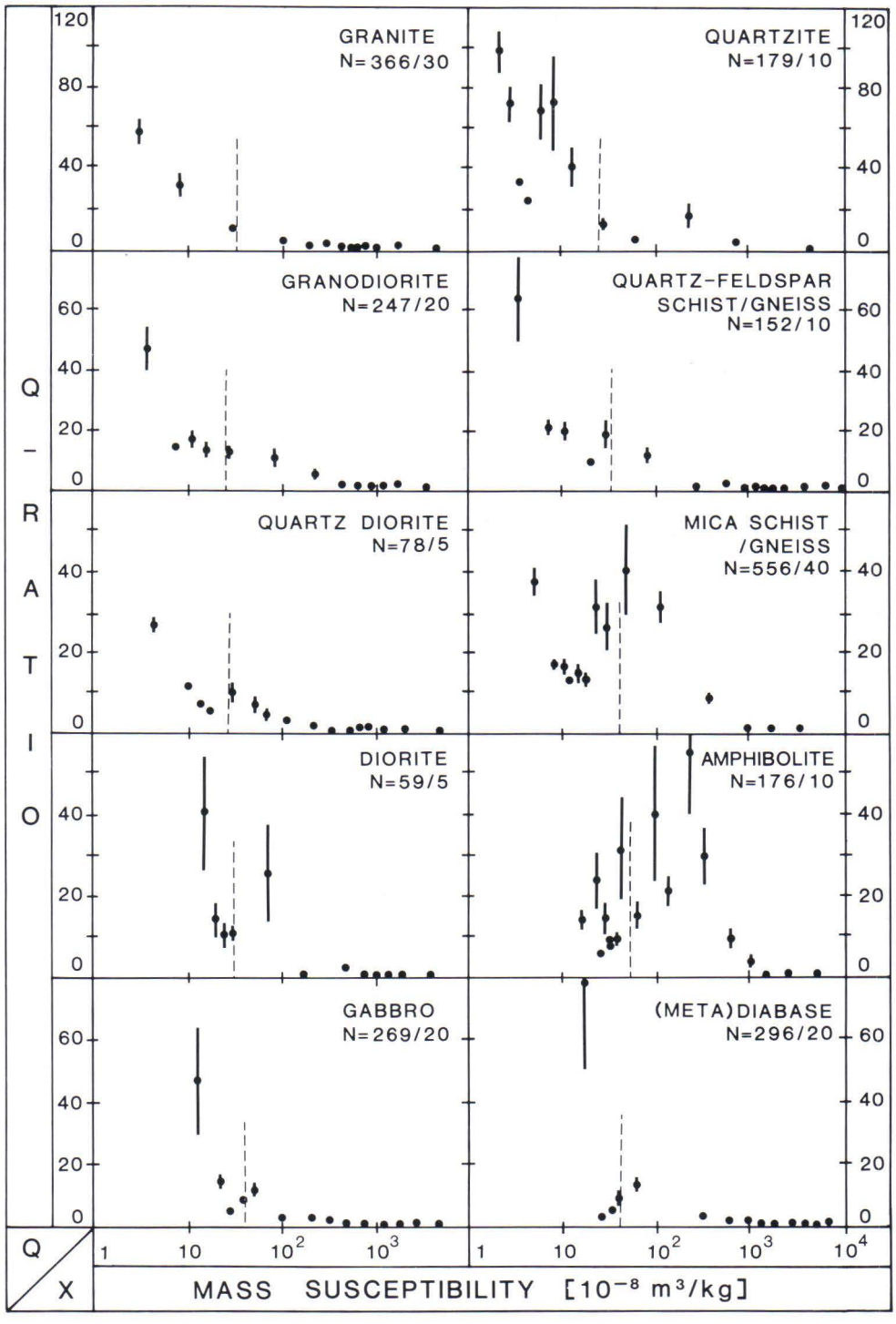

Fig. 17. Dependence between mass susceptibility X and Königsberger's ratio $Q = J_r/X/H$ for example rock types. Samples below measuring threshold for remanence ($J_r < 30 \cdot 10^{-6}$ Am²/kg) or susceptibility ($X < 10^{-9}$ m³/kg) are not included. Vertical bars describe standard errors of Q-ratios and dashed lines divide data into para- and ferrimagnetic parts. Magnetic field H = 41 A/m and N = number of samples/size of smoothing group.

anences that their averages remain below the sensitivity threshold ($30 \cdot 10^{-6}$ Am²/kg) of our remanence meters. The remanence values exceed this threshold only in 12 % of the samples with paramagnetic susceptibilities. Therefore, most of the weakly magnetic rocks can be considered dominantly paramagnetic on the basis of their remanence as well. This statement is valid only in a statistical sense, and the purity of paramagnetism must be verified separately for each sample. This verification can be made, for instance, with the aid of magnetization experiments (Chernyuk, 1971) that reveal even small amounts of ferrimagnetic impurities.

Let us finally examine the dependence between mass susceptibility X and Q-ratio. This ratio can be calculated reliably only, if both its numerator (remanence) and denominator (susceptibility) are known accurately enough. For this reason the samples with susceptibility below 10^{-9} m^3/kg and remanence lower than $30 \cdot 10^{-6}$ Am^2/kg have been excluded from the Q-ratio calculations. The remaining ferrimagnetic data have been smoothed and presented (Fig. 17) in a similar manner as the data of XD-diagrams. In most example rock types the Q-ratios decrease on average with increasing susceptibility values, which is consistent with the trends reported by Henkel (1976). The decrease in Q-ratios is caused by the growing proportion of coarse-grained magnetite (Magnusson, 1983), because coarse (multi-domain) grains are characterized by lower values of Q-ratios than the fine grains. The variation of Q-ratios is at a maximum in the weakly magnetic samples, and smallest in the samples with high susceptibilities.

The XQ-diagrams of igneous rocks are regular and similar to each other except in the case of diorites, whose diagram is based on the smallest number of samples. The values and variation in the Q-ratio are low for most points of the diagrams, which indicates that coarse-grained magnetite is the dominant ferrimagnetic mineral in igneous rocks. Coarse ferrimagnetic minerals also characterize (meta)diabases and quartz-feldspar schists/gneisses, whose XQ-diagrams closely resemble those of gabbros and granitoids, respectively. In quartzites and mica schists/gneisses the proportion of fine-grained magnetite, hematite or pyrrhotite becomes significant, because high values and strong variation of Q-ratios are observed in several points of the XQ-diagrams. The largest proportion of fine-grained ferrimagnetic minerals probably occurs within amphibolites, whose XQ-diagram is dominated by points with high Q-ratios and strong scatter.

In the igneous rocks and (meta)diabases of Finland, the dominant ferrimagnetic phase is probably coarse-grained magnetite, which indicates slow crystallization of magma. Metamorphism of basic (iron-rich) rocks seems to increase the amount of fine-grained magnetite and/or hematite, which are common in the sedimentogenous quartzites as well. In most rock types several secondary processes also tend to produce small amounts of fine-grained hematite and magnetite. Secondary ferrimagnetic minerals seem to be most common in the dominantly paramagnetic rocks that are characterized by low susceptibilities and high Q-values (cf. Fig. 17). The identification of magnetic minerals can be verified, for example, with the aid of AC-demagnetization techniques. Soft remanence is typical for coarse (multi-domain) and extremely fine-grained (superparamagnetic) magnetite, whereas hard remanence characterizes hematite and small (single-domain) grains of magnetite (Stacey & Banerjee, 1974).

IRON AND MAFIC SILICATES

In the next chapters we shall concentrate on the geologic interpretation of petrophysical results and particularly on XD-diagrams in the light of chemical, mineralogic and petrologic data. In the XD-diagrams the iron content of rock W_{Fe} is shown on the paramagnetic part of the susceptibility axis and the abundance of mafic minerals W_{Ms} is reflected on the density axis. Therefore, for every point on the XD-lines it is possible in principle to evaluate the iron content of mafic minerals by the ratio W_{Fe}/W_{Ms}. The paramagnetic susceptibilities can be converted into W_{Fe}-estimates by the linear relation (7). The dependence $W_{Ms} = f(D)$ between the abundance of mafic minerals and rock densities is also linear on average (Puranen et al., 1978), but it is more complicated than the relation (7), because the assemblage, proportions and densities of mafic minerals vary between different rock types. In order to determine the dependence $W_{Ms} = f(D)$ more accurately for each rock type, we should need large groups of paramagnetic samples with known densities and modal compositions.

Because the chemical and mineralogic compositions of petrophysical samples are not known, the compositional variations of example rock types in different parts of XD-diagrams are estimated in a preliminary way on the basis of data published elsewhere. The data on mineralogic compositions have been collected from the explanations to the geologic map of Finland (see Appendix A) and a statistical summary of modal analyses is presented in Appendix B. The chemical compositions of the example rock types are summarized in Appendix C on the basis of classical silicate analyses made at GSF. The mineralogic and chemical

data can be properly combined with each other and with XD-diagrams only after the data are ordered and appropriately subdivided. The low values of susceptibility and density are connected with each other in the XD-diagrams. Accordingly, the iron-poor samples in the chemical data should be combined with the low density samples in the mineralogic data. Similarly, the highest densities are associated with the iron-rich samples so that the chemical analyses of the example rocks have been arranged according to increasing iron content and the mineralogic data according to density values.

The densities of most mineralogic samples had not been measured. Therefore, they had to be calculated from the mineralogy using a density model (Puranen et al., 1978), which is summarized at the end of Appendix B. The modelled densities are approximate, but they sufficiently define the relative density order of the mineralogic samples. The ordered data of each example rock type were divided into five parts of equal size, and corresponding averages M1..M5 were calculated for both mineralogic and chemical compositions (Appendices B and C). In all example rocks the amount of mafic minerals (defined in Appendix B) increases with the calculated density. In acid rock types the density growth is mainly caused by increase of biotite content at the expense of alkali feldspar plus quartz, and in basic rocks by increase of amphiboles at the expense of plagioclase feldspar and quartz. The anorthite content of plagioclase rises systematically from acid to basic (igneous) rocks, which reflects their rising temperature of crystallization (Osborn, 1962). Because the anorthite content increases together with density within igneous rocks (cf. Appendix B), the most dense varieties of rocks (upper ends of XD-lines) seem to represent higher crystallization temperatures than the lighter rock material.

The averages M1..M5 for contents of mafic minerals W_{Ms} and iron W_{Fe} were paired for each example rock type in order to estimate the relative iron contents of mafic minerals W_{FeM}. These estimates are presented in Table 6 together with values of the iron-magnesium ratio FM and the oxidation ratio of iron Ox, which were calculated from the averages of Appendix C. The mafic minerals in the modal analyses may contain some magnetite and the iron in chemical analyses can be derived both from silicates and oxides. The iron estimates W_{FeM} of Table 6 are thus based on unknown combinations of paramagnetic iron silicates and ferrimagnetic oxides, although the silicates are clearly dominant. The uncertainty of W_{FeM}-estimates is increased by the fact that determinations of chemical and mineralogic compositions are based on different samples, although the results are combined at the level of group means. Comprehensive analyses of new sample material are required before relations for W_{FeM}-estimation can be calibrated more precisely.

The above reservations should be remembered when the chemical compositions of the example rocks are examined. In all rock types the TiO_2-content, and in acid rocks the CaO- and MgO-contents as well, increase together with the Fe-content (see Appendix C) mainly at the expense SiO_2-content. According to Table 6 the oxidation ratio of iron Ox varies rather randomly in all example rock types, whereas the iron-magnesium ratio FM shows the strongest scatter in quartzites. In other acid rock types the FM-values are reasonably constant and in basic rocks the FM-ratio systematically rises with iron content. In igneous rocks the W_{FeM}-estimates are constant or rise only slightly with increasing Fe-content of the rocks. In other rock types the W_{FeM}-estimates rise together with iron content, the strongest rise being observed in quartzites. The highest W_{FeM}-values are connected with acid rocks and the lowest with basic rock types, which is consistent with the petrophysical results of preceding chapters.

According to mineralogic handbooks (Deer et al., 1962; Deer et al., 1962a; Deer et al., 1963), the iron content of mafic silicates is generally within the range 5—15 wt % and always in the range 0—30 wt %, whereas the Fe-content of pure iron oxides is about 70 wt %. The W_{FeM}-estimates of Table 6 are thus quite realistic for rocks that contain iron oxides and silicates in suitable ratios. Most of the W_{FeM}-values can be explained by iron silicates alone, but iron oxides are needed to produce the highest value (43 wt %) in quartzites. The other W_{FeM}-values are presumably also affected by iron oxides and the effect probably grows with Fe-content of rocks. Elimination of the effect of iron oxides would decrease the highest W_{FeM}-estimates, and then the constant or slightly increasing trends of W_{FeM}-values could even change to decreasing trends. Therefore, it is not possible to deduce from the data of Table 6, how the iron content of mafic silicates varies between the lower and upper ends of XD-lines.

For the present, only the iron content of rocks can be determined from XD-lines, and accurate W_{FeM}-estimates of mafic silicates will require additional investigations. However, the deviations of observation points from the XD-lines reflect relative changes in the iron content of mafic silicates. If the observations from a rock unit lie above (below) the

Table 6. Iron content of mafic minerals $W_{FeM} = 100 \cdot W_{Fe}/W_{Ms}$, iron-magnesium ratio of rocks $FM = W_{Fe}/(W_{Fe} + W_{Mg})$ and oxidation ratio of iron Ox in different parts of XD-lines for example rock types. Averages M1 are tied to lower ends of XD-lines, where abundances (wt %) of iron W_{Fe} (susceptibility) and mafic minerals W_{Ms} (density) are low. Upper ends of XD-lines are approached through averages M2..M5 as explained in text and Appendices B and C.

GRANITE

	W_{Ms}	W_{Fe}	W_{FeM}	FM	Ox
M1	3.6	0.6	17	0.85	0.44
M2	4.3	1.2	28	0.87	0.38
M3	5.7	1.7	29	0.87	0.32
M4	8.1	2.3	29	0.85	0.36
M5	14.7	4.0	27	0.85	0.33

GRANODIORITE

	W_{Ms}	W_{Fe}	W_{FeM}	FM	Ox
M1	7.6	1.6	21	0.77	0.27
M2	11.0	2.4	22	0.78	0.31
M3	16.4	3.0	19	0.80	0.21
M4	21.4	4.0	19	0.74	0.25
M5	28.9	5.5	19	0.83	0.23

QUARTZ DIORITE

	W_{Ms}	W_{Fe}	W_{FeM}	FM	Ox
M1	15.5	2.4	15	0.67	0.18
M2	22.9	3.5	15	0.73	0.19
M3	28.3	4.3	15	0.72	0.15
M4	34.1	5.3	16	0.76	0.22
M5	40.7	6.6	16	0.79	0.18

DIORITE

	W_{Ms}	W_{Fe}	W_{FeM}	FM	Ox
M1	30.8	4.9	16	0.71	0.25
M2	41.3	5.4	13	0.69	0.16
M3	47.0	5.9	13	0.71	0.23
M4	50.7	6.8	13	0.74	0.22
M5	53.1	7.9	15	0.82	0.13

GABBRO

	W_{Ms}	W_{Fe}	W_{FeM}	FM	Ox
M1	43.3	4.6	11	0.51	0.13
M2	52.3	6.2	12	0.54	0.19
M3	56.6	6.9	12	0.57	0.24
M4	63.6	8.1	13	0.65	0.17
M5	77.1	10.6	14	0.72	0.15

QUARTZITE

	W_{Ms}	W_{Fe}	W_{FeM}	FM	Ox
M1	1.0	0.1	6	0.71	0.70
M2	3.3	0.3	10	0.43	0.66
M3	6.4	0.8	12	0.78	0.49
M4	9.7	1.5	15	0.65	0.72
M5	13.2	5.6	43	0.84	0.49

QUARTZ-FELDSPAR SCHIST/GNEISS

	W_{Ms}	W_{Fe}	W_{FeM}	FM	Ox
M1	6.7	1.0	15	0.76	0.31
M2	10.1	1.6	16	0.78	0.18
M3	13.6	2.8	20	0.80	0.24
M4	15.7	4.0	26	0.78	0.25
M5	25.0	5.3	21	0.76	0.12

MICA SCHIST/GNEISS

	W_{Ms}	W_{Fe}	W_{FeM}	FM	Ox
M1	20.5	2.6	13	0.77	0.23
M2	27.9	4.0	14	0.76	0.28
M3	36.0	5.0	14	0.75	0.24
M4	40.5	6.1	15	0.73	0.18
M5	44.9	8.7	19	0.75	0.36

AMPHIBOLITE

	W_{Ms}	W_{Fe}	W_{FeM}	FM	Ox
M1	41.0	4.3	10	0.51	0.21
M2	53.7	6.7	13	0.66	0.17
M3	63.4	7.9	13	0.64	0.17
M4	77.3	9.2	12	0.66	0.19
M5	76.6	11.0	14	0.72	0.22

(META)DIABASE

	W_{Ms}	W_{Fe}	W_{FeM}	FM	Ox
M1	52.4	5.9	11	0.62	0.22
M2	61.9	8.1	13	0.67	0.28
M3	66.0	9.4	14	0.72	0.20
M4	78.5	11.0	14	0.78	0.27
M5	73.0	14.3	20	0.79	0.21

average XD-line of that rock type, then the iron content of mafic minerals in the unit are lower (higher) than average. In igneous rocks the crystallization temperature is reflected by the iron content of mafic silicates, because gabbros with iron-poor silicates are formed at higher temperatures than granites with iron-rich silicates. In addition, iron-rich biotites within a rock type reflect lower crystallization temperatures than iron-poor biotites (Wones & Eugster, 1965). The iron-rich silicates can also break down into iron oxides and iron-poor silicates under oxidizing conditions.

IRON AND MAGNETITE

The formation of magnetite (Fe_3O_4) requires iron and suitable oxidation conditions with respect to temperature. When the oxygen fugacity is too high for the generation of magnetite, iron goes to hematite and ilmenite. When the oxygen fugacity is low, iron ends up in mafic Fe-Mg-silicates and sometimes also in iron sulfides. The appearance of magnetite in rocks is often closely related to mafic silicates as reviewed by Grant (1985). On the one hand, silicates can use up all the iron thus preventing magnetite formation whereas on the other, they can provide the iron for the formation of magnetite during metamorphic changes. The paramagnetic iron of mafic silicates is reflected in the linear parts of XD-diagrams, and the XD-lines may also include data from samples containing hematite, ilmenite or pyrrhotite. Such samples often have low susceptibilities and high Q-values due to considerable remanence. In the following we shall concentrate on the ferrimagnetic XD-curves, which reflect the relations between iron and magnetite content in the example rock types.

The susceptibilities of XD-curves can be converted by formula (1) into estimates of magnetite content W_m (wt %). The amount of iron in magnetite Fe_m (wt %) is obtained from the relation $Fe_m = 0.724 \cdot W_m$. The effect of magnetite density ($D_m = 5\ 200\ kg/m^3$) on the densities of XD-curves can be eliminated when the magnetite content is known at each point of the curve. The corrected density is also called the silicate density (Henkel, 1976), which can be determined using the formula $D_s = D \cdot D_m \cdot (100—W_m)/(100 \cdot D_m—D \cdot W_m)$. The silicate density D_s characterizes the silicate matrix of ferrimagnetic rocks in a similar way as do the densities of paramagnetic XD-lines. These densities reflect the abundance of mafic minerals and also the iron content of rocks (cf. Table 4). The iron content Fe_s within the mafic silicates of the ferrimagnetic example rocks can thus be estimated by inserting the silicate densities into the regression relations of Table 4. The total iron content of ferrimagnetic rocks is finally obtained as the sum $Fe = Fe_s + Fe_m$.

The relationship between iron abundances and magnetite content in the ferrimagnetic samples are presented in Fig. 18. These relations are based on smaller numbers of samples than the paramagnetic lines of the XD-diagrams (cf. Fig. 14). The paramagnetic XD-lines gave limits for the iron content of the example rocks, and these limits are shown for comparison in Fig. 18. The total iron content in the ferrimagnetic samples stays on average above certain minimum values, which seem to be required before formation of magnetite can commence. The minimum values are characteristic for each rock type, and the minimum is lowest for granites (1—2 %) and highest for gabbros (10 %). Iron content falls below these minima only in the paramagnetic samples located at the lower ends of XD-lines. These paramagnetic samples have high SiO_2-contents and therefore, no iron is left over for magnetite from the silicates (Grant, 1985).

When the iron content increases, magnetite-bearing samples start to appear in the lowest part of XD-curves, as an alternative to the paramagnetic samples. Because the iron in the paramagnetic samples is bound only to iron silicates, and in the ferrimagnetic samples both to silicates and oxides, the oxidation ratio of iron should be higher in the latter samples. The amount of oxidized iron increases further towards the right end of the XD-curves, where magnetite is found abundantly in the iron-rich varieties of the example rocks. Iron-rich rocks also appear at the left end of XD-curves, where the magnetite content is less than 0.1 % and the magnetite grains are small, as indicated by the high Q-ratios (cf. Fig. 17). Small amounts of fine-grained Fe-Ti-oxides are often formed in post-magmatic alterations as a result of replacement processes or partial decomposition of mafic silicates (Haggerty, 1976; Best, 1982). These small particles of magnetite appear in the most mafic varieties of pilot rocks, but more commonly the mafic rocks crystallize without magnetite and are then located at the upper end of the XD-lines.

Let us examine more closely the magnetite-iron curves of igneous rocks (Fig. 18). The abundances of iron and magnetite are highest in the gabbros, but the greatest part (more than half) of iron is bound to magnetite in the ferrimagnetic granites, which are thus characterized by a high oxidation ratio of iron. This is consistent with the chemical analyses of Table 2 and with the oxygen fugacity analyses presented by Haggerty (1976). The high oxidation ratio of iron is also demonstrated by the fact that magnetite has successfully competed with silicates even where iron abundances are low (1—2 %), although the Si-content of granites is high. The total amount of iron has to exceed an average limit of 5 % in granodiorites, quartz diorites and diorites, and of about 10 % in gabbros before iron becomes available for magnetite. The iron content of the silicate matrix stays close to these limits virtually irrespective of magnetite content. Therefore, practically all of the iron exceeding these limits goes into magnetite under proper oxidation conditions.

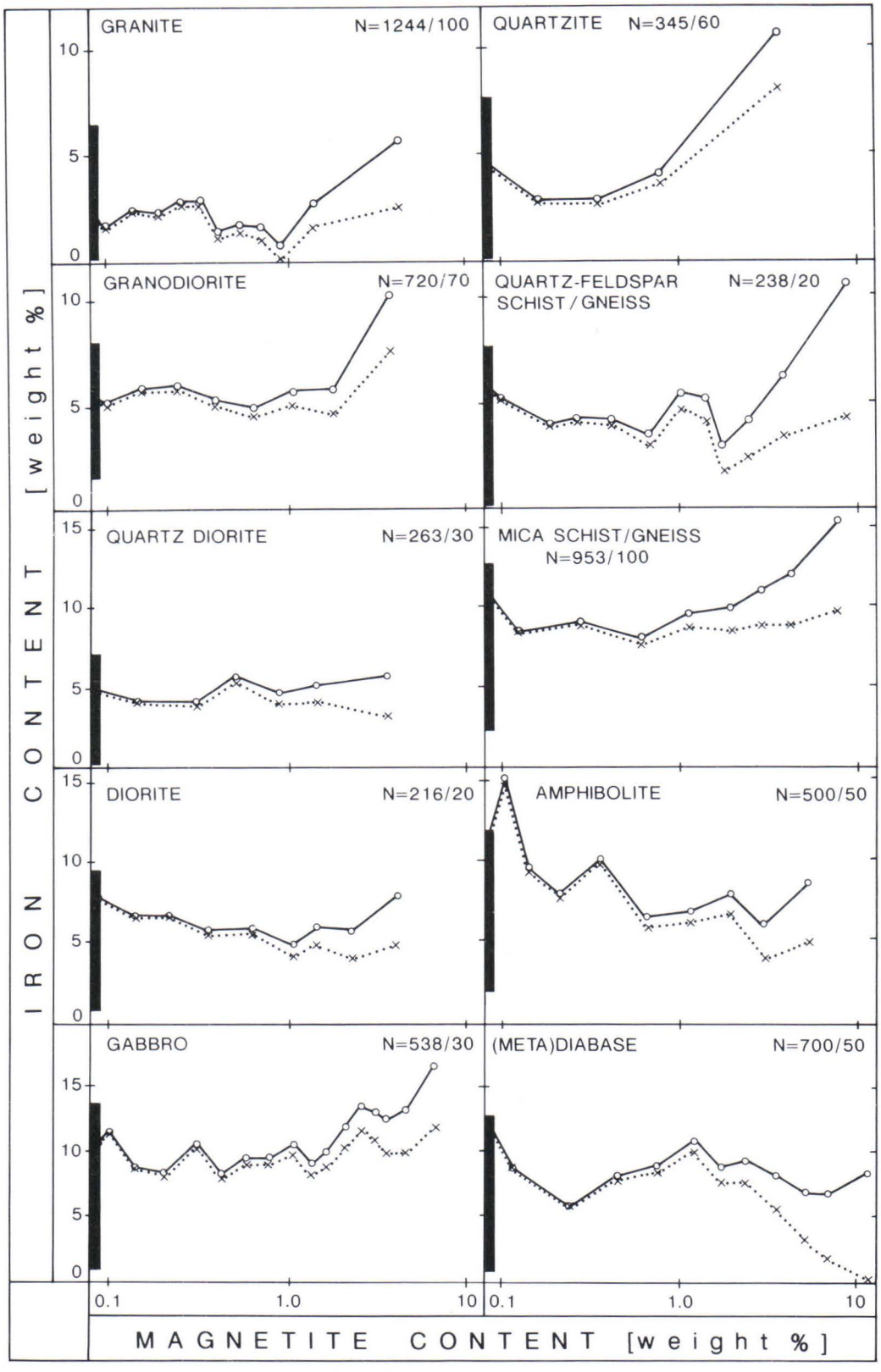

Fig. 18. Abundance of iron in whole rock (circles) and in silicate minerals (crosses) of ferrimagnetic example rocks as function of magnetite content. Abundance estimates are calculated from ferrimagnetic XD-curves as explained in text. Black segments of left margins show iron limits from paramagnetic XD-lines (cf. Fig. 14). N = number of ferrimagnetic samples/size of smoothing group.

The oxidation ratio of iron is highest in the sediments formed at the earth's surface (McIntyre, 1980), which is also reflected in the sedimentogenous quartzites of Finland (cf. Table 2). Metasediments often inherit their oxidation state from the original sediments (Chinner, 1960), although the most common iron oxide (hematite) of sediments is usually

transformed into magnetite in metasediments (McIntyre, 1980). This transformation takes place through dehydration of metasediments. In dehydration processes the oxidation ratio of rocks remains unchanged, because magnetite is simply formed by moving FeO from silicates to hematite (McIntyre, 1980). Dehydration reactions under greenschist facies conditions may produce significant amounts of magnetite, but the reactions can also be inhibited by high fluid pressures (McIntyre, 1980). When the degree of metamorphism rises to amphibolite facies, the magnetite content of rocks can be increased slightly, since iron-rich silicates locally decompose into magnetite and iron-poor silicates (Grant, 1985). Repeated cycles of regional metamorphism can also strengthen the magnetic properties of rocks, whereas metasomatism and granitization tend to destroy magnetite (Grant, 1985).

The magnetite-iron curves of the metamorphic example rock types are demonstrated in Fig. 18. Magnetite already appears in quartzites at rather low iron contents (about 3 %), although the quartzites contain high amounts of silica that competes about iron. The high oxidation ratio of iron probably explains the early appearance of magnetite in quartzites, and also in the quartz-feldspar schists/gneisses. In the most magnetic quartz-feldspar gneisses over half the iron occurs in magnetite, which is even more than in the magnetite-rich granites. The high oxidation ratio of iron is also manifested in the cumulative susceptibility distribution of quartz-feldspar gneisses (Fig. 7), which contains more than 40 % of ferrimagnetic samples. In mica schists/gneisses the total abundance of iron has to reach almost 10 % on average before magnetite starts to appear. Magnetite in mica gneisses is possibly formed by breakdown of iron-rich silicates, whereas magnetite in quartzites and quartz-feldspar gneisses can be transformed from hematite and mafic silicates of sediments. Some of the magnetite-rich quartz-feldspar gneisses may have inherited their oxidation state from acid volcanics, which are usually highly oxidized (Haggerty, 1976).

The right half of the magnetite-iron curve of amphibolites resembles that of (meta)diabases while the left half recalls that of gabbros. This is natural because amphibolites are formed by the metamorphism of basic volcanic or intrusive rocks. In amphibolites and particularly in diabases, the amount of iron in silicates decreases as the magnetite content increases, and in the most magnetic diabases almost all of the iron is bound up in magnetite. Such an abundance of magnetite is probably caused by the differentiation of magma, as the diabase dykes crystallized rapidly at near-surface conditions. The curves of Fig. 18 are suitable as references in areal comparisons, because they reflect average relations between iron and magnetite in the example rock types for the whole of Finland. The curves also reflect the oxidation ratio of iron in the ferrimagnetic example rocks, whereas the cumulative distributions of Fig. 7 characterize the abundance of ferrimagnetic rock material.

In igneous rocks the oxidation ratio of iron is dependent on the development of oxygen fugacity during crystallization, which in turn depends on the rock composition and crystallization environment (Haggerty, 1976). Metamorphic rocks for their part often inherit the oxidation state of their source rocks (McIntyre, 1980). As emphasized by Rumble (1976), different estimates can be obtained for the oxidation state of rocks from their chemical composition on one hand and from the (equilibrium) mineralogic composition on the other. Rocks can contain both hematite (Fe_2O_3) and magnetite (Fe_3O_4), which reflects relatively high oxygen fugacities during crystallization. The oxygen fugacity is kept approximately constant by the buffer reaction $O_2 = 6 \cdot Fe_2O_3 — 4 \cdot Fe_3O_4$, even if the amount of oxygen in the system changes. In progressive metamorphism oxygen can be removed from the system by H_2-rich aqueous fluids. The oxygen fugacity is restored by reduction of hematite to magnetite, which thus raises the magnetite-hematite ratio in the rock. Hence chemically, the amount of oxygen and the oxidation ratio of iron can decrease in the system, although the oxygen fugacity remains approximately constant at the high level indicated by the minerals of buffer reaction.

Corresponding situations are also possible in other buffered reactions of open systems, where reducing or oxidizing fluids (or gases) can move freely. In closed environments the oxygen is not particularly mobile, because the absolute values of oxygen fugacities (pressure gradients) are very low (McIntyre, 1980). Since the oxygen released in the buffer reactions is not dispersed away, the oxygen fugacity at the reaction site soon becomes high enough to stop the reaction and to keep the changes small and local. The reaction may continue only if some other reaction simultaneously reduces the oxygen fugacity or if the temperature is changed suitably with respect to fugacity. Local accumulations of magnetite are thus typical of closed environments, but in open systems magnetite is either uniformly distributed or does not form at all (Korsman, 1985). The relations between formation conditions of rocks and their iron and magnetite contents are thus manifold, and interpretations based on such relations will often remain tentative.

AREAL COMPARISONS

In the preceding chapters the physical properties of example rock types have been considered within Finland as a whole. This means that features from many kinds of geologic units and conditions have been combined into the average XD-diagrams. Therefore, the diagrams as such do not represent any particular geologic environment but provide a frame of reference, within which more specific geologic examples can be compared. In the following, such comparisons are made between certain provinces and geologic units. The provinces are compared separately for granites, mica schists and amphibolites, which have been sufficiently sampled in different areas of Finland. These rock types provide a good coverage of various genetic and compositional aspects of the Finnish bedrock, and the coverage is further enhanced by the treatment of Wiborg rapakivi massif and Kainuu schist belt as special cases. However, the areal distribution of sample material is not even within the provinces, which may cause some bias in the results of comparisons.

The province subdivision and example formations are depicted in Fig. 19. The southern (I), central (II) and northern (III) provinces represent the Svecokarelidic (Early Proterozoic) rocks of Finland, whereas province IV is formed by the Presvecokarelidic (Archean) basement. The simplified outlines of provinces have been drawn from the geologic maps presented by Simonen (1980). The boundary between provinces I and II has been placed along the northern border of the Svecofennidic schist zone of Tampere. The Presvecokarelidic area (P) also includes a granulite complex, but this interesting area cannot be treated due to a lack of petrophysical data. We shall consider instead the Wiborg rapakivi massif (R) and also the Kainuu schist belt (S) that forms a Svecokarelidic inlier within the Pre-

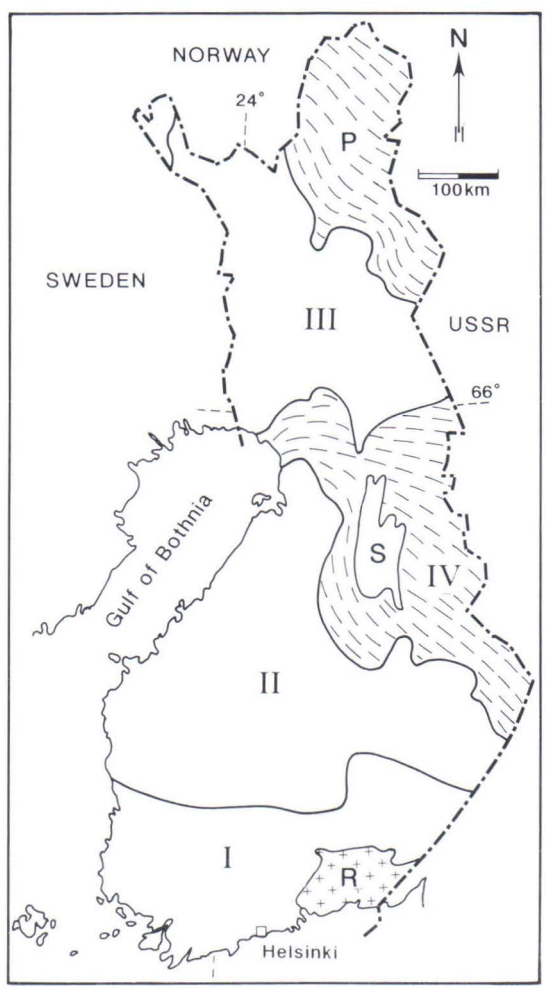

Fig. 19. Province division and location of example formations. Provinces are formed by Svecokarelides of I) southern Finland, II) central Finland, III) northern Finland and by IV) Presvecokarelidic basement. Example formations are R = Wiborg rapakivi massif and S = Svecokarelidic schist belt of Kainuu (with surroundings). P = Presvecokarelidic area in Lapland.

svecokarelidic basement (IV). The areal comparisons will be started with the cumulative susceptibility distributions of example rock types, which are presented according to provinces in Fig. 20.

The distribution curves demonstrate that in Lapland (province III) the mica schists/gneisses and especially the granites are more strongly magnetic than corresponding rocks in other provinces. In the granites of Lapland the proportion of ferrimagnetic samples is more than 70 % and in the mica schists about 50 %, whereas the corresponding proportions are approximately 20 % and 10 % in other provinces. The presence of magnetite in almost all granite samples of Lapland can be seen in Fig. 21, which shows the XD-diagrams of granites in individual provinces compared with the average diagram for granites in Finland. The points in the diagram of province III do not form a paramagnetic XD-line, because even the weakly magnetic granite samples contain small amounts of ferrimagnetic magnetite. For this reason the iron content of Lappish granites cannot be estimated with susceptibility measurements. However, their iron content must be low, because the densities of these granites are also low on all susceptibility values.

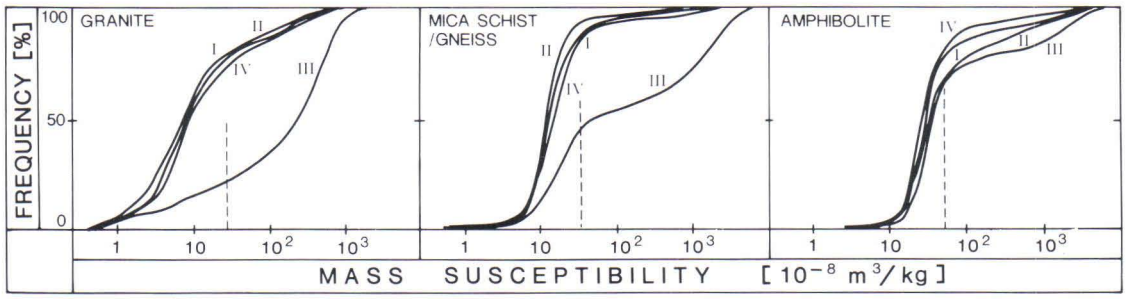

Fig. 20. Cumulative distributions of mass susceptibilities of granites, mica schists/gneisses and amphibolites in provinces I—IV. Dashed lines show limits between para- and ferrimagnetic samples according to Table 3. Numbers of samples as in Figures 21—23.

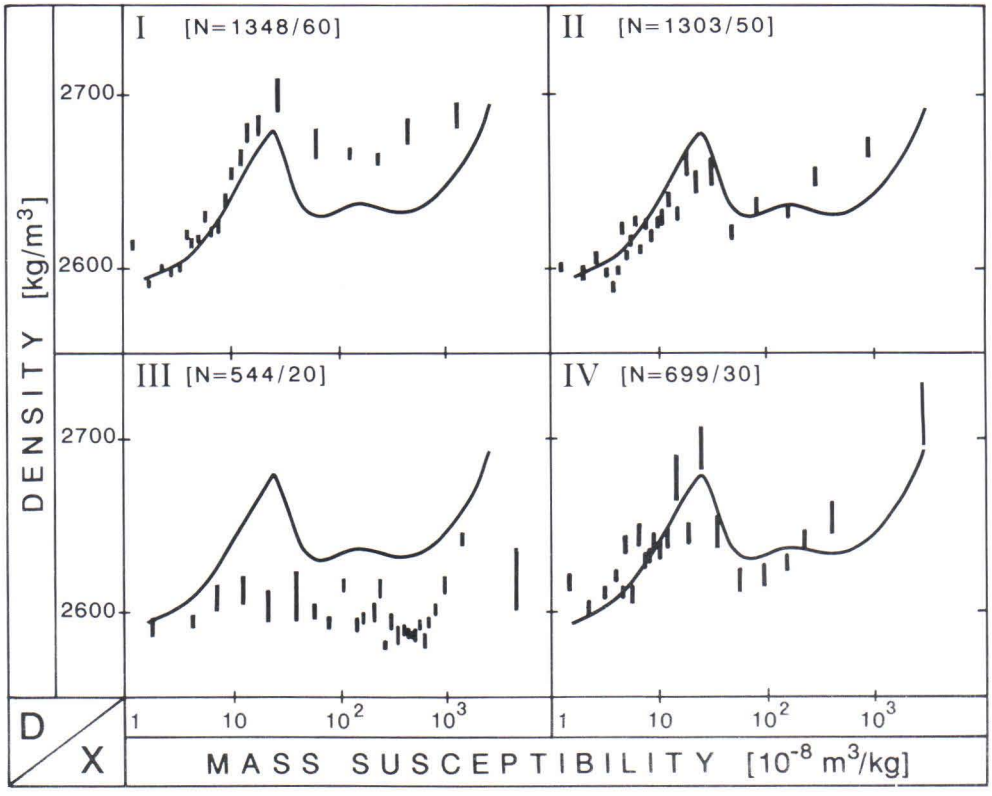

Fig. 21. XD-diagrams of granites in provinces I—IV compared with average XD-curve of all granites in Finland. N = number of samples/size of smoothing group.

In other provinces the XD-data of granites are clearly divided into dominant paramagnetic and minor ferrimagnetic parts. A similar division is observed in the XD-diagrams of mica schists/gneisses (Fig. 22) and amphibolites (Fig. 23). The data points of Figures 21—23 in relation to the average XD-lines qualitatively characterize the areal variation of

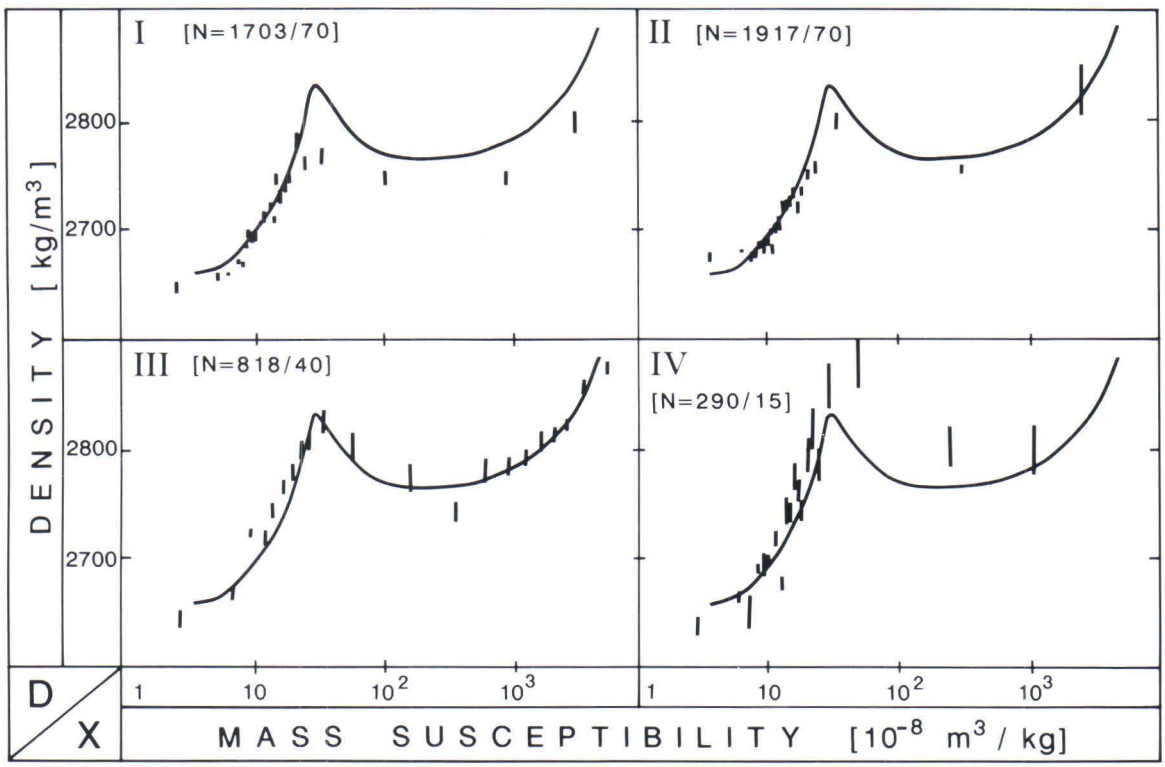

Fig. 22. XD-diagrams of mica schists/gneisses in provinces I—IV compared with average XD-curve of all mica schists/gneisses in Finland. N = number of samples/size of smoothing group.

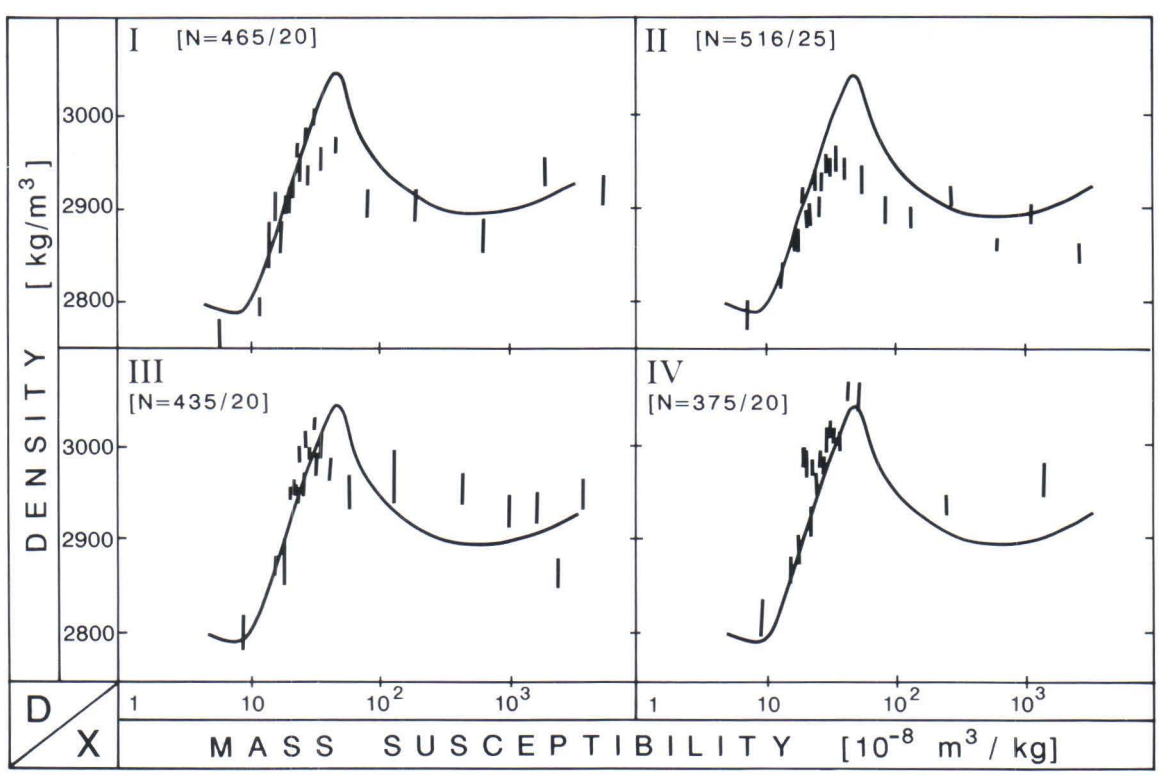

Fig. 23. XD-diagrams of amphibolites in provinces I—IV compared with average XD-curve of all amphibolites in Finland. N = number of samples/size of smoothing group.

iron content in these rocks (and their mafic silicates). Iron and magnetite contents of the rocks have been quantitatively estimated by formulae (1) and (7) after separation of para- and ferrimagnetic samples using the limiting susceptibilities X_b of Table 3. The estimates are presented by provinces in Table 7, which also contains average results from the chemical analyses of these rock types. According to Table 7 the magnetite content (W_m) of granites is on average approximately equal in Lapland and in other provinces, but the proportion (F) of ferrimagnetic samples is clearly largest in Lapland. The distribution of magnetite is thus exceptionally thorough in the granites of Lapland, whereas in other provinces the occurrence of magnetite is more localized and irregular.

Table 7. Average compositions (wt %) of granites (0), mica schists/gneisses (7) and amphibolites (8) in provinces I—IV estimated by petrophysical methods (N samples) and from silicate chemistry (n analyses). Additional explanations in Tables 3 and 6.

ROCK	AREA	W_{Fe}	W_m	F%	N	SiO_2	MgO	TiO_2	Fe	Ox	FM	n
0	I	2.5	0.5	22	1348	72.0	0.43	0.29	1.87	0.30	0.88	48
0	II	2.8	0.5	22	1303	70.6	0.75	0.40	2.14	0.31	0.83	41
0	III	—	0.6	>70	544	73.2	0.35	0.28	1.24	0.58	0.85	14
0	IV	2.9	0.4	26	699	70.0	0.86	0.46	2.43	0.36	0.82	12
7	I	4.7	1.2	12	1703	65.2	2.05	0.76	5.31	0.21	0.81	13
7	II	4.5	1.1	7	1917	64.8	2.80	0.77	4.73	0.21	0.74	28
7	III	5.6	2.3	54	818	56.5	5.14	1.76	7.67	0.33	0.71	9
7	IV	5.2	0.4	11	290	63.2	2.96	0.71	4.97	0.12	0.74	2
8	I	8.5	1.4	20	465	52.3	6.14	1.05	7.51	0.19	0.67	21
8	II	9.0	1.0	32	516	50.1	6.89	1.61	8.50	0.19	0.67	12
8	III	9.9	1.9	32	435	51.3	7.93	1.57	9.05	0.17	0.65	14
8	IV	9.5	0.6	19	375	52.1	8.03	0.62	5.34	0.24	0.52	9

The proportion of ferrimagnetic samples in mica schists/gneisses is also larger in Lapland than in other provinces. In addition, the highest magnetite content of mica schists is observed in northern Finland. The amphibolites of Lapland contain abundant magnetite as well, although the proportion of ferrimagnetic samples is not exceptionally high. The estimates of paramagnetic iron content for each rock type are fairly similar in all provinces. Furthermore, the petrophysical estimates (W_{Fe}) for iron are systematically somewhat higher than the corresponding chemical estimates (Fe), which could be caused by different sample materials. The chemically analysed iron content of granites is clearly lower in Lapland than in other provinces, which is also reflected in the low densities of Lappish granites. The low Fe-content and high SiO_2-content of these granites would have made magnetite formation improbable, because the small amount of iron present could easily have been bound to mafic silicates.

There are, however, three factors favouring magnetite formation in the granites of Lapland: the high oxidation ratio of iron (Ox), the relatively high iron/magnesium-ratio (FM) and the low titanium content. As a result of the high FM-ratio not all iron is consumed by mafic silicates, and due to the low Ti-content only part of the iron can be incorporated into ilmenite (cf. Korsman, 1985). The remaining iron goes into magnetite and possibly also hematite because of the high oxidation ratio. The mica schists/gneisses of Lapland are on average highly oxidized as well, which favours the formation of magnetite. In addition, their low SiO_2-content leaves excess iron from silicates for magnetite generation, but part of the iron forms ilmenite due to the rather high Ti-content of mica schists. In the amphibolites no clear differences are observed between the provinces in the appearance of magnetite or the oxidation state of iron. Because the amphibolites often represent mantle-derived basic material, significant areal variations are not expected. After these physico-chemical considerations we shall try to find some geologic explanations for the common presence of magnetite in Lapland.

The oxidation ratio of iron (0.58) in the Lappish granites is even higher than the average ratio (0.53) in the sedimentogenous quartzites of Finland (cf. Table 2). In the metasediments studied by Chinner (1960) the largest proportion of iron was tied to magnetite, when the oxidation ratio varied in the range 0.4—0.6. The most highly oxidized sedimentary formations are represented by hematite stained red beds, which have mainly originated in terrestrial oxide facies conditions (see McIntyre, 1980). This kind of terrestrial environment may have originally characterized the Karelidic schist zones of Lapland, which now con-

tain abundant quartzites (Simonen, 1980). On the other hand, a marine environment probably characterized the development of Svecofennidic schist zones of southern Finland. These geotectonic environments are in harmony with the observed distribution of magnetite, which indicates oxidizing conditions for Lapland. The common appearance of magnetite in the granites and mica schists of Lapland could reflect inheritance from evenly oxidized protoliths. Alternatively, the distribution of magnetite could have been homogenized by differentiation or convective mixing of granitic magma.

The large granitoid area of central Lapland has undergone partial anatexis and in many places the massive granites grade into migmatites (Lauerma, 1982). Therefore, the even distribution of magnetite is probably not due to mixing or differentiation of magma, but seems rather to require homogeneously oxidized source material. Oxidized iron, generally in the form of hematite, is often abundant in extensive and thick sedimentary formations. Such sedimentary material could be transformed into granites when material from the earth's surface is buried deeper in the crust. In the oxygen-poor crust the oxidized sedimentary material tries to attain a new equilibrium (see McIntyre, 1980), and thus hematite could be reduced into magnetite in the granites. On the other hand, when iron silicates are brought from the crust closer to the oxygen-rich surface, silicates can partially decompose into iron oxides, as the new equilibrium is approached.

According to Sm-Nd isotopic studies (Huhma, 1986) the granitoids of Lapland derive largely from reworked Archean crust, whereas the contribution of Archean material is only minimal in the granitoids of southern and central Finland. If the granitoids of Lapland, as metamorphic rocks elsewhere (see McIntyre, 1980), have inherited their oxidation state from their protoliths, then this implies that the iron of the Archean source material has been highly oxidized. Table 7 indicates however, that iron is not very highly oxidized in the Archean rocks of province IV. Therefore, the oxidized iron is probably derived from sediments formed on the surface of Archean crust. When these sediments were later buried deeper in the crust, the material could have melted and crystallized into magnetite-bearing granite. The mica schists/gneisses of Lapland also contain older crustal material that appears to be partially of Archean origin (Huhma, 1986). The oxidized iron and abundant magnetite of the mica schists could then be derived from a common source with the granites of Lapland.

The granites of southern and central Finland contain on average more iron than the granites of Lapland (Table 7). The abundance of iron can indicate a strong interaction between crust and mantle during formation of rocks (Grant, 1985), and the isotope studies of Huhma (1986) also indicate that granitoids in central and southern Finland consist largely of newly mantle-derived material, with only a minor admixture of older continental crust. The small proportion of oxidized terrestrial material might explain the low oxidation ratio of iron and the scarce and patchy occurrence of magnetite in the granites of southern and central Finland. If the interpretations above are correct, then the oxidation state of iron seems to carry information about the composition of source rocks even through intensive geologic processes, just as do many isotopic systems.

The rapakivi granites of southern Finland have originated in the lower crust as suggested by their close association with mantle-derived mafic rocks (Simonen, 1980), and the Wiborg rapakivi massif was later intruded at a shallower level of only a few kilometers (see Vorma, 1971). The cumulative susceptibility distributions and XD-diagrams of Wiborg rapakivi varieties are compared in Fig. 24 with the corresponding average curves for granites in Finland. The somewhat ambiguous limiting susceptibility between para- and ferrimagnetic rapakivi samples (cf. Fig. 4) is close to letter R on the cumulative distribution curve (Fig. 24A). This limit indicates a high proportion (about 50 %) for the ferrimagnetic samples, but the average magnetite content of Wiborg rapakivi massif is only 0.1 wt %.

The XD-points of Wiborg rapakivi varieties are all clearly located below the average paramagnetic XD-line of granites. This suggests that mafic silicates of rapakivi granites are exceptionally iron-rich, which is consistent with mineralogic observations (see Simonen & Vorma, 1969). Partial decomposition of iron-rich silicates often produces very fine-grained iron oxides, which possibly happened as the rapakivi massif was rising toward the surface and the biotite as well as hornblende attempted to re-equilibrate. Fine-grained magnetite is indicated by the high average Q-ratio (6.7) that characterizes the Wiborg rapakivi samples. The iron oxides of rapakivi granites have been thoroughly studied in the Wolf River massif (Anderson, 1980), where magnetite formed partially during magmatic crystallization, but commonly also in retrograde reactions under subsolidus conditions.

The even distribution of magnetite in the granites of province III is in good accordance with the aeromagnetic map of Finland (Korhonen, 1980), as the areally largest positive

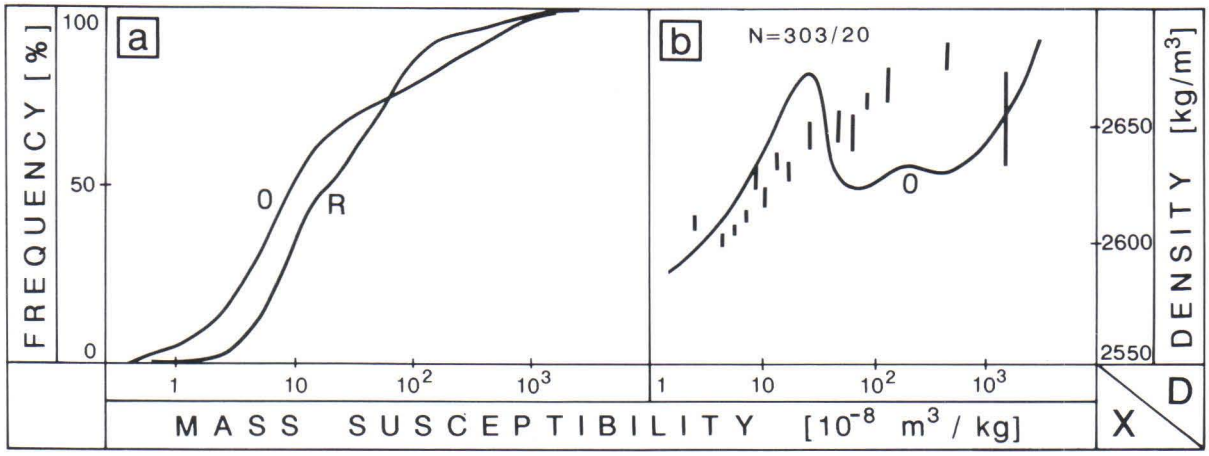

Fig. 24. A) Cumulative susceptibility distributions and B) XD-diagrams of Wiborg rapakivi varieties (R) compared with average curves (0) of all granites in Finland. N = number of rapakivi samples/size of smoothing group.

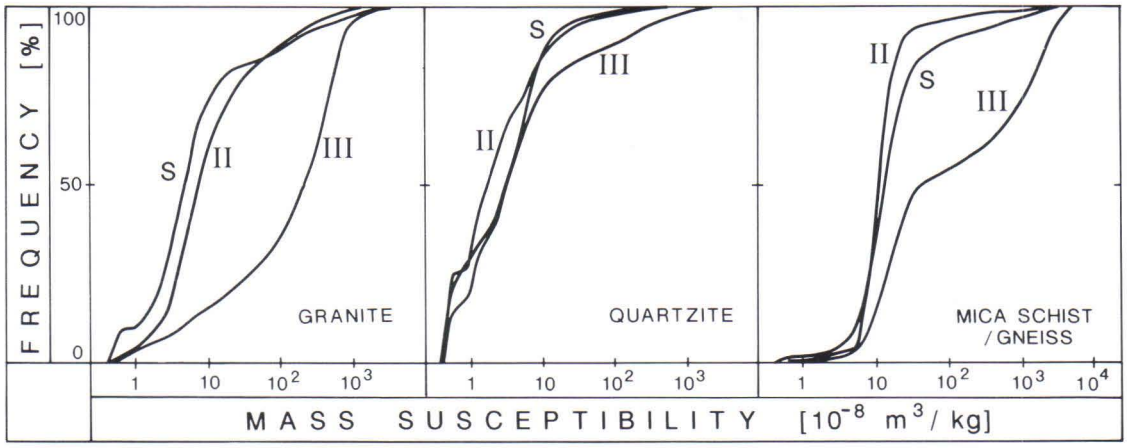

Fig.25. Cumulative susceptibility distributions of granites (349 samples), quartzites (929 samples) and mica schists/gneisses (811 samples) in Kainuu schist belt (S) compared with corresponding distributions in provinces II and III.

anomaly of the magnetic field is associated with the granites of central Lapland. Based on the similarity of regional magnetic anomalies, Korhonen (1981) connects the Kainuu schist belt and its surroundings with the magnetic area of central Lapland. The Kainuu schist area is located within the Presvecokarelidic basement as a Svecokarelian inlier composed of granites, quartzites and mica schists/gneisses (see Fig. 19). The cumulative susceptibility distributions of these rocks are presented in Fig. 25, which also shows the corresponding distributions for provinces II and III. On the basis of susceptibility distributions the rocks of Kainuu schist area differ from the corresponding rocks of province III in Lapland and resemble more the rocks of province II. Because the samples collected from the outcrops of Kainuu area are rather weakly magnetic, the aeromagnetic anomaly above Kainuu schist belt can be explained only after more strongly magnetic rocks have been identified beneath the overburden or deeper in the bedrock.

CONCLUDING REMARKS

The preceding interpretations of petrophysical results were made assuming that magnetite is formed either by incorporating oxidized iron from the earth's surface deeper into the crust or by bringing iron closer to the surface to be oxidized, which makes magnetite for-

mation possible at very different depths. This line of thinking differs somewhat from the interpretation presented by Ishihara (1977). He suggests that magnetite series granitoids are generated at great depth (upper mantle to lower crust), where the granitoid magma has avoided interaction with reducing crustal carbon and is principally oxidized by the dissociation of water and preferential escape of hydrogen. The ilmenite series granitoids that are weakly magnetic, have originated at a shallower level, where magnetite formation is inhibited by the reducing effect of crustal carbon. Ishihara (1977) thus emphasizes the reducing role of carbon in the formation of magnetite, whereas in the present work the significance of oxidized iron is stressed. This difference in emphasis is due to the restricted development of carbonaceous geologic environments in the bedrock of Finland.

The magnetite-series granitoids of Ishihara (1977) were generated at great depths in the lower crust, and the strongly magnetic granitoids of Pecherskiy (1965) were intruded into a fractured environment at a depth of about 1 km. Both these types of magnetic granitoids are in accordance with the preceding interpretations. The magnetic granites of Nattanen-type in Lapland were emplaced at shallow levels (Haapala et al., 1987), where part of their magnetite was possibly formed through re-equilibration of iron silicates. The magnetic granitoids of Lapland cover large areas in Sweden as well, and it would be advantageous to study these granites as a whole. The petrophysical investigations of magnetic granites and other rock units should be continued with the aid of carefully selected sample materials, which should be studied chemically and especially under microscope. Further investigations are also needed to verify how well the oxidation ratio of iron in rocks reflects the composition of source material. However, Tuominen (1961) already observed from the magnetic maps of the Orijärvi area that the oxidation state of source rocks had been preserved after granodioritization.

In conclusion, the susceptibility and density data of geologic units should be summarized into XD-diagrams, which can be used to identify the para- and ferrimagnetic parts of the units. The mere identification of these parts makes it possible to more precisely plan petrologic investigations of magnetite in relation to mafic silicates. The susceptibility measurements of geologic units provide average estimates for the magnetite content of ferrimagnetic samples by relation (1) and the total iron content of paramagnetic samples by relation (7). The relative proportion of magnetite-bearing samples can be estimated from the cumulative susceptibility distributions. This proportion characterizes the mode of occurrence of magnetite and the oxidation ratio of iron, which in turn reflects formation conditions of geologic units and magnetite. Local variations in magnetite content can be mapped directly at outcrop scale with the aid of portable susceptibility meters. When the association of magnetite with other minerals is finally determined under microscope, the crystallization history of geologic units can be traced (Sanderson, 1974).

Samples can be more easily chosen for microscopic studies when, in addition to susceptibilities, the remanences are measured and Q-ratios calculated. High values of Q-ratio help to identify the samples that carry fine-grained iron oxides, which have often been formed during secondary alteration processes. The samples with high Q-ratios are generally characterized by low contents of magnetite and high amounts of mafic minerals. On the XD-diagrams these samples are located in the shifting region between the paramagnetic and ferrimagnetic parts of XD- paths. The paramagnetic XD-lines reflect the total iron content of rocks and also the relative abundance of iron in mafic minerals. If the XD-line of some geologic unit is situated below the average XD-line for that rock type in Finland (Fig. 15), then the mafic minerals of the unit are exceptionally iron-rich. The densities of rocks depend on their SiO_2-contents or the abundances of mafic minerals, but these dependences are only approximately known. Better definition of these relations would require combined petrophysical, chemical and mineralogic analysis of representative sample materials.

The petrophysical method simultaneously offers mineralogic estimates for the grain size and abundance of magnetite as well as chemical estimates for the iron content of rocks and mafic minerals. The method is thus well suited for petrologic studies of magnetite, and such studies are necessary in developing the geologic interpretation of (aero)magnetic maps. Susceptibility plays a central part in this methodology, and a sensitive susceptibility meter (resolution better than 10^{-9} m^3/kg) is needed for accurate measurement of paramagnetic rocks. The usefulness of the petrophysical techniques demonstrated in this work will be tested only with the aid of thoroughly studied case histories. In any case, the petrophysical data as such form a sound basis for quantitative geophysical interpretations.

ACKNOWLEDGEMENTS

Maunu Puranen initiated the petrophysical research in Finland, and he also encouraged throughout the course of this work. Petrologic interpretation of the data was emphasized as a result of several discussions with the late Pentti Rehtijärvi. The final stages of reporting were sped up by Seppo Elo, who bravely listened to endless petrophysical considerations. The manuscript was constructively reviewed by Ilmo Kukkonen and Pekka Nurmi. Processing of petrophysical data would have been very tedious without the computer programs written by Hannu Hongisto and Meri-Liisa Airo. The figures were skillfully drafted by Kirsti Blomster and the English of manuscript was corrected by Peter Ward. The geologists of Petrologic department showed a fine spirit of co-operation by lending both support and samples. To all these persons I want to express my sincere gratitude.

REFERENCES

Akimoto, S., Horai,K. & Boku, T., 1958. Magnetic susceptibility of orthopyroxenes. J. Geomagn. Geoelectr. 10: 7—11.

Anderson, J.L., 1980. Mineral equilibria and crystallization conditions in the Late Precambrian Wolf River rapakivi massif, Wisconsin. Am. J. Sci. 280: 289—332.

Balsley, J.R. & Buddington, A.F., 1958. Iron-titanium oxide minerals, rocks, and aeromagnetic anomalies of the Adirondack area, New York. Econ. Geol. 53 (7): 777—805.

Best, M.G., 1982. Igneous and metamorphic petrology. W.H. Freeman and Company, New York. 630 p.

Beus, A.A. , 1976. Geochemistry of the lithosphere. Mir Publishers, Moscow. 366 p.

Bleaney, B.I. & Bleaney, B., 1976. Electricity and magnetism. Oxford University Press, Oxford: p. 456.

Chernyuk, M.V., 1971. Distribution of the magnetic susceptibility values of intrusive rocks. Phys. Solid Earth 3: 225—229.

Chevallier, R. & Martin, R., 1959. Le moment magnétique de l'ion ferreux dans une série de pyroxènes monocliniques. Bull. Soc. chim. France: 9—10.

Chevallier, R. & Mathieu, S., 1958. Susceptibilité magnétique spécifique de pyroxénes monocliniques. Bull. Soc. chim. France 5: 726—729.

Chinner, G.A., 1960. Pelitic gneisses with varying ferrous/ferric ratios from Glen Clova, Angus, Scotland. J. Petrol. 1 (2): 178—217.

Clark, D.A., 1983. Comments on magnetic petrophysics. Bull. Aust. Soc. Explor. Geophys. 14: 49—62.

Cornwell, J.D., 1975. The magnetization and densities of Precambrian rocks and iron-ores of northern Sweden. Geoexploration 13: 201—214.

Criss, R.E. & Champion, D.E., 1984. Magnetic properties of granitic rocks from the southern half of the Idaho Batholith: Influences of hydrothermal alteration and implications for aeromagnetic interpretation. J. Geophys. Res. 89 (B8): 7061—7076.

Deer, W.A., Howie, R.A. & Zussman, J., 1962. Rock-forming minerals 3: Sheet silicates. Longmans, London. 270 p.

Deer, W.A., Howie, R.A. & Zussman, J., 1962a. Rock-forming minerals 5: Non-silicates. Longmans, London. 371 p.

Deer, W.A., Howie, R.A. & Zussman, J., 1963. Rock-forming minerals 2: Chain silicates. Longmans, London. 379 p.

Dortman, N.B., 1976. Fiziceskie svoistva gornich porod i polesnich iskopaemych (petrofisika). Nedra, Moskva. 527 p.

Dudarev, A.N., 1964. Magnetic properties of country rock and ores in the Altay-Sayan region. Intern. Geol. Rev. 6 (12): 2127—2131.

Emerson, D.W., 1979. Comments on applied magnetics in mineral exploration. Bull. Aust. Soc. Explor. Geophys. 10 (1): 3—5.

Enmark, T. & Nisca, D.H., 1983. The Gallejaur intrusion in northern Sweden — a geophysical study. GFF 105: 287—300.

Feniak, M.W., 1944. Grain sizes and shapes of various minerals in igneous rocks. Am. Mineral. 29: 415—421.

Fox, P.J. & Opdyke, N.D., 1973. Geology of the oceanic crust: magnetic properties of oceanic rocks. J. Geophys. Res. 78 (23): 5139—5154.

Grant, F.S., 1985. Aeromagnetics, geology and ore environments, I. Magnetite in igneous, sedimentary and metamorphic rocks: an overview. Geoexploration 23: 303—333.

Gupta, V.K. & Burke, K.B.S., 1977. Density and magnetic susceptibility measurements in southeastern New Brunswick. Can. J. Earth Sci. 14: 128—132.

Haapala, I., Front, K., Rantala, E. & Vaarma, M., 1987. Petrology of Nattanen-type granite complexes, northern Finland. Precambrian Res. 35: 225—240.

Hageskov, B., 1984. Magnetic susceptibility used in mapping of amphibolite facies recrystallisation in basic dykes. Tectonophysics 108: 339—351.

Haggerty, S.E., 1976. Opaque mineral oxides in terrestrial igneous rocks. In D. Rumble III (ed.): Oxide Minerals. Mineral. Soc. Am. Short Course Notes: Hg101—Hg300.

Henkel, H., 1976. Studies of density and magnetic properties of rocks from northern Sweden. Pageoph 114: 235—249.

Henkel, H. & Guzmán, M., 1977. Magnetic features of fracture zones. Geoexploration 15: 173—181.
Huhma, H., 1986. Sm-Nd, U-Pb and Pb-Pb isotopic evidence for the origin of the Early Proterozoic Svecokarelian crust in Finland. Geol. Surv. Finland, Bull. 337: 48 p.
Imaoka, T. & Nakashima, K., 1983. Temporal and spatial variations of magnetic susceptibility of Cretaceous to Neogene igneous rocks from the central and western Chugoky Province, Japan. J. Sci. Hiroshima Univ., Ser. C (8): 1—30.
Irving, E., Molyneux, L. & Runcorn, S.K., 1966. The analysis of remanent intensities and susceptibilities of rocks. Geophys. J. R. astron. Soc. 10 (5): 451—464.
Ishihara, S., 1977. The magnetite-series and ilmenite-series granitic rocks. Min. Geol. 27: 293—305.
Ishihara, S., 1981. The granitoid series and mineralization. Econ. Geol., 75th Anniv. Volume: 458—484.
Jäger, W. & Kopf, M., 1975. Dichte- und Suszeptibilitätswerte von Gesteinen aus dem Gebiet Südskandinaviens. Gerlands Beitr. Geophys. 84 (3/4): 297—310.
Kopf, M., 1976. Zur Anwendung der Petrophysik in der Petrographie. Z. geol. Wiss. 4 (7): 1049—1067.
Korhonen, J., 1980. The aeromagnetic map of Finland. Geol. Surv. Finland, Espoo.
Korhonen, J., 1981. Major structures of the bedrock as revealed by aeromagnetic maps. In K. Puustinen (ed.): Geological, geochemical and geophysical investigations in the eastern part of the Baltic Shield. The Committee for Scientific and Technical Co-operation between Finland and the Soviet Union, Helsinki. Pp. 71—85.
Korsman, K., 1985. Metamorfiset vyöhykkeet ja metamorfoosin merkitys. Abstract: Metamorphic zones and the significance of metamorphism. In K. Puustinen (ed.): Geologiaa geofyysikoille. Geol. Surv. Finland, Rep. Invest. 69: 21—28.
Krutikhovskaya, Z.A., Silina, I.M., Bondareva, N.M. & Podolyanko, S.M., 1979. Relation of magnetic properties of the rocks of the Ukrainian Shield to their composition and metamorphism. Can. J. Earth Sci. 16: 984—991.
Kukkonen, I., Sarapää, O & Heino, T., 1985. Mustaliuskeiden synty, koostumus ja esiintyminen. Abstract: Black schists, their origin, composition and occurrence. In K. Puustinen (ed.): Geologiaa geofyysikoille. Geol. Surv. Finland, Rep. Invest. 69: 70—84.
Lapointe, P., Morris, W.A. & Harding, K.L., 1986. Interpretation of magnetic susceptibility: a new approach to geophysical evaluation of the degree of rock alteration. Can. J. Earth Sci. 23: 393—401.
Lauerma, R., 1982. On the ages of some granitoid and schist complexes in northern Finland. Bull. Geol. Soc. Finland 54: 85—100.
Laurila, E., 1964. A new instrument for determination of magnetite content of powdered samples. Acta Polytech. Scand., Chem. Incl. Metall. Ser. 30: 19 p.
Lauterbach, R., 1959. Vorwort. Geophysik und Geologie 1: 1.
Lidiak, E.G., 1974. Magnetic characteristics of some Precambrian basement rocks. J. Geophys. 40: 549—564.
Lokka, L., 1934. Neuere chemische Analysen von finnischen Gesteinen. Bull. Comm. géol. Finlande 105: 64 p.
Lokka, L., 1950. Chemical analyses of Finnish rocks. Bull. Comm. géol. Finlande 151: 75 p.
Magnusson, K.-Å., 1983. A petrophysical and paleomagnetic study of the Nordingrå region in eastern Sweden. Sver. Geol. Unders., Ser. C (801): 70 p.
McIntyre, J.I., 1980. Geological significance of magnetic patterns related to magnetite in sediments and metasediments — a review. Bull. Aust. Soc. Explor. Geophys. 11 (1/2): 19—33.
Mooney, H. M., 1952. Magnetic susceptibility measurements in Minnesota. Part I: Technique of measurement. Geophysics 17 (3): 531—543.
Mooney, H.M. & Bleifuss, R., 1953. Magnetic susceptibility measurements in Minnesota. Part II: Analysis of field results. Geophysics 18: 383—393.
Mutton, A.J. & Shaw, R.D., 1979. Physical property measurements as an aid to magnetic interpretation in basement terrains. Bull. Aust. Soc. Explor. Geophys. 10 (1): 79—91.
Nagata, T., 1961. Rock Magnetism. Maruzen Company, Tokyo. 350 p.
Nagata, T., Yukutake, T. & Uyeda, S., 1957. On magnetic susceptibility of olivines. J. Geomagn. Geoelectr. 9: 51—56.
Okko, V., 1964. Maaperä. In K. Rankama (ed.): Suomen geologia. Kirjayhtymä, Helsinki: p. 243.
Osborn, E.F., 1962. Reaction series for subalkaline igneous rocks based on different oxygen pressure conditions. Am. Mineral. 47: 211—226.
Parasnis, D.S., 1973. Mining Geophysics. Elsevier, Amsterdam. 395 p.
Parry, L.G., 1965. Magnetic properties of dispersed magnetite powders. Philos. Mag. 11: 303—312.
Paterson, N.R. & Reeves, C.V., 1985. Applications of gravity and magnetic surveys: The state-of-the-art in 1985. Geophysics 50 (12): 2558—2594.
Pecherskiy, D.M., 1965. Statistical analysis of the reasons for the varying magnetization of the granitoids of the Verkhoyansk-Chukotka fold region and the Okhotsk-Chukotka volcanic belt. Intern. Geol. Rev. 7(11): 1963—1976.
Pesonen, L.J. & Stigzelius, E., 1972. On petrophysical and paleomagnetic investigations of the gabbros of the Pohjanmaa region, Middle-West Finland. Geol. Surv. Finland, Bull. 260: 27 p.
Pulkkinen, E., Puranen, R. & Lehmuspelto, P., 1980. Interpretation of geochemical anomalies in glacial drift of Finnish Lapland with the aid of magnetic susceptibility data. Geol. Surv. Finland, Rep. Invest. 47: 39 p.
Puranen, M., 1978. Fluxgate-tyyppinen mittauslaite kivinäytteiden remanenssimagnetismin tutkimista varten (Oersted-mittari). Summary: Fluxgate type instrument for measurement of remanent magnetization of rock samples. Geol. Surv. Finland, Interim Rep. Q16.1/27.2/78/1: 24 p.
Puranen, M., Marmo, V. & Hämäläinen, U., 1968. On the geology, aeromagnetic anomalies and susceptibilities of Precambrian rocks in the Virrat region (Central Finland). Geoexploration 6: 163—184.
Puranen, M. & Puranen, R., 1977. Apparatus for the measurement of magnetic susceptibility and its anisotropy. Geol. Surv. Finland, Rep. Invest. 28: 46 p.
Puranen, R., 1976. Magneettisen suskeptibiliteetin ja tiheyden sisältämästä geologisesta informaatiosta. Summary: On the geological significance of magnetic susceptibility and density. Geologi 28 (4/5): 59—63.
Puranen, R., 1977. Magnetic susceptibility and its anisotropy in the study of glacial transport in northern Finland. Prospecting in Areas of Glaciated Terrain 1977. IMM, London: 111—119.
Puranen, R., Elo, S. & Airo, M.-L., 1978. Geological and areal variation of rock densities, and their relation to some gravity anomalies in Finland. Geoskrifter 10: 123—164.

Puranen, R. & Sulkanen, K., 1985. Technical description of microcomputer-controlled petrophysical laboratory. Geol. Surv. Finland, Interim Rep. Q15/27/85/1: 252 p.

Puzicha, K., 1942. Der Magnetismus der Gesteine als Funktion ihres Magnetitgehaltes. Beitr. Angew. Geophys. 9 (2): 158—186.

Rumble, D. III, 1976. Oxide minerals in metamorphic rocks. In D. Rumble III (ed.): Oxide Minerals. Mineral. Soc. Am. Short Course Notes: R1-R24.

Sanderson, D.D., 1974. Spatial distribution and origin of magnetite in an intrusive igneous mass. Geol. Soc. Am. Bull. 85: 1183—1188.

Schön, J., 1983. Petrophysik. Ferdinand Enke Verlag, Stuttgart. 405 p.

Sederholm, J.J., 1925. The average composition of the Earth's crust in Finland. Bull. Comm. géol. Finlande 70: 20 p.

Simonen, A., 1980. The Precambrian in Finland. Geol. Surv. Finland, Bull. 304: 58 p.

Simonen, A. & Vorma, A., 1969. Amphibole and biotite from rapakivi. Geol. Surv. Finland, Bull. 238: 28 p.

Speer, J.A., 1981. The nature and magnetic expression of isograds in the contact aureole of the Liberty Hill pluton, South Carolina: Summary. Geol. Soc. Am. Bull. 92: 603—609.

Stacey, F.D., 1967. The Koenigsberger ratio and the nature of thermoremanence in igneous rocks. Earth Planet. Sci. Lett. 2: 67—68.

Stacey, F.D. & Banerjee, S.K., 1974. The physical principles of rock magnetism. Elsevier, Amsterdam. 195 p.

Subrahmanyam, C. & Verma, R.K., 1981. Densities and magnetic susceptibilities of Precambrian rocks of different metamorphic grade (Southern Indian Shield). J. Geophys. 49: 101—107.

Syono, Y., 1960. Magnetic susceptibility of some rock forming silicate minerals such as amphiboles, biotites, cordierites and garnets. J. Geomagn. Geoelectr. 11: 85—93.

Tarling, D.H., 1966. The magnetic intensity and susceptibility distribution in some Cenozoic and Jurassic basalts. Geophys. J. 11 (4): 423—431.

Tuominen, H.V., 1961. The structural position of the Orijärvi granodiorite and the problem of synkinematic granites. Bull. Comm. géol. Finlande 196: 499—515.

Vernon, R.H., 1961. Magnetic susceptibility as a measure of total iron plus manganese in some ferromagnesian silicate minerals. Am. Mineral. 46: 1141—1153.

Vorma, A ., 1971. Alkali feldspars of the Wiborg rapakivi massif in southeastern Finland. Bull. Comm. géol. Finlande 246: 72 p.

Wenk, H.-R. & Wenk, E., 1969. Physical constants of Alpine rocks (density, porosity, specific heat, thermal diffusivity and conductivity). Beitr. Geol. Schweiz, Kleinere Mitt. 45: 343—357.

Werner, S., 1945. Determinations of the magnetic susceptibility of ores and rocks from Swedish iron ore deposits. Sver. Geol. Unders., Ser. C (472): 79 p.

Westerlund, K., 1973. Instruction manual for the susceptibility meter of Geological Survey of Finland. Geol. Surv. Finland, Interim Rep. Q16.1/27.2/73/9: 14 p.

Wones, D.R., & Eugster, H.P., 1965. Stability of biotite: Experiment, theory, and application. Am. Mineral. 50: 1228—1272.

Yudin, B.A. & Katseblin, P.L., 1981. Petrophysical characteristics of gabbro-labradorite complexes, Kola Peninsula. Intern. Geol. Rev. 23 (5): 517—523.

SOURCE REFERENCES FOR MINERALOGIC DATA

Bergman, L., 1981. Geological map of Finland 1:100000, Sheets 0034 + 0043 Signilskär, 1012 Mariehamn and 1021 Geta. Geological Survey of Finland, Explanation to the maps of Pre-Quaternary rocks: 72 p.

Ehlers, C. & Ehlers, M., 1981. Geological map of Finland 1:100000, Sheet 1023 Kumlinge. Geological Survey of Finland, Explanation to the maps of Pre-Quaternary rocks: 60 p.

Härme, M., 1978. Geological map of Finland 1:100000, Sheets 2043 Kerava and 2044 Riihimäki. Geological Survey of Finland, Explanation to the maps of rocks: 51 p.

Huhma, A., 1975. Geological map of Finland 1:100000, Sheets 4222 Outokumpu, 4224 Polvijärvi and 4311 Sivakkavaara. Geological Survey of Finland, Explanation to the maps of rocks: 151 p.

Huhma, A., Salli, I. & Matisto, A., 1952. Geological map of Finland 1:100000, Sheet 2122 Ikaalinen. Geological Survey of Finland, Explanation to the map of rocks: 74 p.

Hyppönen, V., 1983. Geological map of Finland 1:100000, Sheets 4411 Ontojoki, 4412 Hiisijärvi and 4413 Kuhmo. Geological Survey of Finland, Explanation to the maps of Pre-Quaternary rocks: 60 p.

Korsman, K. & Lehijärvi, M., 1973. Geological map of Finland 1:100000, Sheet 3144 Sulkava. Geological Survey of Finland, Explanation to the map of rocks: 24 p.

Laitakari, I., 1980. Geological map of Finland 1:100000, Sheet 2134 Lammi. Geological Survey of Finland, Explanation to the maps of Pre-Quaternary rocks: 34 p.

Laitakari, I. & Simonen, A., 1963. Geological map of Finland 1:100000, Sheet 3022 Lapinjärvi. Geological Survey of Finland, Explanation to the map of rocks: 48 p.

Laitala, M., 1961. Geological map of Finland 1:100000, Sheet 2032 Siuntio. Geological Survey of Finland, Explanation to the map of rocks: 32 p.

Laitala, M., 1984. Geological map of Finland 1:100000, Sheets 3012 Pellinki and 3021 Porvoo. Geological Survey of Finland, Explanation to the maps of Pre-Quaternary rocks: 53 p.

Lehijärvi, M., 1957. Geological map of Finland 1:100000, Sheet 2021 Salo. Geological Survey of Finland, Explanation to the map of rocks: 31 p.

Lehijärvi, M., 1962. Geological map of Finland 1:100000, Sheet 2133 Kärkölä. Geological Survey of Finland, Explanation to the map of rocks: 26 p.

Lehijärvi, M., 1964. Geological map of Finland 1:100000, Sheet 3111 Lahti. Geological Survey of Finland, Explanation to the map of rocks: 40 p.

Lehijärvi, M., 1979. Geological map of Finland 1:100000, Sheet 3112 Heinola. Geological Survey of Finland, Explanation to the maps of Pre-Quaternary rocks: 25 p.

Lehijärvi, M., 1980. Geological map of Finland 1:100000, Sheet 3121 Sysmä. Geological Survey of Finland, Explanation to the maps of Pre-Quaternary rocks: 25 p.

Lehtonen, M., 1984. Geological map of Finland 1:100000, Sheet 2723 Muonio. Geological Survey of Finland, Explanation to the maps of Pre-Quaternary rocks: 71 p.

Marmo, V., 1963. Geological map of Finland 1:100000, Sheet 2232 Keuruu. Geological Survey of Finland, Explanation to the map of rocks: 55 p.

Marmo, V., 1965. Geological map of Finland 1:100000, Sheet 2214 Virrat. Geological Survey of Finland, Explanation to the map of rocks: 63 p.

Matisto, A., 1961. Geological map of Finland 1:100000, Sheet 2213 Kuru. Geological Survey of Finland, Explanation to the map of rocks: 40 p.

Matisto, A., 1971. Geological map of Finland 1:100000, Sheet 2121 Vammala. Geological Survey of Finland, Explanation to the map of rocks: 44 p.

Neuvonen, K.J., 1956. Geological map of Finland 1:100000, Sheet 2113 Forssa. Geological Survey of Finland, Explanation to the map rocks: 39 p.

Neuvonen, K.J., 1971. Geological map of Finland 1:100000, Sheet 2324 Kannus. Geological Survey of Finland, Explanation to the map of rocks: 28 p.

Nykänen, O., 1959. Geological map of Finland 1:100000, Sheets 2441 Raahe and 2443 Paavola. Geological Survey of Finland, Explanation to the maps of rocks: 38 p.

Nykänen, O., 1960. Geological map of Finland 1:100000, Sheet 1242 Korsnäs. Geological Survey of Finland, Explanation to the map of rocks: 34 p.

Nykänen, O., 1963. Geological map of Finland 1:100000, Sheet 2334 Kinnula. Geological Survey of Finland, Explanation to the map of rocks: 42 p.

Nykänen, O., 1968. Geological map of Finland 1:100000, Sheet 4232 + 4234 Tohmajärvi. Geological Survey of Finland, Explanation to the map of rocks: 68 p.

Nykänen, O., 1971. Geological map of Finland 1:100000, Sheet 4241 Kiihtelysvaara. Geological Survey of Finland, Explanation to the map of rocks: 68 p.

Nykänen, O., 1975. Geological map of Finland 1:100000, Sheets 4213 Kerimäki and 4231 Kitee. Geological Survey of Finland, Explanation to the maps of rocks: 45 p.

Nykänen, O., 1983. Geological map of Finland 1:100000, Sheets 4124 + 4142 Punkaharju and 4123 + 4114 Parikkala. Geological Survey of Finland, Explanation to the maps of Pre-Quaternary rocks: 81 p.

Paavola, J., 1984. Geological map of Finland 1:100000, Sheet 3334 Nilsiä. Geological Survey of Finland, Explanation to the maps of Pre-Quaternary rocks: 57 p.

Pipping, F., 1972. Geological map of Finland 1:100000, Sheet 3311 Viitasaari. Geological Survey of Finland, Explanation to the map of rocks: 23 p.

Salli, I., 1953. Geological map of Finland 1:100000, Sheet 2111 Loimaa. Geological Survey of Finland, Explanation to the map of rocks: 41 p.

Salli, I., 1965. Geological map of Finland 1:100000, Sheets 2432 Pyhäjoki and 2434 Vihanti. Geological Survey of Finland, Explanation to the maps of rocks: 52 p.

Salli, I., 1967. Geological map of Finland 1:100000, Sheets 2341 Lestijärvi and 2343 Reisjärvi. Geological Survey of Finland, Explanation to the maps of rocks: 43 p.

Simonen, A., 1949. Geological map of Finland 1:100000, Sheet 2131 Hämeenlinna. Geological Survey of Finland, Explanation to the map of rocks: 45 p.

Simonen, A., 1956. Geological map of Finland 1:100000, Sheet 2024 Somero. Geological Survey of Finland, Explanation to the map of rocks: 31 p.

Simonen, A., 1982. Geological map of Finland 1:100000, Sheets 3123 Mäntyharju and 3142 Mikkeli. Geological Survey of Finland, Explanation to the maps of Pre-Quaternary rocks: 36 p.

Simonen, A. & Tyrväinen, A., 1981. Geological map of Finland 1:100000, Sheet 3132 Savitaipale. Geological Survey of Finland, Explanation to the maps of Pre-Quaternary rocks: 30 p.

Sjöblom, B., 1984. Geological map of Finland 1:100000, Sheet 2241 Ähtäri. Geological Survey of Finland, Explanation to the maps of Pre-Quaternary rocks: 39 p.

Tyrväinen, A., 1983. Geological map of Finland 1:100000, Sheets 3713 Sodankylä and 3714 Sattanen. Geological Survey of Finland, Explanation to the maps of Pre-Quaternary rocks: 59 p.

Tyrväinen, A., 1984. Geological map of Finland 1:100000, Sheets 2223 Alavus and 2224 Kuortane. Geological Survey of Finland, Explanation to the maps of Pre-Quaternary rocks: 36 p.

Vorma, A., 1965. Geological map of Finland 1:100000, Sheet 3134 Lappeenranta. Geological Survey of Finland, Explanation to the map of rocks: 72 p.

MINERALOGIC SUMMARY AND MODEL DENSITIES

Composition estimates are based on modal analyses published in explanations to geologic maps of Finland (see Appendix A). Densities are calculated from mineralogic compositions by the density model of Puranen et al. (1978) presented below. Analyses of each rock type were arranged into ascending order on the basis of calculated densities, and then subdivided into five groups of equal size. Averages were calculated for each group (M1..M5) and for all analyses (M). Mineral abundances are expressed in volume %, and calculated densities D of rocks and average densities D_{Ms} of mafic minerals in kg/m³. Formula $W_{Ms} = 100 \cdot (D_{Ms}/D) \cdot V_{Ms}$ is used to calculate abundance of mafic minerals W_{Ms} (wt %) from their volume fraction V_{Ms}.

GRANITE (115 analyses)

Mean	QUAR	PLAG	anor	ALKA	MUSC	BIOT	AMPH	PYRO	OTHE	D_{Ms}	D	W_{Ms}
M	32.7	30.0	19.0	30.5	0.5	4.5	0.3	0.0	1.5	3110	2660	7.3
M1	33.0	26.3	17.2	36.8	0.4	2.9	0.0	0.0	0.3	3040	2630	3.6
M2	35.7	31.1	19.0	28.9	0.3	3.6	0.0	0.0	0.3	2990	2640	4.3
M3	32.5	30.3	17.7	31.4	0.9	3.8	0.0	0.0	1.1	3110	2650	5.7
M4	31.1	31.6	18.6	29.3	1.0	5.4	0.1	0.1	1.5	3140	2660	8.1
M5	30.9	30.5	22.6	26.1	0.0	6.9	1.3	0.0	4.3	3260	2700	14.7

GRANODIORITE (189 analyses)

Mean	QUAR	PLAG	anor	ALKA	MUSC	BIOT	AMPH	PYRO	OTHE	D_{Ms}	D	W_{Ms}
M	25.6	46.9	24.8	12.1	0.1	10.1	3.1	0.2	1.8	3020	2700	17.0
M1	30.1	46.4	21.2	16.5	0.0	6.2	0.4	0.0	0.4	2970	2660	7.6
M2	28.3	49.3	22.9	12.2	0.2	7.9	1.0	0.0	1.0	3000	2680	11.0
M3	25.8	47.6	24.4	11.7	0.1	10.7	2.4	0.0	1.6	3020	2700	16.4
M4	23.7	47.4	26.5	9.6	0.1	12.1	4.4	0.6	2.1	3040	2720	21.4
M5	20.1	43.7	29.1	10.2	0.0	13.9	7.6	0.4	4.1	3080	2760	28.9

QUARTZ DIORITE (170 analyses)

Mean	QUAR	PLAG	anor	ALKA	MUSC	BIOT	AMPH	PYRO	OTHE	D_{Ms}	D	W_{Ms}
M	20.3	51.7	29.8	2.0	0.2	14.5	8.3	0.1	3.0	3040	2760	28.3
M1	27.7	54.5	26.9	3.2	0.5	11.2	1.3	0.1	1.4	3020	2700	15.5
M2	22.8	53.2	27.6	3.0	0.2	12.9	5.2	0.1	2.4	3030	2730	22.9
M3	18.6	54.4	29.6	1.3	0.0	15.5	6.8	0.2	3.2	3040	2760	28.3
M4	18.4	48.8	31.5	1.6	0.0	16.5	11.2	0.0	3.5	3050	2780	34.1
M5	14.0	47.5	33.5	0.7	0.3	16.2	16.7	0.1	4.5	3070	2820	40.7

DIORITE (50 analyses)

Mean	QUAR	PLAG	anor	ALKA	MUSC	BIOT	AMPH	PYRO	OTHE	D_{Ms}	D	W_{Ms}
M	5.0	53.2	37.6	0.5	0.0	11.8	25.6	0.5	3.4	3070	2840	44.6
M1	7.8	61.9	33.4	2.0	0.1	12.9	12.5	0.8	2.0	3050	2770	30.8
M2	6.5	55.1	37.4	0.3	0.0	12.1	23.0	0.7	2.3	3060	2820	41.3
M3	3.1	53.3	35.8	0.0	0.0	13.6	26.6	0.1	3.4	3060	2840	47.0
M4	4.5	48.3	37.0	0.0	0.0	13.5	28.8	0.7	4.2	3080	2870	50.7
M5	3.2	47.4	44.5	0.0	0.0	7.1	37.2	0.2	4.9	3120	2900	53.1

GABBRO (84 analyses)

Mean	QUAR	PLAG	anor	ALKA	MUSC	BIOT	AMPH	PYRO	OTHE	D_{Ms}	D	W_{Ms}
M	1.2	43.8	51.1	0.1	0.1	4.6	34.1	12.3	3.8	3160	2940	58.4
M1	1.9	57.8	46.3	0.5	0.0	7.3	23.5	6.9	2.1	3120	2860	43.3
M2	2.1	49.0	50.9	0.2	0.0	7.0	31.6	7.7	2.5	3120	2900	52.3
M3	0.9	46.3	51.7	0.0	0.0	3.3	35.1	10.3	3.9	3160	2930	56.6
M4	0.5	39.6	53.8	0.0	0.0	3.2	43.9	6.6	6.1	3170	2980	63.6
M5	0.6	25.0	52.8	0.1	0.3	2.0	36.7	30.9	4.4	3210	3070	77.1

QUARTZITE (49 analyses)

Mean	QUAR	PLAG	anor	ALKA	MUSC	BIOT	AMPH	PYRO	OTHE	D_{Ms}	D	W_{Ms}
M	78.3	7.9	17.1	5.1	3.3	2.2	0.2	0.3	2.7	3430	2690	6.6
M1	78.2	10.0	19.4	9.7	1.2	0.5	0.0	0.0	0.3	3350	2650	1.0
M2	77.7	9.1	19.9	5.8	4.6	1.8	0.0	0.0	1.0	3390	2670	3.3
M3	75.3	9.7	16.4	6.2	3.5	2.7	0.0	0.0	2.5	3420	2680	6.4
M4	79.7	4.8	14.4	1.3	6.0	4.8	0.0	0.0	3.3	3420	2700	9.7
M5	81.0	5.6	15.3	2.2	0.9	1.1	0.9	1.6	6.6	3580	2740	13.2

QUARTZ-FELDSPAR SCHIST/GNEISS (64 analyses)

Mean	QUAR	PLAG	anor	ALKA	MUSC	BIOT	AMPH	PYRO	OTHE	D_{Ms}	D	W_{Ms}
M	34.9	41.3	25.2	7.5	3.7	9.1	0.7	0.1	2.6	3120	2710	14.1
M1	38.9	34.3	22.2	19.4	1.5	5.1	0.2	0.0	0.6	3100	2660	6.7
M2	35.0	47.7	25.7	6.3	1.8	7.8	0.0	0.2	1.1	3090	2680	10.1
M3	36.5	44.3	26.4	4.2	3.0	9.4	0.3	0.3	2.1	3090	2700	13.6
M4	32.4	41.8	27.3	6.0	6.0	9.8	0.2	0.0	3.7	3150	2720	15.7
M5	31.7	38.1	24.6	1.2	6.7	13.5	3.2	0.0	5.6	3150	2770	25.0

MICA SCHIST/GNEISS (70 analyses)

Mean	QUAR	PLAG	anor	ALKA	MUSC	BIOT	AMPH	PYRO	OTHE	D_{Ms}	D	W_{Ms}
M	33.4	30.0	27.5	3.2	1.9	28.1	1.2	0.0	2.3	2950	2750	33.6
M1	33.4	35.2	27.9	11.3	0.9	17.8	0.5	0.0	0.7	2920	2690	20.5
M2	39.1	32.8	27.3	1.1	0.9	24.6	0.1	0.0	1.5	2920	2720	27.9
M3	32.0	29.6	24.9	2.3	2.4	31.0	0.4	0.0	2.4	2980	2750	36.0
M4	26.9	30.0	27.9	1.5	3.4	34.2	1.0	0.0	3.0	2940	2770	40.5
M5	35.7	20.3	29.7	0.0	1.8	33.9	4.2	0.0	4.1	2980	2790	44.9

AMPHIBOLITE (54 analyses)

Mean	QUAR	PLAG	anor	ALKA	MUSC	BIOT	AMPH	PYRO	OTHE	D_{Ms}	D	W_{Ms}
M	4.3	36.5	44.2	0.0	0.2	3.4	46.4	5.7	3.4	3120	2940	62.1
M1	12.1	49.7	36.3	0.0	0.6	5.4	29.5	1.3	1.4	3080	2830	41.0
M2	4.8	44.8	45.5	0.2	0.0	3.6	42.2	2.1	2.2	3100	2890	53.7
M3	1.1	38.8	47.7	0.0	0.3	3.4	44.9	8.7	2.9	3130	2950	63.4
M4	1.9	23.5	43.0	0.0	0.0	3.6	66.5	0.0	4.5	3110	3000	77.3
M5	1.6	24.8	48.8	0.0	0.0	0.9	49.1	17.6	6.0	3180	3050	76.6

(META)DIABASE (26 analyses)

Mean	QUAR	PLAG	anor	ALKA	MUSC	BIOT	AMPH	PYRO	OTHE	D_{Ms}	D	W_{Ms}
M	1.8	35.3	41.3	0.0	0.0	5.6	41.3	11.3	4.7	3150	2970	66.4
M1	4.1	46.9	39.0	0.0	0.0	15.8	28.4	1.4	3.5	3060	2870	52.4
M2	1.8	40.0	43.1	0.0	0.0	5.8	41.5	6.3	4.7	3140	2950	61.9
M3	1.1	36.7	43.3	0.0	0.0	2.1	40.4	14.9	4.7	3190	2990	66.0
M4	2.3	22.0	33.0	0.0	0.0	2.8	66.9	0.0	6.0	3130	3020	78.5
M5	0.1	30.4	47.6	0.1	0.0	2.3	29.4	33.3	4.4	3230	3050	73.0

Abbreviations of mineral names:

FELSIC
QUAR = quartz
PLAG = plagioclase
anor = anorthite
ALKA = alkali feldspar
MUSC = muscovite

MAFIC
BIOT = biotite
AMPH = amphibole
PYRO = pyroxene
OTHE = other minerals

MODEL DENSITIES OF MINERALS

Di	QUAR	ALKA	MUSC	BIOT	AMPH	PYRO	OTHE	PLAG
kg/m^3	2650	2580	2800	2860	3080	3280	3760	$2625 + 125 \cdot anor/90$

SUMMARY OF CHEMICAL ANALYSES

The summary is based on classical silicate analyses made at the Geological Survey of Finland. Analysis results were collected from publications (Lokka, 1934; Lokka, 1950) and from the open data register that contains analyses from the years 1957—1981. Analysis results of each rock type were arranged into ascending order on the basis of total iron content Fe, and the data so arranged were divided into five parts of equal size. Averages of different elements were calculated for each part (M1..M5) and for all analyses (M).

GRANITE (120 analyses)

Mean	SiO_2	TiO_2	Al_2O_3	Fe_2O_3	FeO	MnO	MgO	CaO	Na_2O	K_2O	P_2O_5	Fe
M	71.41	0.35	14.20	0.99	1.68	0.05	0.56	1.71	3.46	4.64	0.12	1.97
M1	75.15	0.08	13.66	0.38	0.44	0.02	0.17	0.74	3.48	5.17	0.05	0.60
M2	73.66	0.21	13.87	0.66	1.00	0.02	0.31	1.17	3.42	4.86	0.07	1.22
M3	72.83	0.33	13.86	0.77	1.47	0.03	0.43	1.53	3.10	4.81	0.10	1.68
M4	71.04	0.32	14.08	1.19	2.02	0.07	0.69	1.81	3.59	4.42	0.13	2.33
M5	64.40	0.78	15.54	1.90	3.47	0.09	1.22	3.32	3.70	3.96	0.26	4.03

GRANODIORITE (48 analyses)

Mean	SiO_2	TiO_2	Al_2O_3	Fe_2O_3	FeO	MnO	MgO	CaO	Na_2O	K_2O	P_2O_5	Fe
M	66.33	0.60	15.68	1.16	3.21	0.08	1.48	3.46	3.71	3.08	0.19	3.31
M1	71.06	0.29	15.28	0.61	1.46	0.05	0.77	2.71	4.28	2.71	0.09	1.56
M2	67.31	0.37	16.03	1.08	2.18	0.08	1.15	3.33	3.70	3.09	0.16	2.45
M3	67.44	0.57	15.46	0.92	3.10	0.08	1.24	3.14	3.42	3.51	0.16	3.05
M4	63.72	0.72	16.10	1.44	3.87	0.09	2.38	3.82	3.71	2.95	0.22	4.01
M5	62.15	1.05	15.48	1.79	5.50	0.09	1.84	4.30	3.47	3.09	0.35	5.53

QUARTZ DIORITE (34 analyses)

Mean	SiO_2	TiO_2	Al_2O_3	Fe_2O_3	FeO	MnO	MgO	CaO	Na_2O	K_2O	P_2O_5	Fe
M	61.69	0.76	16.86	1.19	4.63	0.09	2.54	5.21	3.71	2.13	0.23	4.43
M1	64.02	0.44	18.10	0.60	2.49	0.05	1.91	4.94	4.35	1.89	0.16	2.36
M2	65.29	0.77	16.11	0.95	3.67	0.06	2.18	4.18	3.54	2.32	0.17	3.52
M3	61.31	0.71	16.78	0.95	4.72	0.09	2.83	5.39	3.49	2.48	0.25	4.34
M4	60.29	0.73	16.95	1.66	5.32	0.13	2.85	5.80	3.60	1.81	0.22	5.30
M5	57.49	1.15	16.35	1.72	6.95	0.14	2.97	5.78	3.52	2.18	0.34	6.61

DIORITE (33 analyses)

Mean	SiO_2	TiO_2	Al_2O_3	Fe_2O_3	FeO	MnO	MgO	CaO	Na_2O	K_2O	P_2O_5	Fe
M	55.88	1.30	17.01	1.75	6.42	0.14	3.70	6.55	3.51	2.09	0.46	6.18
M1	58.66	0.89	17.38	1.73	4.72	0.09	3.31	5.00	4.06	2.37	0.42	4.88
M2	58.51	1.05	16.14	1.27	6.00	0.13	4.10	6.29	3.35	1.90	0.30	5.43
M3	56.11	1.19	17.00	1.97	5.84	0.10	4.04	6.87	3.18	2.04	0.53	5.92
M4	53.50	1.64	17.39	2.18	6.82	0.16	3.94	7.43	3.55	1.77	0.67	6.82
M5	52.56	1.73	17.24	1.51	8.79	0.24	2.94	7.03	3.46	2.46	0.42	7.89

GABBRO (74 analyses)

Mean	SiO_2	TiO_2	Al_2O_3	Fe_2O_3	FeO	MnO	MgO	CaO	Na_2O	K_2O	P_2O_5	Fe
M	49.89	1.21	16.04	1.82	7.75	0.15	7.79	10.49	2.44	0.78	0.31	7.30
M1	51.02	0.60	18.55	0.86	5.20	0.11	7.39	11.81	2.50	0.54	0.16	4.64
M2	50.15	0.86	15.80	1.66	6.41	0.17	8.59	11.55	2.38	0.72	0.16	6.15
M3	50.85	0.93	15.68	2.38	6.77	0.16	8.72	9.47	2.33	1.27	0.36	6.93
M4	49.11	1.39	15.62	1.99	8.62	0.18	7.35	10.88	2.20	0.65	0.44	8.10
M5	48.39	2.39	14.53	2.27	11.66	0.16	6.96	8.66	2.80	0.73	0.49	10.65

Appendix C. (continued)

QUARTZITE (31 analyses)

Mean	SiO_2	TiO_2	Al_2O_3	Fe_2O_3	FeO	MnO	MgO	CaO	Na_2O	K_2O	P_2O_5	Fe
M	86.62	0.16	5.43	1.32	1.03	0.03	0.82	1.33	0.52	1.34	0.05	1.62
M1	96.58	0.03	2.40	0.06	0.02	0.00	0.04	0.12	0.03	0.28	0.02	0.06
M2	90.56	0.10	5.21	0.31	0.20	0.01	0.73	0.18	0.30	1.64	0.02	0.33
M3	89.62	0.11	4.52	0.55	0.52	0.02	0.36	1.50	0.31	1.46	0.03	0.79
M4	79.65	0.22	9.74	1.52	0.52	0.06	1.34	1.12	1.35	2.12	0.13	1.47
M5	76.17	0.37	5.43	3.95	3.68	0.06	1.73	3.70	0.65	1.19	0.03	5.62

QUARTZ-FELDSPAR SCHIST/GNEISS (26 analyses)

Mean	SiO_2	TiO_2	Al_2O_3	Fe_2O_3	FeO	MnO	MgO	CaO	Na_2O	K_2O	P_2O_5	Fe
M	71.34	0.42	13.42	0.83	3.02	0.06	1.44	2.15	2.97	3.16	0.18	2.93
M1	75.91	0.13	13.34	0.45	0.93	0.03	0.53	1.35	3.57	3.20	0.08	1.03
M2	75.47	0.25	12.31	0.40	1.68	0.03	0.75	1.37	2.47	4.31	0.11	1.58
M3	70.96	0.44	13.61	0.96	2.70	0.08	1.13	2.58	3.26	3.04	0.24	2.77
M4	71.05	0.54	12.18	1.45	3.87	0.06	1.89	2.22	3.04	2.40	0.19	4.02
M5	63.38	0.76	15.65	0.89	6.00	0.09	2.75	3.14	2.46	2.87	0.24	5.28

MICA SCHIST/GNEISS (54 analyses)

Mean	SiO_2	TiO_2	Al_2O_3	Fe_2O_3	FeO	MnO	MgO	CaO	Na_2O	K_2O	P_2O_5	Fe
M	63.56	0.92	15.80	2.06	5.21	0.06	2.95	1.75	2.34	3.26	0.19	5.34
M1	74.20	0.50	12.13	0.87	2.90	0.05	1.30	2.25	3.05	1.71	0.15	2.64
M2	65.88	0.61	16.02	1.62	3.70	0.05	2.13	1.40	2.61	3.97	0.17	4.01
M3	62.23	0.83	17.10	1.68	5.38	0.05	2.70	2.57	2.51	3.44	0.21	4.98
M4	60.45	0.97	17.25	1.54	6.43	0.09	3.77	1.51	2.00	3.08	0.25	6.08
M5	56.03	1.64	16.16	4.46	7.23	0.08	4.71	1.05	1.57	3.97	0.19	8.74

AMPHIBOLITE (57 analyses)

Mean	SiO_2	TiO_2	Al_2O_3	Fe_2O_3	FeO	MnO	MgO	CaO	Na_2O	K_2O	P_2O_5	Fe
M	51.43	1.33	14.95	2.17	8.12	0.17	7.02	9.00	2.89	0.98	0.27	7.83
M1	57.34	0.60	15.04	1.28	4.35	0.11	6.74	7.48	3.58	1.47	0.17	4.27
M2	51.22	1.07	16.78	1.65	7.18	0.15	5.82	10.32	2.96	1.16	0.32	6.74
M3	50.21	1.21	14.90	1.94	8.47	0.17	7.51	10.37	2.65	0.60	0.23	7.94
M4	49.95	1.50	14.56	2.49	9.56	0.20	7.93	8.31	2.59	1.22	0.42	9.17
M5	48.16	2.26	13.58	3.46	11.10	0.21	7.13	8.70	2.62	0.46	0.23	11.04

(META)DIABASE (94 analyses)

Mean	SiO_2	TiO_2	Al_2O_3	Fe_2O_3	FeO	MnO	MgO	CaO	Na_2O	K_2O	P_2O_5	Fe
M	50.04	1.84	14.93	3.29	9.58	0.20	5.97	8.17	2.74	1.29	0.33	9.75
M1	54.40	1.00	16.22	1.82	5.98	0.21	5.99	7.81	3.27	1.66	0.27	5.92
M2	49.72	1.37	16.27	3.30	7.45	0.17	6.49	8.23	2.52	1.60	0.32	8.10
M3	49.20	1.62	15.89	2.71	9.71	0.18	6.23	9.34	2.52	1.14	0.34	9.44
M4	49.50	2.33	14.23	4.25	10.30	0.19	5.01	7.80	2.96	1.13	0.40	10.98
M5	47.35	2.95	12.06	4.36	14.46	0.27	6.13	7.70	2.41	0.90	0.31	14.28

Tätä julkaisua myy
GEOLOGIAN
TUTKIMUSKESKUS (GTK)
Julkaisumyynti
02150 Espoo
☎ 90-46931
Teleksi: 123 185 geolo sf
Telekopio: 90-462 205

GTK, Väli-Suomen
aluetoimisto
Kirjasto
PL 1237
70701 Kuopio
☎ 971-164 698
Telekopio: 971-228 670

GTK, Pohjois-Suomen
aluetoimisto
Kirjasto
PL 77
96101 Rovaniemi
☎ 960-297 219
Teleksi: 37 295 geolo SF
Telekopio: 960-297 289

Denna publikation säljes av
GEOLOGISKA
FORSKNINGSCENTRALEN (GFC)
Publikationsförsäljning
02150 Esbo
☎ 90-46931
Telex: 123 185 geolo sf
Telefax: 90-462 205

GFC, Distriktsbyrån för
Mellersta Finland
Biblioteket
PB 1237
70701 Kuopio
☎ 971-164 698
Telefax: 971-228 670

GFC, Distriktsbyrån för
Norra Finland
Biblioteket
PB 77
96101 Rovaniemi
☎ 960-297 219
Telex: 37 295 geolo SF
Telefax: 960-297 289

This publication can be obtained from
GEOLOGICAL SURVEY
OF FINLAND (GSF)
Publication sales
SF-02150 Espoo, Finland
☎ 90-46931
Telex: 123 185 geolo sf
Telefax: 90-462 205

GSF, Regional office for
Mid-Finland
Library
P.O. Box 1237
SF-70701 Kuopio, Finland
☎ 971-164 698
Telefax: 971-228 670

GSF, Regional office for
Northern Finland
Library
P.O. Box 77
SF-96101 Rovaniemi, Finland
☎ 960-297 219
Telex: 37 295 geolo SF
Telefax: 960-297 289

ISBN 951-690-352-5
ISSN 0781-4240

Vammala 1989
Vammalan Kirjapaino Oy